



**TRIBHUVAN UNIVERSITY**  
**INSTITUTE OF ENGINEERING**  
**PULCHOWK CAMPUS**

**THESIS NO.:PUL075MSGtE001**

**Seepage Characteristics of Concrete Face Rockfill Dhap Dam**

by

Anup Lamichhane

A THESIS

SUBMITTED TO THE DEPARTMENT OF CIVIL ENGINEERING  
IN PARTIAL FULFILLMENT OF THE REQUIREMENTS FOR THE  
DEGREE OF MASTERS OF SCIENCE IN  
GEOTECHNICAL ENGINEERING

DEPARTMENT OF CIVIL ENGINEERING  
LALITPUR, NEPAL

September, 2021

## **COPYRIGHT**

The author has agreed that the library, Department of Civil Engineering, Pulchowk Campus, Institute of Engineering, may make this thesis freely available for inspection.

Moreover, the author has agreed that permission for extensive copying of this thesis for scholarly purpose may be granted by the professor(s) who supervised the work recorded herein or, in their absence, by the Head of the Department wherein the thesis was done. It is understood that the recognition will be given to the author of this thesis and to the Department of Civil Engineering, Pulchowk Campus, Institute of Engineering in any use of the material of this thesis. Copying or publication or the other use of this thesis for financial gain without approval of the Department of Civil Engineering, Pulchowk Campus, Institute of Engineering and author's written permission is prohibited.

Request for permission to copy or to make any other use of the material in this thesis in whole or in part should be addressed to:

.....

Head

Department of Civil Engineering

Pulchowk Campus, Institute of Engineering

Lalitpur, Nepal

**TRIBHUVAN UNIVERSITY**  
**INSTITUTE OF ENGINEERING**  
**PULCHOWK CAMPUS**  
**DEPARTMENT OF CIVIL ENGINEERING**

The undersigned certify that they have read, and recommended to the Institute of Engineering for acceptance, a thesis entitled “**Seepage Characteristics of Concrete Face Rockfill Dhap Dam**” submitted by Mr. Anup Lamichhane (PUL075MSGte001) in partial fulfillment of the requirements for the degree of Master of Science in Geotechnical Engineering.

.....  
Supervisor  
Dr. Bhagaban Acharya  
Senior Dam/Geotechnical Engineer,  
Entura, Australia

.....  
Supervisor  
Associate Prof. Dr. Indra Prasad Acharya  
Institute of Engineering, Pulchowk Campus

.....  
External Examiner  
Dr. Mohan Prasad Acharya  
Senior Geotechnical Engineer  
NEA Engineering Company Limited

.....  
Program Coordinator  
Dr. Santosh Kumar Yadav  
Institute of Engineering, Pulchowk Campus

## ABSTRACT

Dhap dam is the first CFRD type dam under construction in the Gokarneshwor Municipality in Bagmati Province, Nepal. The dam is constructed in the gneiss rock foundation underlain by the colluvium deposit. This thesis presents the seepage assessment by varying the hydraulic conductivity function and anisotropy of foundation materials. As a part of this study, an ongoing geotechnical investigation organized by the Bagmati River Basin Improvement Project was supervised and necessary data relevant to this thesis was calculated. The geotechnical investigations consisted of drilling boreholes, Lugeon tests, Lefranc tests and grouting undertaken around the plinth region of the upstream toe of the dam. A geotechnical model was proposed based on the information collated from borehole logs. The hydraulic conductivity of the foundation materials was interpreted from the Lugeon and Lefranc tests. Besides, top colluvium sample was brought to lab and geotechnical characterization as well as constant head test was performed to carry out coefficient of permeability value. Permeability value of the colluvium obtained from laboratory tests and field permeability value vary significantly implying lab permeameter is never in the same condition as in the site. Finally, two-dimensional Seep/W numerical models were prepared considering dam sections and foundation materials to estimate the seepage through the dam. Additionally, numerical models were analyzed by incorporating grouting in the models to evaluate the influence of grouting on the seepage performance of the dam. Reduction of seepage after grouting, seepage variation by varying foundation materials and anisotropy is presented in this research.

Keywords: CFRD, Seepage, Permeability, Lugeon test, Lefranc test, Grouting



## ACKNOWLEDGEMENT

I am so grateful to the Institute of Engineering, Pulchowk Campus which provides me a platform to do this study. I wish to express my deepest and sincere appreciation to my supervisors Dr. Bhagaban Acharya and Associate Professor Dr. Indra Prasad Acharya for their guidance, encouragement, and critical suggestion throughout this study without whom, this research and thesis work couldn't achieve this state. I am highly indebted to them for their tireless patience during the thesis and for bearing with all the troubles and extending necessary help towards accomplishing this task. I highly appreciate their scholastic attitude and pragmatic thinking over thesis problems. My sincere thanks to Dr. Santosh Kumar Yadav for his valuable guidance and understanding during this study.

I have the deepest gratitude to Bagmati River Basin Improvement Project personnel Mr. Krishna Prasad Rijal, Mr. Nischchal Chhatkuli, Ms. Jaya Laxmi Singh, and Mr. Devendra Rimal for providing me a platform to collect and transport the test samples and facilitation on supervising site investigation activities including rock Coring, drilling, testing, and grouting. Financial support and motivation offered by BRBIP personnel during this study are highly appreciated.

In addition, I would like to thank Mr. Suvash Gyawali and classmates for their constant support during my thesis. I am also grateful to the friends from SLG for their constant motivation.

I offer my regards to my loving parents whose love and blessings brought me here. Further, I would like to thank my family members along with my relatives and friends for their advice, instructions, and guidelines that bring encouragement on this research. I would like to extend further thanks to all individuals for their direct and indirect help.

## TABLE OF CONTENTS

Copyright.....	i
Abstract.....	iii
Acknowledgement .....	iv
Table of contents.....	v
List of figures: .....	ix
List of tables: .....	xi
List of charts: .....	xii
Abbreviations .....	xiii
CHAPTER ONE: INTRODUCTION.....	1
1.1 Introduction .....	1
1.2 Background .....	2
1.3 Location.....	3
1.4 Topography/Geology .....	4
1.5 Problem Statement/ Motivation .....	5
1.6 Objectives.....	6
1.7 Scope of the work.....	6
1.8 Justification of Study.....	7
CHAPTER TWO: LITERATURE REVIEW.....	8
2.1 Dam.....	8
2.1.1 Embankment Dam .....	9
2.1.2 Concrete Face Rockfill Dam (CFRD).....	9
2.2 Permeability and Seepage .....	11
2.2.1 Viscosity of the pore fluid (usually water) .....	13
2.2.2 The void ratio of the soil:.....	13

2.2.3	The size and shape of the soil particles:.....	15
2.2.4	Saturation ‘S’: .....	15
2.3	Laboratory test for hydraulic conductivity.....	16
2.4	Field Test.....	17
2.4.1	Lugeon Test .....	17
2.4.2	Lefranc Test .....	20
2.5	Seepage in CFRD .....	22
2.6	Curtain Grout as Seepage Barrier.....	22
2.7	Numerical Modelling .....	23
2.7.1	Finite Element Technique .....	24
2.7.2	Anisotropy.....	24
CHAPTER THREE: RESEARCH METHODOLOGY .....		25
3.1	General .....	25
3.2	Introduction .....	25
3.3	Sample Collection Program (Test Pits Sample).....	26
3.4	Laboratory Program .....	27
3.4.1	Index Property.....	27
3.4.2	Maximum Dry Density: .....	28
3.4.3	Constant Head Test .....	28
3.4.4	Free Swell Index Test .....	31
3.4.5	XRD .....	31
3.5	Site Investigation Program .....	31
3.5.1	Rock Coring and Drilling.....	31
3.6	Geological Model.....	32
3.7	Grout Curtain.....	33
3.8	Numerical Analysis .....	34
CHAPTER FOUR: RESULTS AND DISCUSSIONS.....		37

4.1	General .....	37
4.2	In-situ Test Results.....	37
4.3	Laboratory Test Results .....	37
4.3.1	Particle Size Distribution .....	38
4.3.2	Compaction Test Result.....	40
4.3.3	Permeability Test Results .....	40
4.3.4	XRD .....	45
4.4	Geotechnical Investigation.....	46
4.4.1	Core Recovery and RQD Profile .....	46
4.4.2	Geotechnical Model.....	46
4.4.3	Lugeon Profile .....	47
4.5	Grouting .....	49
4.6	Numerical Analyses .....	50
4.6.1	General.....	50
4.6.2	GeoStudio Seep/W Software .....	51
4.6.3	Model Function.....	52
4.6.4	Numerical Model .....	55
4.7	Numerical Analyses Results.....	57
4.8	Sensitivity Analysis.....	58
4.9	Numerical Analyses Considering Anisotropy.....	60
4.10	Seepage potential when water level is up to permanent outlet.....	63
4.11	Sensitivity analysis on grouted dam .....	64
4.12	Discussion.....	65
CHAPTER FIVE: CONCLUSIONS AND RECOMMENDATIONS .....		67
5.1	General .....	67
5.2	Conclusions .....	67
5.3	Recommendations .....	69

REFERENCES .....	71
APPENDICES .....	75
APPENDIX A: TRENCH SAMPLE COLLECTION.....	76
APPENDIX B: CORE LOGGING .....	77
APPENDIX C: FIELD TESTS.....	87
APPENDIX D: CORELOG PHOTOGRAPHS.....	92
APPENDIX E: NUMERICAL MODEL .....	97
APPENDIX F: WORK SCHEDULE .....	100

## LIST OF FIGURES:

Figure 1.1: Dhap Dam Project Location .....	3
Figure 1.2: Drone Image of Under Construction Dhap CFRD.....	4
Figure 2.1 Zoning of a modern CFRD(Cruz et al., 2010).....	11
Figure 2.2 Relation between void ratio $e$ and $k$ for variable head test ((Lambe and Whitman, 1979) .....	14
Figure 2.3: Permeability versus degree of saturation for various sand. (From Wallace, 1948) .....	15
Figure 2.4: Permeability test data from Literature (Lambe and Whitman Page 286).....	16
Figure 2.5: Schematic Diagram of Lugeon test (Fell et al., 2005).....	17
Figure 2.6 Two ways to conduct Lefranc CH test .....	21
Figure 3.1 Constant Head Permeameter and Constant Head permeameter placed in sink.....	30
Figure 3.2 Geological Profile along the hole MP15 (Ref. Section 4.4).....	33
Figure 3.3: Typical curve of 1500 GIN intensity with 15bar $P_{max}$ .....	34
Figure 4.1: Grain Size Distribution Curve of Samples .....	39
Figure 4.2 Compaction test Result.....	40
Figure 4.3: Plot of Permeability vs. Void ratio of Samples .....	42
Figure 4.4 Plot of $k$ vs. $e^3/(1+e)$ .....	43
Figure 4.5 Plot of Permeability values of Sample 1 and 10 in plot digitizer of Lambe and Whitman chart.....	44
Figure 4.6: XRD test data of sample (Sample No. 10) .....	45
Figure 4.7: RQD and Core Recovery obtained plot while rock coring .....	46
Figure 4.8: Geotechnical Model of Dam Plinth.....	47
Figure 4.9: Lugeon Pattern .....	48
Figure 4.10: Graphical Presentation of Lugeon Values.....	48
Figure 4.11: Frequency Chart of Permeability Values in Lugeon Units .....	49
Figure 4.12: Sample GIN curve at 15 bar pressure.....	50
Figure 4.13 Dhap Dam and cross-sections adopted for Seepage Model .....	51
Figure 4.14: Hydraulic Conductivity function of materials.....	53
Figure 4.15: Volumetric Water Content Function of Materials.....	53

Figure 4.16: Seepage Model of Dam along section B-B before grouting .....	55
Figure 4.17: Seepage Model of Dam along section B-B after grouting .....	56
Figure 4.18: Seepage Model of Dam along section A-A before grouting .....	56
Figure 4.19: Seepage Model of Dam along section A-A after grouting .....	56
Figure 4.20: Seepage Model of Dam along section C-C before grouting .....	57
Figure 4.21: Seepage Model of Dam along section C-C after grouting .....	57
Figure 4.22: Sensitivity Analysis at Dam Section (A-A) .....	59
Figure 4.23: Sensitivity Analysis at Dam Section (B-B).....	60
Figure 4.24: Sensitivity Analysis at Dam Section (C-C).....	60
Figure 4.25: Sensitivity Analysis by varying Anisotropy at section (A-A).....	61
Figure 4.26: Sensitivity Analysis by Varying Anisotropy ratio at section (B-B)..	61
Figure 4.27: Sensitivity Analysis by Varying Anisotropy ratio at section (C-C)..	62
Figure 4.28: Seepage without group on up to permanent outlet level .....	63
Figure 4.29: Seepage with grout on up to permanent outlet level .....	64

## LIST OF TABLES:

Table 1.1: Salient Features of Dhap Dam (BRBIP, 2018).....	2
Table 2.1: Variation of ratio with temperature .....	13
Table 2.2: Classification of Soil Permeability .....	16
Table 2.3: Situations of Rock mass with reference to Lugeon Values (Camilo Quinones-Rozo and Andrew Yu, 2010) .....	19
Table 2.4: Lugeon Interpretation as their pattern.....	20
Table 4.1 Field density (Sand Replacement Method) Test Result.....	37
Table 4.2 Soil Classification of Collected Samples.....	38
Table 4.3: Compaction test data from laboratory .....	40
Table 4.4: Permeability Test Result of Sample No. 1.....	41
Table 4.5: Permeability Test Result of Sample No. 10.....	41
Table 4.6 Summary of Permeability Test of samples.....	41
Table 4.7: Permeability in correlation with Grain size distribution.....	43
Table 4.8: Typical Lugeon Test Result.....	47
Table 4.9: Summary of saturated water content and hydraulic conductivity of materials .....	52
Table 4.10: Geotechnical Model Along Section B-B .....	54
Table 4.11: Geotechnical Model along section A-A .....	54
Table 4.12: Geotechnical Model along C-C .....	55
Table 4.13: Summary of Estimated Seepage on the dam .....	57
Table 4.14: Summary of Sensitivity Analysis .....	59
Table 4.15: Estimated Seepage variation along Section A-A.....	61
Table 4.16: Estimated Seepage variation along Section B-B .....	62
Table 4.17: Estimated Seepage variation along Section C-C .....	62
Table 4.18: Summary with Anisotropy.....	63
Table 4.19: Summary of estimated seepage after grout interface with sensitivity analysis.....	64



**LIST OF CHARTS:**

Chart 3.1: Flow Chart of Research Methodology .....25

## ABBREVIATIONS

ASTM	American Society for Testing and Materials
CFRD	Concrete Face Rockfill Dam
$C_u$	Coefficient of Uniformity
$C_c$	Coefficient of Curvature
CH	Constant Head
CMTL	Central Material Testing Laboratory
FEM	Finite Element Method
GIN	Grout Intensity Number
GSD	Grain Size Distribution
ICOLD	International Commission on Large Dams
HCF	Hydraulic Conductivity Function
Lu	Lugeon
NMC	Normal Moisture Content
OMC	Optimum Moisture Content
USCS	Unified Soil Classification System
VWF	Volumetric Water content Function
XRD	X-Ray Diffraction

## CHAPTER ONE: INTRODUCTION

### 1.1 Introduction

A dam is used to impound water for several reasons viz. flood control, water supply for human or livestock, irrigation, energy generation, recreation, or pollution control. Dams are of various types and can be categorized under various conditions. The dam can be a storage dam, diversion dam, detention dam, cofferdam, debris dam depending upon its functions. According to ICOLD (2010), dam is classified based on the height of the dam including Low, Medium, High and Very High head dam. Based on construction material dam can be of Concrete, Embankment, Wooden, Steel, and Masonry. Concrete Dam can also be Gravity dam (the most common and famous one), Arch dam or Buttress Dam.

The embankment dam is the oldest and common one as it is built using locally and naturally available materials such as soil and rock. Embankment dams can be seen of earth fill or rock fill or composite of both which are most common these days. Based on section embankment dams can be homogeneous, zoned or diaphragm type.

Dhap dam is the first concrete face rockfill dam (CFRD) type dam being built in Nepal. Dhap dam is a diaphragm-type zoned embankment dam with a reasonably impervious layer of inclined concrete slab on the upstream face of the dam.

A cut-off wall and grout curtain are usually adopted as the foundation anti-seepage measures in water retention dams such as CFRD (Li, 2007). However, the seepage control system of high CFRD may have anti-seepage deficiencies during both construction and operation. The incomplete and defective nature of the dam face slab during construction and operation phases may lead to seepage through the CFRD (Chen & Zhang, 2016). Based on an assessment of more than 30 CFRDs with height ranging from 25 m to 185.5 m, (Gavan & Fell, 2003) demonstrated that maximum leakage rate at first filling observed was from 5 l/s to more than 3000 l/s, which reduced during operation.

The evaluation of seepage through the foundation and abutment is of prime importance to assure its safety and prevent the downstream life and property during the incident of dam failure, if any. Thus, the permeability characteristics of various types of soil and rock in the dam foundation need to be studied thoroughly to understand the seepage

behavior of the foundation of the dam. The correct estimation of permeability of the foundation soils will assist in the prediction of potential seepage through the dam foundation and remedial measures can be implemented in the design of the dam.

The research here is solely focused on estimating the seepage on downstream of Dhap dam using finite element numerical modeling by thoroughly analyzing the permeability characteristics of foundation material. In addition, the influence of the ground improvement technique such as grouting in seepage performance of the CFRD dam foundation is studied

## 1.2 Background

Dhap dam is aimed to impound the water head upstream and raise the existing Chisapani Lake to store 850,000 m<sup>3</sup> of water. It will collect the monsoon rain and discharge the outflow to maintain the flow in the Bagmati River during dry seasons. (BRBIP, 2018)

Dhap dam being 24 m high in the deepest section and 172.7 m long along the crest, 203m along the plinth. As per ICOLD (2010), Dhap dam is classified as High dam.

The salient features of the Dhap dam are presented in Table 1.1.

**Table 1.1: Salient Features of Dhap dam (BRBIP, 2018)**

Item	Description
Dam type	Concrete Face Rockfill Dam
Maximum Dam height (D/S toe to crest)	24.0 m
Dam length	172.7 m
Dam crest elevation	2090.14 m asl
Upstream slope inclination	1V: 1.7H
Downstream slope inclination	1V: 1.7H
Crest width	8 m
Concrete face thickness	300 mm
Dam volume	53000 m <sup>3</sup>
Normal Water Level (NWL)	2087.14 m asl
Freeboard	3 m

This project was initiated to build a water impounding reservoir by the construction of a dam at the toe level of the Dhap area within Shivapuri-Nagarjun National Park. The reservoir is expected to serve as ground recharge to the upper catchment of Bagmati and Manamati river.

The dam here is mainly oriented to supply a continuous flow of water even in the dry season in Bagmati river, which flows through a major capital city along the way of Pashupatinath Temple. So, this project has national as well as religious significance (BRBIP, 2018).

### 1.3 Location

Dhap dam site is located in the eastern part and almost at the top of Shivapuri hills near Chisapani. The site lies on Gokarneshwor Municipality, Kathmandu District, Bagmati Province bordering with Sindhupalchowk and Nuwakot districts. At the latitude and longitude of 27°48'21.96"N and 85°27'20.13"E, and at approximately 2090m above sea level axis of Dhap dam situates. The project area can be accessed by either Chisapani Nagarkot road or Chisapani-Sundarijal road and is located at 18 km road distance in the north from Sundarijal. The project location for the Dhap dam is shown in Figure 1.1 and a drone image is shown in Figure 1.2.

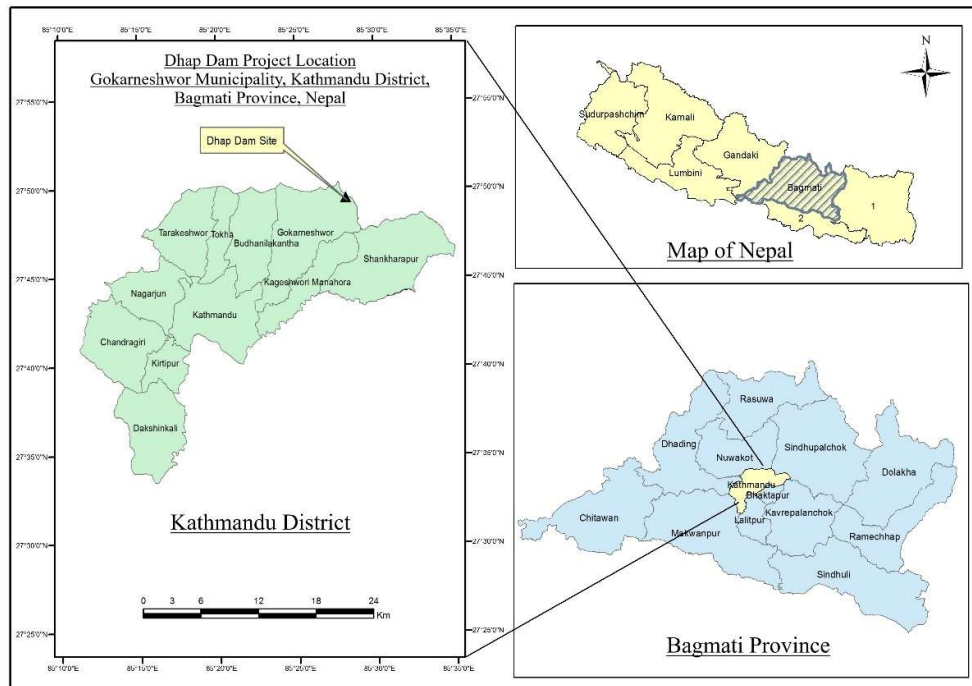


**Figure 1.1: Dhap dam Project Location**



**Figure 1.2: Drone Image of Under Construction Dhap CFRD**

#### **1.4 Topography/Geology**

The topography of the site is relatively rolling around a small lake (the existing Chisapani Lake) which is surrounded by small hilltops reaching up to 2090 m asl, covered by slightly dense forest.

Regionally, the proposed dam site is located within highly metamorphosed basement rocks of the Higher Himalaya Tectonic Zone. Physiographically, the region lies within the Fore Himalaya Geomorphic Unit. The bedrock of the project area is described as ‘Sheopuri Gneiss Formation’ is of Precambrian age (Shrestha, 2000). These rocks are described as “mica gneiss and biotite schist with intrusions of muscovite granite, intensively weathered at the surface.” (Dhital, 2015) in his book *Geology of the Nepal Himalaya* describes the Sheopuri Gneiss as varying from fine to coarse grained banded gneiss, ribbon gneiss, and Augen gneiss composed of quartz, feldspar (plagioclase and K-feldspar), biotite, muscovite and other accessory minerals.

The main rock types in the dam site are gneiss with bands of schists and some intrusions of granites. The bedrock is high to moderately weathered due to which the bedrock underneath the top organic soil is the product of completely weathered/decomposed gneiss resulting in residual soil. The plinth of the dam lies on the fresh to completely weathered gneiss interbedded with some quartzite, schist intruded by quartz, granite, and pegmatite veins. Gneiss is thin to thickly foliated, high to moderately jointed,

medium to coarse-grained, white to dark grey in a fresh color. Quartzite is thin to massive, fresh, light grey, and fine-grained.

### **1.5 Problem Statement/ Motivation**

Dhap dam is a diaphragm type zoned dam with concrete-faced on the upstream side and concrete is supported by a series of rock fill layers in the downstream slope of the dam so-called CFRD is the first dam under construction in Nepal. This dam here is considered as an anti-seepage dam which is a basic characteristic of the concrete face rockfill dam. Though, from the literature, it has been found that there can be significant leakage even through CFRD. One of the major causes of failure of the embankment dam is seepage through the foundation and in the case of CFRD seepage through the foundation is more prominent than from the dam body.

A detailed seepage assessment is necessary for the safe operation of the dam. Thus, seepage characteristics of the CFRD built on gneiss rock formation need to be evaluated to understand the seepage behavior of the Dhap dam. Some of the existing pond formations on the upstream area of the Dhap dam indicated the seepage through colluvium formation. Additionally, the preliminary assessment of the available geotechnical data may be insufficient to evaluate the seepage characteristics of the Dhap dam. Thus, the requirement to undertake an additional geotechnical investigation was felt which would assist in the evaluation of seepage characteristics of the materials encountered in the dam foundation.

Dhap dam being a storage dam with innovative concept of CFRD, accounting leakage here is a very important factor. Furthermore, data from existing investigations show a varying geology which makes it more complex to assess the seepage performance of the Dhap dam. The uncertainty on the reliability of the existing geotechnical investigation data suggested the need for sensitivity analysis that could provide the range of estimated seepage through the dam foundation so that necessary action could be taken earlier. Residual soil on top and completely weathered rocks seems highly permeable so a detailed field and laboratory permeability test is necessary. In addition, numerical analysis of the embankment geometry with grouting and without grouting needs to be undertaken to assess the seepage characteristics of the Dhap dam.

*“To pass judgment on the quality of a dam foundation is one of the most difficult and responsible tasks. It requires both careful consideration of the geological conditions*

*and the capacity for evaluating the hydraulic importance of the geological facts.” Karl Terzaghi, 1929.*

## **1.6 Objectives**

The main objective of this thesis is:

- i. To evaluate the seepage assessment of Dhap dam.

To achieve the main objective, the following general objectives are also established during the study:

- i. Geotechnical characterization of the foundation of Dhap dam,
- ii. Investigate the permeability characteristics of subsurface material from the laboratory as well as field tests, and
- ii. Sensitivity analyses by varying the permeability of foundation soil and anisotropy ratio.

## **1.7 Scope of the work**

This thesis provides insight regarding the seepage behavior of CFRD. The permeability characteristics of residual and highly weathered gneiss rock are studied in the field and laboratory. Various approaches to field tests are studied and practiced with their significance and importance. Laboratory and field tests of residual soil are observed. Quantitative analysis of seepage using GeoStudio, a Finite Element Method, software was undertaken. This study is an attempt to assess the potential seepage from the dam and associated safety issues related to seepage around the toe region of the dam.

To achieve the main objective of the study, the scope of work is summarized below:

- i. Undertake excavation of test pits to collect samples for the laboratory testing,
- ii. Laboratory testing to determine the permeability of the colluvium samples,
- iii. Site investigations including borehole drillings, Lugeon tests, Lefranc tests and grouting,



- iv. Numerical modelling using GeoStudio software to predict the seepage through the dam including evaluation of the effectiveness of the grouting in the seepage performance of the dam, and
- v. Sensitivity analyses in the estimation of seepage considering the varying permeability characteristics of foundation materials.

Although this study is limited to estimate the permeability and seepage characteristics of the Dhap dam, the outcome of the research would be a basis for a similar CFRD such as “Nagmati dam” proposed to build on the downstream side of the Dhap dam.

### **1.8 Justification of Study**

Although the CFRD dam is said to be an anti-seepage, many investigators in the literature indicated that there may be considerable leakage of water through the dam foundation and main body. So, this research will identify the seepage behavior of the Dhap dam through the foundation and dam body.

A fundamental assumption with the CFRD dam is that the dam type lets us use local material from the riverbed and the obligatory excavations in the rock-fill dam body, in contrary to using expensive material from quarries which may have to be transported far from the construction area. In Nepal, there can be a number of potential locations for the CFRD however it has not been sufficiently practiced yet, which motivates to conduct more research about the CFRD in the context of Nepal.

Based on the preliminary study of the geology around the Dhap Dam, the proposed “Nagmati Dam” is also sharing similar geology. Thus, this study would provide an insight into the seepage characteristics of CFRD built on a gneiss rock foundation.

## CHAPTER TWO: LITERATURE REVIEW

Literature relevant, recent and reliable to this study have been reviewed to gain more knowledge about research work. For those available papers, books, journals, articles, abstracts have been studied.

### 2.1 Dam

Dam is a water-retaining physical structure and can be classified under based on function, based on head and on construction material.

According to the hydraulic design dams can be categorized as overflow dam (to permit overflow of surplus water from its crest, non-over flow dam (water is not allowed to overflow over its crest) and rigid dams which are constructed with rigid materials and non-rigid dams which are constructed with earth and rock-fill. According to The Purpose, the dam can be classified as: Storage dam, diversion dam, detention dam, debris dam and coffer dam. Storage dams are constructed to store the spring runoff to use in dry season, a diversion dam is constructed for the purpose of diverting water of the river into an off-taking canal (or a conduit), a debris dam is constructed to retain debris such as sand, gravel, and drift wood flowing in the river with water, detention dams are constructed for flood control i.e. to retards the flow in the river on its downstream during floods by storing some flood water and cofferdam also known as temporary dam is usually constructed at the upstream of the main dam site to exclude water so that the construction can be done in dry state (Bhattarai et al., 2016).

Dam can be of low head (<15m), medium head (15-50m), High head (50-250m), Very High head (>250m).

Besides ICOLD (International Commission on Large Dams) defines large dams as: Either, A dam that is more than 15 meters in height (measured from the lowest point in the general foundations to the crest of the dam) Or, any dam between 10 meters and 15 meters in height which meets one of the following conditions: the crest length is not less than 500 meters; the capacity of the reservoir formed by the dam is not less than one million cubic meters; the maximum flood discharge dealt with by the dam is not less than 2000 cubic meters per second; The dam is of unusual design. (Icold, 2010)

Based on construction Material dam can be concrete dam, embankment dam, wooden dam, steel dam or masonry dam.

### **2.1.1 Embankment Dam**

Embankment dams are earth dams and rockfill dams and their composites. They can be homogeneous composed of only one material, generally material is semi-impervious or impervious soil to limit seepage, built where only one type of material is economically available.

Some embankment dams are zoned earth dam composed of more than one type of soil material, generally consists of central impervious core flanked by pervious material on u/s and d/s sides. And diaphragm type earth dams are the one that consists of thin impervious core called diaphragm. Based on method of construction also Embankment dam can be rolled filled earth dam, hydraulic filled earth dam and semi-hydraulic filled earth dam.

Concrete dams were ruling since earlier because of the lack of large earth moving equipment. Later in the 18<sup>th</sup> century construction of rockfill dams started with proper knowledge and technology. The first rockfill dam was constructed in the 1850's in California, America, followed by English which consists of a 24 m high rockfill dam (Chen & Zhang, 2016).

An impervious membrane is placed on the rock fill on the upstream side to reduce the seepage through the dam. The membrane is usually made of cement concrete or asphaltic concrete. In early rock fill dams, steel and timber membrane were also used, but now they are obsolete.

### **2.1.2 Concrete Face Rockfill Dam (CFRD)**

Concrete faced rock-fill dams, CFRD, is the term used to describe a type of barrier that has a dam body of rock-fill or gravel materials that is compacted and an anti-seepage system using a concrete face slab on upstream (Clements, 1984). The concrete slab works like an impervious layer when the rock-fill body includes granular material which has a high permeability and supports the concrete face slab by giving the dam stability (Gavan & Fell, 2003).

One of the main characteristics of CFRD is that, the dam can be constructed taking full advantages of local excavated materials at the dam site (as opposed to using expensive

material from quarries which may have to be transported a long way), simple construction technique, economic and best adaptability to geology and topography and safer in operation (Bhattarai et al., 2016).

A Concrete Face Rockfill Dam (CFRD) contains of different zones of materials with specific functions in the dam construction. Cooke and Sherard developed the basic designs and presented the result in papers 1987 and they are now standard for CFRD's (Cruz et al., 2010). Figure 2.1 shows the zoning. The main zones and parts in a CFRD are listed here:

- The *concrete face slab* is situated on the upstream side and serves as the impervious element. It consists of 0.25 – 0.6 m thick reinforced concrete (Fell et al., 2005).
- *Zone 1 – Impervious*: Consists of compacted soil, silt is preferable, which is impervious (Zone 1A). It will serve as a cover for the perimetric joints in the lower part of the face slab. It will thus seal potential cracks in the concrete face. Zone 1A can be supported by a less costly material (Zone 1B). CFRD's without Zone 1 have been successfully constructed, therefore it is not always necessary, but it is useful if problems develop. It is an economical matter but it is recommended to have this zone in high CFRD's.
- *Zone 2 – Filter/transition zone*: This layer is a filter and transition zone between the face slab and the rockfill. It consists of fine graded soil material, in the range from sand-sized particles to fines. It has two purposes; to make a stable and even surface for the face slab and a semi-impervious layer with a filtering function. Since the material is well-graded, it will prevent any large leaking.
- *Zone 3: – The main rockfill*: Zone 3A is a transition zone between Zone 2 and 3B and consists of finer rockfill. Zone 3B will transfer most of the water load into the foundation. It consists of well-compacted rockfill and need to have low compressibility. Large settlements of Zone 3B should be avoided because it can make the face slab deflect with cracks and leakage as a result. Zone 3C is not subjected to the same amount of load as Zone 3B. To save compaction and material costs, this zone can be allowed to have higher compressibility.

- *Zone T – Central zone:* This “dead zone” is situated between Zone 3B and 3C. To save costs, it can be constructed with poorer rockfill quality since the area is not subjected to large loads compared to the other zones. (Cruz et al., 2010).

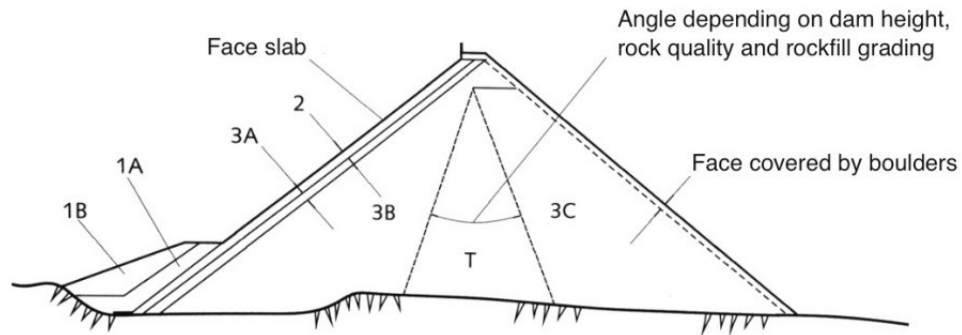


**Figure 2.1 Zoning of a modern CFRD(Cruz et al., 2010)**

## 2.2 Permeability and Seepage

*“In engineering practices, difficulties through soils are almost exclusively not due to soils themselves but to water contained in their voids. On a planet without any water there would have been no need for Soil Mechanics.”* (Karl Terzaghi, 1939)

So, it can be said that; no water no soil mechanics, water inhibit itself at different place in mysterious ways, harmful accumulation of water is a great concern, most of problems are due to uncontrolled seepage and consequences of uncontrolled seepage are disastrous.

These consequences can be understood by simple physical property called PERMEABILITY. Permeability is facility with which water flows through soil. Soil is permeable due to the existence of voids between soil grains that are interconnected and allow flow from points of higher potentials towards points of lower potentials (energy). While estimating seepage losses coefficient of permeability also known as hydraulic conductivity is used.

Coefficient of permeability signifies the capacity of water flowing through porous materials (Todd & Mays, 2005). Empirical approaches, laboratory experiments, and in-situ tests are normally used to obtain the saturated  $K$  value. To estimate the hydraulic conductivity empirically, many predictive equations were projected based on the particle size distribution, porosity and other properties of the soil, reviewed by

(Chapuis, 2012). In the laboratory, the saturated  $K$  values of granular soils can be determined with either a constant or falling head test in a rigid-wall or flexible-wall (triaxial cell) permeameter. The detailed specifications are included in ASTM standards ((ASTM D 2434), 2006; ASTM D5084, 2016). The pumping and field permeability tests are performed to evaluate the in-situ  $K$  values.

Knowledge of the in-situ  $K$  values of aquifers is critical for many hydrogeological, geotechnical, and environmental problems, such as seepage through dams and their foundations, infiltration from disposal fields, and monitoring groundwater contamination (Chapuis et al., 1990).

As mentioned, coefficient of Permeability of soil can be obtained both in laboratory and field but one must be fortunate enough to obtain the same result because sample in the permeameter is never in the same condition as that of site. Also, the flow through the stata in field is not same in the lab anymore. The ratio of horizontal to vertical conductivity in sand at field would be  $k_h / k_v \geq 3$  which can't be duplicated in the lab even after the sample is carefully compacted at desired void ratio. Boundary condition in the lab is never same also the clean walls of permeameter make water movement better than when it will be rough.. (Bowles, 1992)

Many of the reseraches shows that the Darcy's law is nonlinear at bigger value of hydraulic gradient  $i$ . Thus,

$$v = k i^n \quad \text{not} \quad v = k i$$

The air present on the laboratory sample has significant effect even for small air voids as the soil taken is less.

The hydraulic conductivity ( $k$ ) of soil can be defined as the approach velocity of permeant for flow through soil of unit area under a unit gradient. The permeability value depends on the nature of permeant and soil.

An equation reflecting the influence of the permeant and the soil was developed by (Taylor, 1948) using Poiseuille's law for laminar flow. The equation is given as:

$$k = D_s^2 \frac{\gamma}{\mu} \frac{e^3}{(1 + e)} C \quad (2.1)$$

The following is an expression for the permeability of porous media, known as the Kozeny-Carman equation since it was proposed by Kozeny and improved by Carman:

$$k = \frac{1}{k_o} \frac{\gamma}{S^2} \frac{e^3}{\mu (1 + e)} C \quad (2.2)$$

$k_o$  = factors depending on pore size and ratio of length of actual flow path to soil bed thickness,  $S$  = specific surface area

Since  $D_s$  is defined by the diameter of particle having surface  $S$ , on equation (2.2) can be considered as the simplification of Kozeny-Carman equation.

### 2.2.1 Viscosity of the pore fluid (usually water)

The more temperature lesser will be the viscosity of water and more will be the coefficient of permeability. For the standard 20° C has been set and the coefficient of permeability at other temperature is related by:

$$k_{20} = k_t \frac{v_t}{v_{20}} \quad (2.3)$$

where  $v_t$  and  $v_{20}$  are the viscosity of the water at recorded temperature and at 20° C respectively. The variation of  $(v_t/v_{20})$  with the test temperature  $T$  varying from 15 to 30°C is given in table below.

**Table 2.1: Variation of ratio with temperature**

Temperature, T°C	( $\eta_{T^\circ C}/\eta_{20^\circ C}$ )	Temperature, T°C	( $\eta_{T^\circ C}/\eta_{20^\circ C}$ )
15	1.135	23	0.931
16	1.106	24	0.910
17	1.077	25	0.889
18	1.051	26	0.869
19	1.025	27	0.850
20	1.000	28	0.832
21	0.976	29	0.814
22	0.953	30	0.797

### 2.2.2 The void ratio of the soil:

Many of the earlier studies tried to relate the hydraulic conductivity ( $k$ ) with void ratio ( $e$ ) and presented coefficient of permeability as a function of void ratio by relations such as:

$$k_2 = k_1 \left( \frac{e_2}{e_1} \right)^2 \quad (2.4)$$

$$k_2 = k_1 \frac{e_2^3(1 + e_1)}{e_1^3(1 + e_2)} \quad (2.5)$$

In both these equations (2.4) and (2.5) the hydraulic conductivity  $k_1$  is the value from laboratory test of soil for void ratio  $e_1$  and the hydraulic conductivity for void ratio  $e_2$  is required which will be  $k_2$ . Nowadays, determining coefficient of permeability at various void ratio and curve fitting to obtain relationship between  $e$  and  $k$  is recommended.

Further, the equation (2.1) designates that plot of  $k$  versus  $e^3/(1+e)$  should be straight line. Other theoretical equations have suggested that  $k$  versus  $e^2/(1+e)$  or  $k$  versus  $e^2$  should be straight line. There are considerable experimental data which shows that  $e$  versus  $\log k$  is frequently a straight line.

If the permeability of soil at void ratio 0.85 is known, then its value for another void ratio can be determined using the following equation given by Casagrande.

$$k = 1.4 k_{0.85} e^2 \quad (2.6)$$

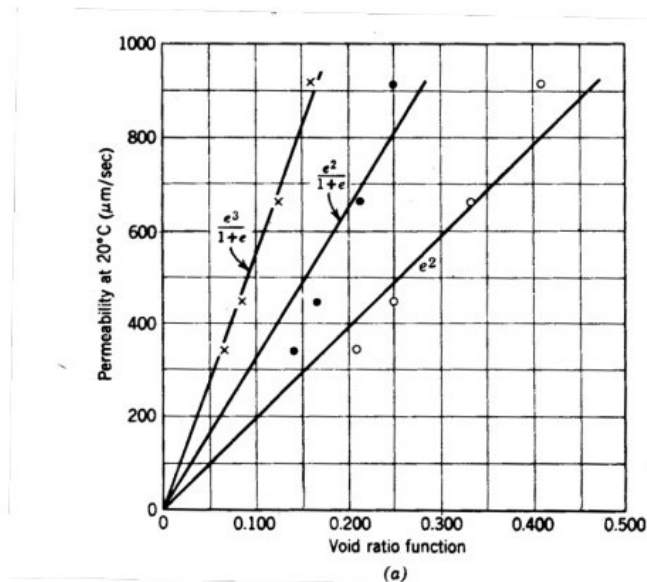


**Figure 2.2 Relation between void ratio  $e$  and  $k$  for variable head test (Lambe & Whitman, 1979)**



### 2.2.3 The size and shape of the soil particles:

If angular and platy particles are predominant over rounded and spherical coefficient of permeability would be less. A study on filter sands by Allan Hazen for use in water works filters performed (ca. 1890) and determined a relationship between coefficient of permeability and  $D_{10}$  which is specifically for clean sands and gravels:

$$k = 100 D_{10}^2 \quad (2.7)$$

Where  $k$  is in cm/s and  $D$  is in cm.

### 2.2.4 Saturation 'S':

The more the degree of saturation the more the value of hydraulic conductivity. This might be due to increase in surface tension partly and the remaining is an unknown quantity.

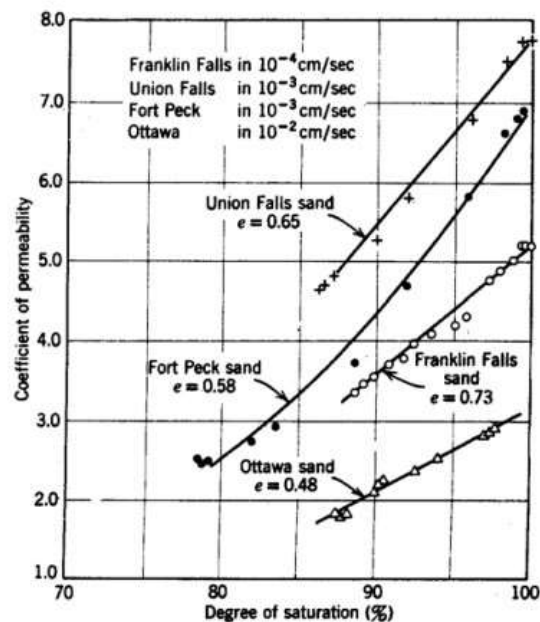


**Figure 2.3: Permeability versus degree of saturation for various sand. (From Wallace, 1948)**

Terzaghi and Peck in 1967 classified the soil permeability according to the coefficient of permeability as in table:

**Table 2.2: Classification of Soil Permeability**

Degree of permeability	values of k (cm/sec)
High	over $10^{-1}$
Medium	$10^{-1}$ to $10^{-3}$
Low	$10^{-3}$ to $10^{-5}$
Very low	$10^{-5}$ to $10^{-7}$
Practically impermeable	less than $10^{-7}$

The permeability test data result obtained from (Lambe & Whitman, 1979) literature is attached:

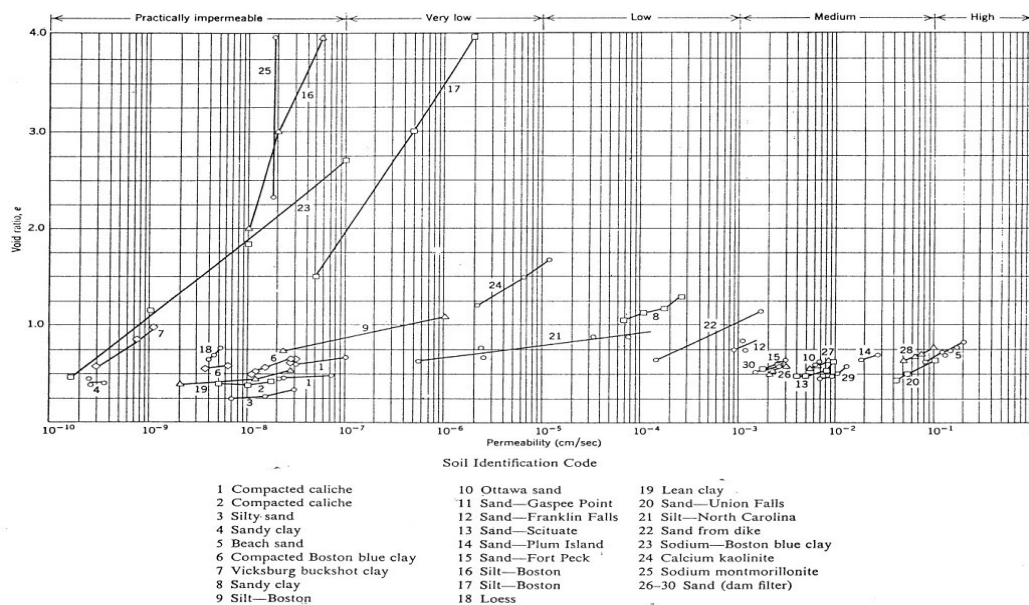


**Figure 2.4: Permeability test data from Literature (Lambe and Whitman Page 286)**

### 2.3 Laboratory test for hydraulic conductivity

In lab soil test for hydraulic conductivity is done either by variable head test or constant head test depending on the grain size. The samples that are to be tested can be both disturbed and undisturbed and further undisturbed sample of cohesionless soil is difficult to obtain so in laboratory sample is tried to reconstruct to the same density as in nature. That's why field tests are more preferred over laboratory test.

However in lab, knowing the height of the soil sample column  $L$ , the sample cross section  $A$ , and the constant pressure difference  $h$ , the volume of passing water  $Q$ , and

the time interval  $T$ , one can calculate the permeability on Constant head permeameter as:

$$k = \frac{Q \cdot L}{A \cdot h \cdot t} \quad (2.8)$$

## 2.4 Field Test

### 2.4.1 Lugeon Test

The most common and effective method of measuring rock mass permeability is the water pressure test (also known as the Lugeon or ‘packer’ test). The test consists of isolating a section of drill hole and pumping water under pressure into that section until the flow rate for any given pressure is constant (i.e., it is a constant head test). (Fell et al., 2005)

The purpose of the test is to obtain permeability of the rock. Results can be used either to assess the quantity of grouting material required to inject or to check the effectiveness of grouting or to predetermine the possible flow type along the drill hole section.

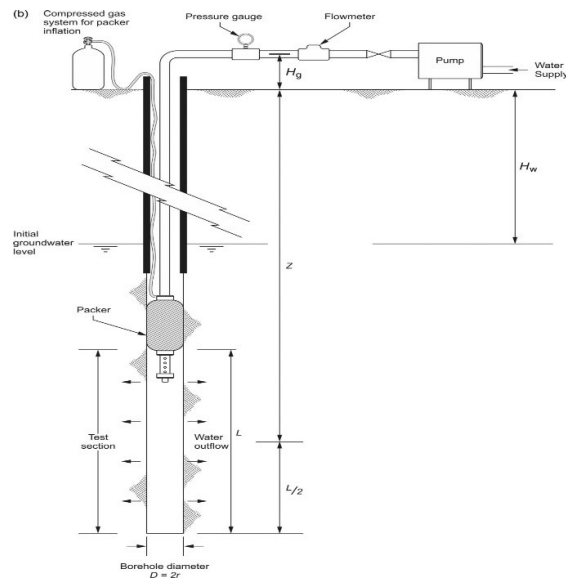


**Figure 2.5: Schematic Diagram of Lugeon test (Fell et al., 2005)**

Test method proposed by (Lugeon, 1933), 1 Lugeon is defined as the water amount pumped to the 1-meter length of test zone under 10 atm hydraulic pressure in 1 minute.

The pressure applying to the test zone is also specified by engineering judgement depending on the physical properties of rock but generally we practice pressure of 1, 2.5, 5, 2.5, 1 bar for comprehensive Lugeon test. Also (0.5, 1.5, 3, 1.5, 0.5) in top most.

Lugeon value ( $L_u$ ) is calculated by the equation (2.9) below:

$$L_u = \frac{Q * 10}{P * L} \quad (2.9)$$

In this expression,  $L_u$  is Lugeon value (lt/min/m),  $Q$  is water amount given to the rock formation (lt/min),  $P$  is hydraulic head applied to the test zone (kg/cm<sup>2</sup>) and  $L$  is test length (m). The permeability class corresponding to the Lugeon values is presented in table 2.4.

$P$  is calculated as:

$$P = P_0 + 0.1(H_1 + H_2) \quad (2.10)$$

where,  $P_0$  is Pressure at pressure gauge, kg/cm<sup>2</sup>

$H_1$  is hydrostatic heads in meter between the pressure gauge and the ground level ( $H_g$ ) in Figure 2.5.

$H_2$  is hydrostatic heads in meter between the ground level and the centre of test section or between the ground level and the water table whichever is smaller. ( $H_w$ ) in Figure 2.5.

The following table describes the conditions typically associated with different Lugeon values, as well as the typical precision for reporting these values (Camilo Quinones-Rozo & Andrew Yu, 2010).

Under homogeneous and isotropic condition 1 Lugeon is equivalent to a hydraulic conductivity  $1.3 \times 10^{-5}$  cm/s proposed by (Fell et al., 2005).

**Table 2.3: Situations of Rock mass with reference to Lugeon Values (Camilo Quinones-Rozo & Andrew Yu, 2010)**

<b>Lugeon Range (Lu)</b>	<b>Classification</b>	<b>Permeability value Range (m/sec)</b>	<b>Situations of Rock mass discontinuities</b>	<b>Precision (Lu Value)</b>
<1	Very Low	$< 1 \times 10^{-7}$	Very tight	<1
1-5	Low	$1 \times 10^{-7} - 6 \times 10^{-7}$	Tight	$\pm 0$
5-15	Moderate	$6 \times 10^{-7} - 2 \times 10^{-6}$	Few partly open	$\pm 1$
15-50	Medium	$2 \times 10^{-6} - 6 \times 10^{-6}$	Some open	$\pm 5$
50-100	High	$6 \times 10^{-6} - 1 \times 10^{-5}$	Many open	$\pm 10$
>100	Very High	$> 1 \times 10^{-5}$	Open closely spaced or voids	>100

Nowadays, Lugeon interpretation is derivative from the work of (Houlsby, 1978). He for the requirement on grouting proposed the typical hydraulic conductivity value based on the performance of Lugeon values computed for the different pressure values applied. He characterized the behaviors into five groups for practice.

-Laminar Flow: The permeability of the rock mass do not depends upon the water pressure applied. In the rock masses where seepage velocities are comparatively small and hydraulic conductivity would also be low.

-Turbulent Flow: The permeability in this pattern indicate the decrease in Lugeon value as the pressure applied increases. This is typical of rock masses exhibiting partly open to moderately wide cracks.

-Dilation: In this case Lugeon values increases as the pressure applied increases and later decrease when pressure applied would decrease. This performance – which is sometimes also observed at medium pressures – occurs when the water pressure applied is greater than the minimum principal stress of the rock mass, thus causing a temporary dilatancy (hydro-jacking) of the fissures within the rock mass.

-Wash-Out: Permeability value will increase as the test goes on whatever would be the pressure applied. This performance indicates that seepage induces permanent and irrecoverable damage on the rock mass, usually due to infillings wash out and/or permanent rock movements.

-Void Filling: Permeability value decreases as the test goes on whatever would be the pressure applied. This performance shows that either: (i) water progressively fills

isolated/non-persistent discontinuities, (ii) swelling occurs in the discontinuities, or (iii) fines flow slowly into the discontinuities building up a cake layer that clogs them.

Table 2.4 presents a graphic summary of the five behavior groups defined by (Houlsby, 1978), as well as the representative Lugeon value that should be reported for each group.

**Table 2.4: Lugeon Interpretation as their pattern**

BEHAVIOR	PRESSURE STAGES	LUGEON PATTERN	DESCRIPTION	REPRESENTATIVE LUGEON VALUE
LAMINAR			All Lugeon values about equal regardless of the water pressure	Average of Lugeon values for all stages
TURBULENT			Lugeon values decrease as the water pressures increase. The minimum Lugeon value is observed at the stage with the maximum water pressure (3 <sup>rd</sup> stage)	Lugeon value corresponding to the highest water pressure (3 <sup>rd</sup> stage)
DILATION			Lugeon values vary proportionally to the water pressures. The maximum Lugeon value is observed at the stage with the maximum water pressure	Lowest Lugeon value recorded, corresponding either to low or medium water pressures (1 <sup>st</sup> , 2 <sup>nd</sup> , 4 <sup>th</sup> , 5 <sup>th</sup> stage)
WASH-OUT			Lugeon values increase as the test proceeds. Discontinuities' infillings are progressively washed-out by the water	Highest Lugeon value recorded (5 <sup>th</sup> stage)
VOID FILLING			Lugeon values decrease as the test proceeds. Either non-persistent discontinuities are progressively being filled or swelling is taking place	Final Lugeon value (5 <sup>th</sup> stage)

### 2.4.2 Lefranc Test

The constant-head (CH) and variable-head (VH) tests in casing borehole were first projected by the French civil engineer (Lefranc, 1936, 1937), known as the Lefranc test. It is a reliable test method to obtain the local  $K$  value when the pumping test is not available for homogeneous and isotropic aquifers (Houti's course note), included in several textbooks (Cassan, 1980, 2005; Monnet, 2015) and the French, International and Canadian standards (AFNOR NF P94-132, 1992, 2000; CAN/BNQ 2501-135, 2014; ISO 22282-2, 2012). It was also used to assess the groutability of the soil ground (Bell, 2004; Cambefort, 1987) and the anisotropy coefficient of the aquifer (Cassan, 2000; Lafhaj & Shahrour, 2004).

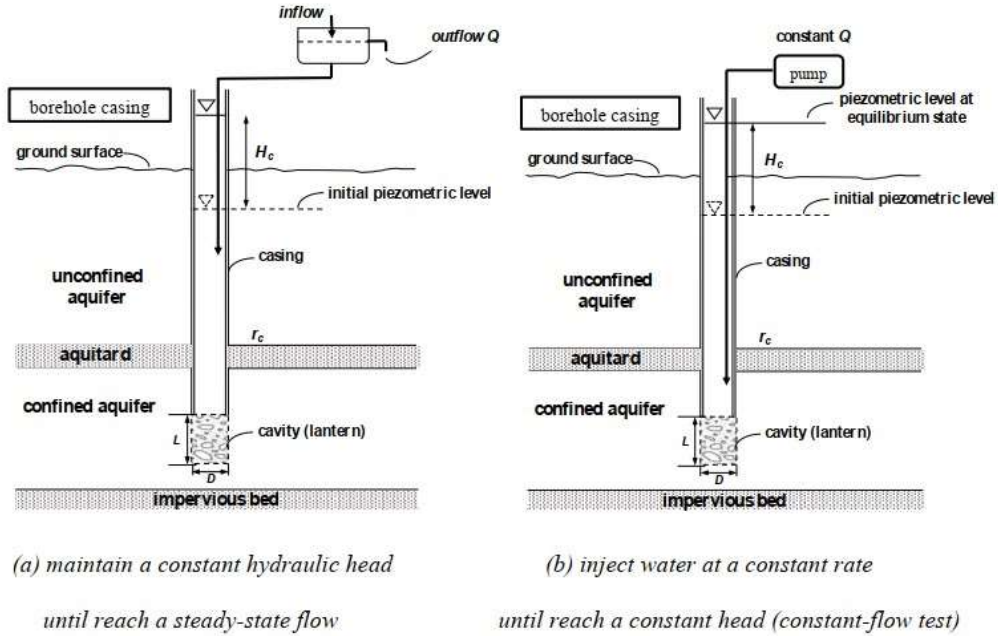


**Figure 2.6: Two ways to conduct Lefranc CH test**

The numerical shape factor of the water injection zone given by Constant Head tests, for either steady-state or transient analysis, can be calculated from the equation of (Lefranc, 1936, 1937):

$$c = \frac{Q}{k H_c} \quad (2.11)$$

where  $k$  is the hydraulic conductivity,  $Q$  is the constant flow rate through the screen, obtained from the numerical result, and  $H_c$  is the applied hydraulic head difference.

The formula for the theoretical shape factor were derived from the solutions of the Laplace equation, based on approximate shapes of the cylindrical injection zone, either a sphere of equal surface or an ellipsoid (Chapuis & Sabourin, 1989), in an infinite medium. The complete ellipsoid formula was given by (Dachler, 1936):

$$c = \frac{2\pi L}{\ln \left[ \frac{L}{D} + \sqrt{1 + \left( \frac{L}{D} \right)^2} \right]} \quad (2.12)$$

where  $L$  and  $D$  is the length and diameter of the water injection zone, respectively. It was simplified by (Hvorslev, 1951) as,

$$c = \frac{2\pi L}{\ln\left(\frac{2L}{D}\right)} \quad (2.13)$$

If  $L/D > 4$

The sphere formula is expressed as,

$$c = 2\pi D \sqrt{\frac{L}{D} + \frac{1}{4}} \quad (2.14)$$

if  $1 \leq L/D \leq 8$

## 2.5 Seepage in CFRD

Seepage in already completed CFRD in other countries were studied and significant amount of seepage has been found.

Some names of the dam studied are: Aguaamilpa, Alto Anchicaya, Bastyan, Brogo, Cethana, Chengbing, Crotty, Foz Do Areia, Golillas, Guanmenshan, Ita, Kangaroo Creek, Kotmale, Little Para, Mackintosh, Mangrove Creek, Muchinson, Salvajina, Scotts Peak, Segredo, Shiroro, Tianshengqia-1, Tullabardine, White spur, Winneke, Xingo, Cogswell, Courtright, Dix River, Lower Bear No. 1, Salt Springs, Strawberry and Wishon. Leakage rate of these Concrete face rockfill dams are found from (G. Hunter, 2003).

Height of these dams vary from 25m to 185.5m and Max Leakage Rate at first filling varies from 5 l/s to more than 3000l/s. which is reduced during operation.

## 2.6 Curtain Grout as Seepage Barrier

To reduce leakage through the dam foundation, seepage erosion potential, uplift pressures and settlements grout curtain can be introduced in the dam foundation.

Grout curtain are thin, vertical, cylindrical grout walls which act as a water barrier in a foundation. They are made directly into the soil/rock by injecting grout on certain pressure at closely spaced intervals. They are constructed in a certain defined spacing according to its design. Spacing is design in such a way that each column of grout



intersects the next. Then, there will be formation of a continuous wall or curtain (Weaver and Bruce, 2013).

(Lomabardi, 1985) studied about the cementation properties of grout and grout curtain designed for the impermeability of dams and underlined that the cohesion of the grout increases the viscosity and grout cannot penetrate into the discontinuities. (Nonveiller, 1989) studied about the different techniques for the construction of grout curtain.

There are many methods for the determination of grout curtain depth ( $h'$ ) (Bureau of Indian Standard, 1993 Equation (2.15); (Pettersen & Molin, 1999) Equation (2.16); (Ewert, 2003) Equation (2.17) ; (Şekercioğlu, 2007) Equation (2.19); (Schleiss & Pougatsch, 2011) Equation (2.18)) . This methods in which the grout curtain depth is a function of dam height ( $h$ ), are expressed in equation (2.15) (2.16) (2.17) (2.18) (2.19).

$$h' = \left(\frac{2}{3}\right) h + 8 \quad (2.15)$$

$$h' = \left(\frac{3}{4}\right) h \quad (2.16)$$

$$h' = h \quad (2.17)$$

$$h' = \left(\frac{2}{3}\right) h \quad (2.18)$$

$$h' = \left(\frac{1}{2}\right) h + 15 \quad (2.19)$$

A curtain grout of 15m depth is proposed for a head of 24m in Dhap Dam.

## 2.7 Numerical Modelling

The numerical model has a huge advantage over a physical model. The complex geometry with considerations of different parameters can be modelled. The critical parameters for modelling can be found out with ease in numerical modelling through trial. The numerical model of dam can solve complex physical model comparatively faster. The numerical modelling of dam and foundation material can be done by different numerical modelling technique. The value of deformation, pore pressure, vertical stress, strain and seepage can be found out. The different numerical modelling approach are: Finite Element Method and Finite Difference method.

### **2.7.1 Finite Element Technique**

Finite element analysis is a numerical method used to solve the engineering problems using array of mathematical techniques. The name comes from the fact that the methods subdivided the larger parts problem into smaller simpler parts called finite elements. In each element, there is a simplified relationship between loads and displacements. The equations that modelled these finite elements are solved and reassemble back into larger system of equation that modelled the entire problem. The continuity equations links all of the equations that are in all of the elements. When we linked up together, we end up in single matrix equation. A boundary conditions is applied that specifies what points are known to displacements and loads. Finally, in post-processing it returns to each element to interpolate local displacements and stresses. Finite element analysis can solve boundary value problems like stress analysis, heat transfer, fluid flow and electric or magnetic potential.

As discussed, seepage analysis is very important issues that must be considered. For this purpose, a finite element method through a computer program, Geo Studio through its sub-program named SEEP/W, was used to determine the surface seepage line, amount of seepage through the dam and its foundation.

### **2.7.2 Anisotropy**

The ratio of vertical to horizontal permeability ( $k_v/k_h$ ) represents the contrast in permeability between the vertical and horizontal planes within a formation (called anisotropic permeability). This ratio is important in reservoir simulation studies because it is applicable in vertical wells and more important in partially penetrated or horizontal wells. In layered reservoirs, the vertical permeability of each layer is quite different from surrounding layers (Shedid, 2019).

## CHAPTER THREE: RESEARCH METHODOLOGY

### 3.1 General

This chapter presents the research methodology adopted to meet the objectives. Different modes of data collection to achieve the result including laboratory test procedures and field investigations are discussed. Finally, the numerical modeling of dam under various scenarios using the field and laboratory test data are discussed.

### 3.2 Introduction

In order to conduct the seepage assessment of Dhap CFRD, various approaches have been adopted. A list of completed stages of works is summarized in schematic form and presented in Chart 3.1.

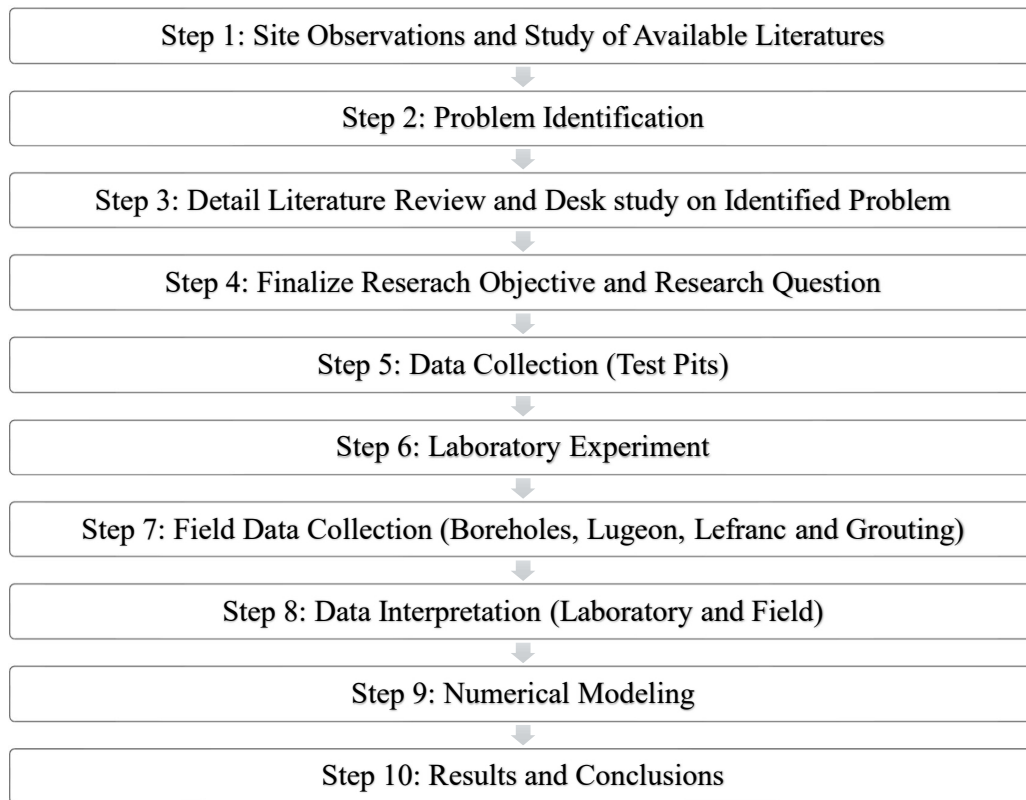


**Chart 3.1: Flow Chart of Research Methodology**

In order to achieve the main objective of seepage estimation through the foundation of dam, hydraulic conductivity function of the foundation materials is necessary. Though

the main objective is seepage estimation, the scope of the study is not only limited to calculating hydraulic conductivity but also geotechnical characterization of the foundation materials which forms the basis of the finite element numerical model of the dam.

First step towards the research is Geotechnical characterization of the foundation material encountered at shallow depth by the Laboratory test program and the second step is to identify the subsurface material offered by site investigations. Site investigation consisted of series of activities including drillings boreholes, Lugeon tests, Lefranc tests and grouting in the plinth area of the foundation of the dam. Each field activity presented in this study was supervised by the researchers to gain insight into the geological characteristics of the foundation and collect relevant data required for the subsequent numerical modeling.

### **3.3 Sample Collection Program (Test Pits Sample)**

To meet the supporting objective of geotechnical characterization of foundation soil of dam, a total of 10 test pits were selected along the cross-section of the dam at about 20 m above the upstream toe of the embankment dam. In each location test pit was dug using pick and shovel and backhoe was also used in some locations found to be feasible to dig. Representative soil samples were collected from the two locations along each excavated pit to undertake index properties and permeability tests.

In addition, bulk samples were collected from 3 test pits to undertake the maximum dry density test. Before extracting the bulk sample, field density testing was also conducted calculated using Sand replacement method. Samples were collected in sample bags preserving natural moisture content. Proper labeling was completed and photographs of the collected samples were recorded. All the samples were packed in a large bag and were transported to IOE, Pulchowk Campus for laboratory tests. The coordinate and description of the sample collections and photographs are presented in Appendix A. All the samples received in Central Material Testing Laboratory (CMTL), Pulchowk campus were stored in the dry shade with proper labeling.

### **3.4 Laboratory Program**

#### **3.4.1 Index Property**

**Moisture Content:** An oven-drying method was used to determine the moisture contents of the samples. For the oven-drying method, small, representative specimens obtained from large bulk samples were weighed as received, then oven-dried at 105 degree celsius for 24 hours. The sample was then reweighed, and the difference in weight was assumed to be the weight of the water driven off during drying. The difference in weight was divided by the weight of the dry soil, giving the water content on a dry weight basis.

**Particle Size Distribution:** More than 1000 gm of soil of each sample were oven-dried and softly hammered followed by sieved through a series of standard sieve numbers and % passing was determined. Grain size distribution curves were plotted for those soils. The soil material is sieved through 4.75mm, 3.35mm, 2.36mm, 1.7mm, 1.18mm, 0.6mm, 0.3mm, 0.15mm, 0.075mm. For particle size, less than 75-micron hydrometer analyses have been performed on this soil. For hydrometer analyses, approximately 50 grams of dry soil passing 75 microns was treated with a dispersing agent Sodium hexametaphosphate for 72 hours. Then hydrometer analyses were performed to measure the amount of silt and clay size particles. After that combined grain size distribution curves are plotted for these soils.

**Atterberg Limit:** Representative samples were subjected to Atterberg limits testing to determine the plasticity of the soils. A Casagrande apparatus was used to determine the liquid limit of sample passing a 425 micrometer (No. 40) sieve following (ASTM D 4318). The plastic limit of the soil was not able to undertake because of non-plastic nature of soil

**Specific Gravity:** Specific gravity is the ratio of the mass of a unit volume of soil at a stated temperature to the mass of the same volume of de-aired or distilled water at a stated temperature of 25° C. The specific gravity of soil samples was determined using ASTM D 854. For this test, a volumetric flask and sand bath were used to remove air from the sample.

**Soil Classification:** Soil samples were classified using the Unified Soil Classification System (USCS). Using the particle size distribution and the Atterberg limits, the USCS designates two-letter symbols and a group name for each soil.

### **3.4.2 Maximum Dry Density:**

The soil sample was softly crumbled and sieve analysis was conducted. The sieved sample was then subjected to Standard Proctor Test as per ASTM 698-78. Maximum dry density and optimum moisture content are obtained from the standard proctor test. The maximum dry density and optimum moisture content values produced from standard proctor test were used to prepare sample for permeability test and will be discussed in following section.

### **3.4.3 Constant Head Test**

The hydraulic conductivity or permeability test was conducted using the constant head test as the soil sample contains less than 2 percent fines and is granular soil.

In the Constant head test, a reservoir with an overflow weir was adopted which is connected to water intake and a sample is kept in permeameter following (ASTM: D 2434 – 68, 2000) and AASHTO T 215-70 standards and Bowles, 1992 testing procedure.

A permeameter used in this study is the standard compaction mold consisting of a special cover and base plate presented in Figure 3.1. The base contains a porous stone, and the cover takes a valve for joining the inflow tube and a petcock for de-aeration. Rubber gaskets were for covering the mold to the base and to the cap.

This arrangement is capable of compacting soil at any density (as for a dam core or the clay liner of a landfill) and then placing the mold of the permeability base and swapping the collar with the special cap piece.

The permeameter used in this study is associated with some limitations. The one is for sand, there can be a large head loss across the 12 mm porous stone in the base. Also, there is no facility for the diffusion of the inflow across the sample area. And, with a down-flow and no potential for sample observation, it is difficult to get all the air out of the sample during saturation phase of the test. The third shortcoming was reduced to some extent by submerging sample assembly in a basin of water (after putting an exit

tube on the inflow valve) so water flows in the sample from the bottom to top and hence enhanced saturation process.

For the test of hydraulic conductivity de-aired water is required. The use of de-aired water have advantage, since the influence of air bubbles coming out sample tends to speed up the saturation process. Moreover, using distilled water in a constant head test speed up the saturation process and the test quality.

There are two methods to reduce the dissolved air-problem. One is to use warmer than the sample so that water cools as it infiltrates through the sample; this shall attract air from the sample into the solution. The other is to use a large enough gradient  $h/L$  that the pressure holds or forces the free air into the solution.

A permeameter mold used in the lab was of diameter 10 cm and length 12.7 cm making a volume of 1000 cc. In this mold, sample can be compacted in desired density such as the soil is placed loosely then putting it with some shaking and also with significant energy. Oven-dried samples were taken and test samples were prepared with varying compacting efforts for varying void ratios and densities. The permeameter with the sample was weighed and a void ratio was calculated in each test.

A filter paper is placed on upper end of sample in the vessel; then the rim of the mold is carefully cleaned and a rubber gasket is placed on the rim and then the cover is firmly seated. The cover has a see-through piece of plastic tubing about 150 mm long connected to the inlet valve over which the water inlet tube can be skidded. A 150 to 200 mm length of rubber tubing to the outlet pipe is attached.

The permeameter is placed on a container or sink in which the water level is about 50 mm above the cover. The valve of outlet tube is kept open so that water can flow through the sample thus removing entrapped air and facilitate the saturation process. After the water level in the plastic tube on top of the mold become same to the water level in the sink then a process of saturation is assumed to be completed

After the water level stabilized in the inlet tube, a hose clamp is taken and clamped to the exit hose. The permeameter is removed from the sink and the inlet tube is attached to a rubber hose from the constant-head standpipe. The air from the tubing is removed at the top of the soil sample by opening the petcock in the mold cover. Then the clamp from the hose is removed slowly so water can drop into the sample and any entrapped

air under the cover or in the entry line is flushed out through the petcock. Then the hydraulic head across the sample was measured.

As the sample has completely saturated the flow-through will be laminar. A 500 ml glass jar is taken and water flow from the outlet pipe is recorded every 5 minutes. If the volume of collected water came within 10% for two consecutive 5 minutes, then data is recorded and the subsequent coefficient of permeability is calculated. Later on, temperature correction at 25°C was also be applied in the recorded permeability value.

Using the Specific Gravity ( $G$ ) obtained earlier, the void ratio for each density is calculated using equation (3.1). A curve is plotted  $k_{20}$  versus  $e$  and the equation is fitted through the curve and the value of the coefficient of permeability is obtained at the required void ratio or required density.

$$e = \frac{G \gamma_w}{\gamma} - 1 \quad (3.1)$$



**Figure 3.1 Constant Head Permeameter and Constant Head permeameter placed in sink**

Limitations faced while conducting laboratory test:

1. The de-aired water couldn't be used; instead tap water was directly used in the test.
2. The permeability characteristics of undisturbed soil sample couldn't be determined as the sample collected was disturbed.
3. While compacting on maximum dry density or field density water flow blocked on permeameter and discharge was not observed.



#### **3.4.4 Free Swell Index Test**

Free swell or differential free swell is the increase in volume of soil without any external restraint while submerging in water. Free swell index test was conducted following IS: 2720-1977 . For this test two graduated glass cylinder of 100ml capacity and 10g each of pulverized oven-dried soil passing through 425 micron IS sieve was taken. 100ml of distilled water was poured on one glass cylinder and 100ml of kerosene oil on another cylinder and 10g sample was poured in each. The suspension was allowed to attain the state of equilibrium for not less than 24 hrs. Final volume of soil in each of the cylinder was read.

#### **3.4.5 XRD**

Although the samples were classified as well graded to poorly graded sand, medium swell behavior was noticed, perhaps because of existence of clay mineralogy. Also, it was impractical to conduct hydraulic conductivity test at minimum void ratios. Thus, to study its unusual behavior sample was sent to the research center to identify the mineral contents.

There the sample was subjected to X-ray diffraction test and a plot of count vs. 2 theta was received. The mineral contents further can be identified using X'Pert High score software.

### **3.5 Site Investigation Program**

Dhap dam is nearly at the end of the construction phase and an additional site investigation was underway by BRBIP during the course of this study. In order to conduct a seepage assessment core drillings producing underground geological profiles and corresponding field tests are essential. So, data for this thesis was primarily collected by the direct supervision of the BRBIP ongoing geotechnical investigation program including drillings, Lugeon test, Lefranc test and grouting. Thus, necessary data collected during the BRBIP site investigation program was used in this research to achieve the objective of this study.

#### **3.5.1 Rock Coring and Drilling**

A series of rock coring was conducted already more than three years ago along the foundation of the dam. A set of drilling and coring was conducted during the feasibility study and another set after commencement of dam construction. As earlier drill holes

were far from the dam axis and plinth, the interpretation of foundation conditions based on available geotechnical investigation data was difficult. Thus, a series of drilling boreholes supervised during the site investigation program was used to produce the subsurface profile of the dam foundation.

A series of boreholes naming MP01, MP03, MP05, MP07, MP09, MP15, MP17, MP19, MP21, MP25 and MP27 were directly supervised and their field test values were recorded. These boreholes are ranging from 25 to 35 m depth and are drilled with rotary drilling machine (Core drilling Rig XUL-100). The core drilling was supervised by following the ASTM D2113-1989 R93 (E1) (Standard Practice for Rock Core Drilling and Sampling of Rock for site exploration) standard. Details of borehole logs, photographs and field test results are included in Appendix B C and D.

To classify the degree of permeability of subsurface material, two types of in-situ tests were carried out depending on the material encountered along the depth of the drill hole. The constant head permeability test (Lefranc test) was performed along with the thickness of colluvium material with the advancement of drilling work simultaneously whereas the water pressure test (Lugeon) was performed along the bedrock section of the drill hole. These in-situ permeability tests establish permeability, porosity, and tightness of different types of material encountered during the drilling operation.

### **3.6 Geological Model**

Based on the core drilling and core logs a representative geological model was prepared. In addition, a longitudinal profile showing Lugeon value was prepared along the axis of dam. A plot of Rock Quality Designation (RQD) and Core recovery ratio along with depth was also analyzed to characterize the strength of rock encountered. Lugeon pattern that includes Laminar, Turbulent, Dilation, Void Filling and Washout are studied to carry out the nature of rock opening referring to Houlsby, 1976.

A typical borehole log, core recovery and RQD and Lugeon profile for borehole MP15 is shown in Figure 3.2. Detailed geological model for the foundation of the dam is discussed in chapter 4.

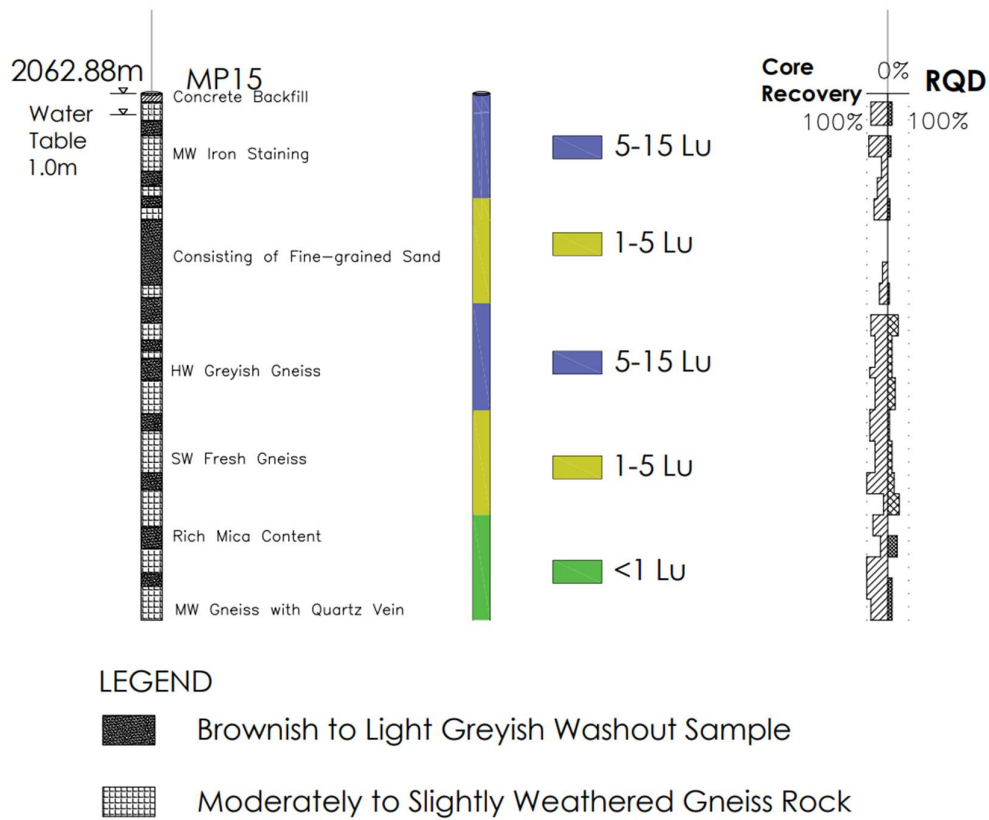


**Figure 3.2 Geological Profile along the hole MP15 (Ref. Section 4.4)**

### 3.7 Grout Curtain

To ensure a competent seepage barrier in rock foundation as well to improve the properties of plinth foundation both curtain and consolidation grouting was conducted along the plinth of approximately 203 m long section on the upstream of Dhap dam. Curtain grout of 15 m depth, proposed specially for seepage barrier, was being implemented during the course of research.

Regular monitoring during the operation will help to understand the seepage behavior rock under the dam foundation. In order to evaluate the effect of grouting on seepage it would be beneficial to involve in design and construction of grouting as well as monitor seepage post-construction. So, some of the curtain grouting undertaken in the upstream plinth regions of the dam are observed during this research. A stable grout mix after the trial grouting was adopted and planned to analyze the water consumption in water test and consumption of grout in same hole. The curtain grouting was conducted with the aim of achieving a tight grout curtain with permeability not exceeding 3 Lugeons which corresponds to hydraulic conductivity of  $3.9 \times 10^{-7}$  m/sec (Fell et al., 2005). Initially

only the primary holes are drilled and grouted which are spacing at 8m, then secondary holes at the center of primary holes such that holes are equidistant (i.e. at 4m spacing) and the tertiary holes in between secondary holes so that all the holes are at equidistant at a spacing of 2m each. This way a curtain of grouting was established to prevent seepage through the foundation of dam.

The design mix as finalized during the trial grouting was comprised of water cement ratio by 0.6 (by weight), Bentonite 0.5% by water, Admixture (Kunal Plast) 0.2% by cement. And as a quality control the standard specifications by ASTM for bleeding, consistency, specific gravity and mud balance test were conducted on site. Furthermore, according to geological parameters of site a GIN intensity of 1500 is foreseen with two limitation pressures i.e., 10 bars for top stage and 15 bars for bottom stage.

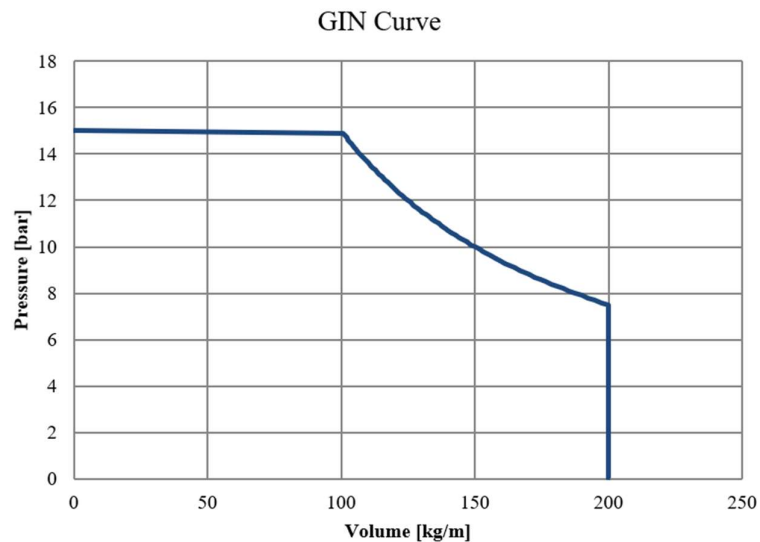


**Figure 3.3: Typical curve of 1500 GIN intensity with 15bar Pmax**

### 3.8 Numerical Analysis

To estimate seepage through the dam, two-dimensional seepage analyses were carried out using the finite element method (FEM) which is a mathematical method that was developed to find numerical solutions to complicated differential equations. Using FEM complex geometrics and boundary conditions can be described easily. The finite element theory is dividing the continuum, representing the geometry of the model, into smaller volume elements. Quadrilateral and triangular elements were used for the two-dimensional analyses which are linked with nodes, called node points.

The numerical analysis conducted in this research employed Seep/W software developed by Geo-Slope international. At first using the draw function, a geometry was established representing the cross-section of the dam. The KeyIn function allowed to manually enter points along a cross-section and also to define region and material property of the various zones. Suitable axes; distance on X-axis and elevation on Y-axis were drawn to confine the model inside the axes. While defining the foundation materials as well as corresponding depth of material in model borehole logs were utilized from the field test as mentioned in section 3.5. The hydraulic conductivity of the colluvium material encountered at shallow depth is assigned using laboratory test results and that for highly weathered to moderately weathered gneiss rock was adopted from Lugeon test result.

Volumetric water content function of the materials was defined using sample function and corresponding saturated water content, coefficient of volume compressibility of the various zones is referred from standard. Likewise, Hydraulic conductivity function was estimated using Fredlund and Xing method and the value was adopted as mentioned above for individual materials. Three types of material model Saturated only, Saturated/Unsaturated and Interface were defined based on zone. Saturated only was defined for a material which will remain saturated for the entire domain of the simulation. Saturated/Unsaturated model was defined where unsaturated zones are expected to occur. Grouting was modelled by adopting interface type material which is considered relatively impermeable compared to existing foundation material. It should be noted that the steady state analysis was conducted for all analysis throughout the research.

The important step here in the numerical modeling was to assign boundary conditions. For this research, boundary conditions can only be one of two fundamental options i.e., to specify H (head) or Q (total flux). Head boundary condition was used where water present within the domain as reservoir in the upstream side of the dam. A Potential seepage face was defined along the downstream slope around the toe region of the dam where both the head and total flux are unknown. The total water head of dam adopted was 2087.19 m which corresponds to the designed operational water level in the dam.

Knowing the flow rate through a dam is main agenda of this thesis and Seep/w provided a feature that one can easily calculate flow rates through a section by drawing a flux

section across any plane of interest. A flux section was drawn on the downstream seepage face at which seepage can be measured automatically along the flux section. The measured seepage gives the seepage quantity per m length of the dam section.

Further, for each material the anisotropy ratio at initial condition was defined as 1 and later its effect was realized by varying this value to 0.5 and 0.1 which is discussed in Chapter 4. Moreover, a sensitivity analyses was conducted by varying the hydraulic conductivity value of foundation material by  $\pm 10\%$  to understand the uncertainty of the in-situ test results on Lugeon and Lefranc tests and corresponding seepage through the dam.

## CHAPTER FOUR: RESULTS AND DISCUSSIONS

### 4.1 General

This chapter presents the discussion on the test results obtained from laboratory tests and data collection during the site investigation. Geological model produced from the field investigation is presented and discussed. At the end of the chapter numerical models and sensitivity analyses is conducted to estimate the seepage behavior of the Dhap dam are discussed.

### 4.2 In-situ Test Results

To carry out the permeability behavior of shallow depth colluvium material a sample collection program was organized as a part of the research to find its index properties as well as permeability behavior. The location of sample collected for the laboratory testing is included in Appendix A. During sample collection, a total of 3 field density testing was conducted by following the sand replacement method in some of the test pits and test results are presented in Table 4.1.

**Table 4.1 Field density (Sand Replacement Method) Test Result**

Description	Sample 1	Sample 10	Sample 9
Mass of Soil (M) (kg)	3.71	3.66	3.27
Mass of Cylinder and Sand ( $M_1$ ) (kg)	15	15	15
Mass of Sand in Cone ( $M_2$ ) (kg)	1.0	1.0	1.0
Mass of Cylinder and Sand after replacement ( $M_4$ ) (kg)	11.17	11.04	11.17
Mass of Sand in Hole ( $M_s$ ) (kg)	2.82	2.96	2.83
Density of Sand ( $\text{kg/m}^3$ )	1480	1480	1480
Volume of Sand ( $V_s$ ) ( $\text{cm}^3$ )	1908.11	1997.30	1908.78
Density of Sample ( $M_s/V_s$ ) ( $\text{kg/m}^3$ )	1945.38	1833.48	1713.13
Unit Weight ( $\text{kN/m}^3$ )	19.08	17.98	16.80

From the field density test presented in Table 4.1, it can be observed that the field density of the sample varies from  $16.8 \text{ kN/m}^3$  to  $19.08 \text{ kN/m}^3$ .

### 4.3 Laboratory Test Results

A series of tests including particle size distribution, liquid limit, plastic limit, maximum dry density and constant head permeability were conducted following standard testing procedures. Index properties test results are presented in Table 4.2.

**Table 4.2 Soil Classification of Collected Samples**

Soil Sample	Cu	Cc	USCS classification	NMC (%)	Liquid Limit (%)	Specific Gravity
Sample 1	4.72	0.85	SP	10.4	37	2.57
Sample 2T	2.73	4.85	SP	10.1		
Sample 2B	8.33	0.96	SW	9.2		
Sample 3	4.75	1.89	SP		31	
Sample 4	13.89	0.94	SW	7.2		
Sample 6	7.33	0.55	SW			
Sample 7	13.89	0.94	SW	10.1		
Sample 8T	12.72	0.68	SW			
Sample 8B	9	0.83	SW			
Sample 9T	7.37	1.4	SW	17.9		
Sample 9B	5.61	1.11	SP	10.8		
Sample 10T	6.11	1.26	SW			
Sample 10B	4.17	0.67	SP		32	
Sample 1Re	3.53	0.61	SP			
Sample 3Re	6.36	0.95	SW			
Slope	5.28	1.46	SP			

It can be observed in Table 4.2 that the value of the coefficient of uniformity varies from 2.73 to 13.89 and the coefficient of curvature varies from 0.55 to 4.85. Based on Unified Soil Classification System (USCS), soil is classified as Poorly Graded Sand (SP) to Well Graded Sand (SW). The natural moisture content of the sample varies from 7.2% to 17.9%.

It should be noted that the moisture content of the samples was tested in the Pulchowk Campus laboratory during the campaign of index properties testing. The liquid limit of the sample varies from 31% to 37%. Plastic limit tests were unable to undertake and are likely to be the presence of non-plastic silt in the sample. The specific gravity of a sample was found to be 2.51.

#### **4.3.1 Particle Size Distribution**

Particle size distribution tests and hydrometer tests results presented in Figure 4.1.



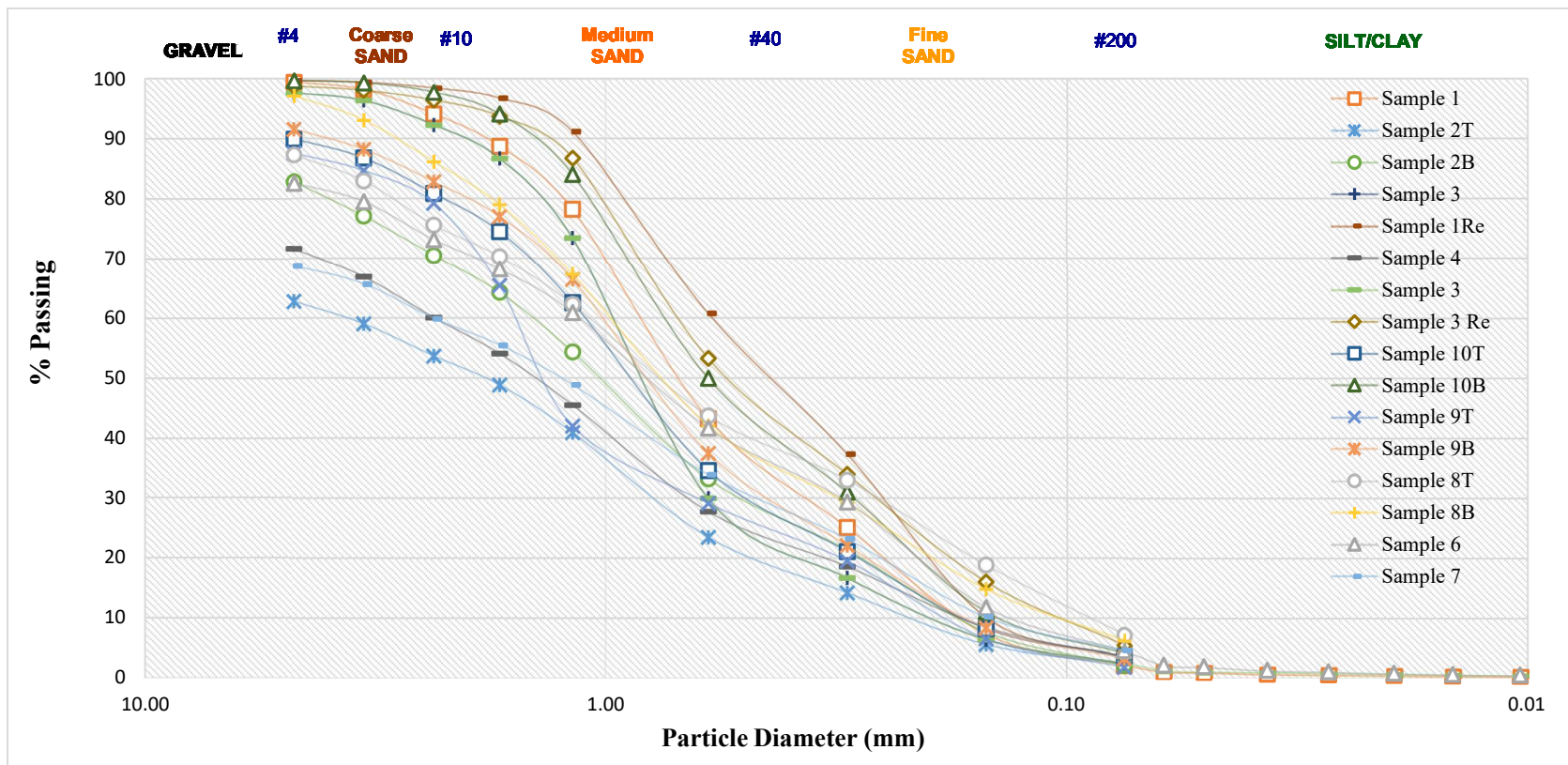


Figure 4.1: Grain Size Distribution Curve of Samples

### 4.3.2 Compaction Test Result

Compaction test result obtained from standard proctor test in the laboratory is presented in Table 4.3 and the dry density versus moisture content plot is shown in Figure 4.2.

**Table 4.3: Compaction test data from laboratory**

Sample No.	Maximum Dry Density (kN/m <sup>3</sup> )	Optimum Moisture Content (%)	Normal Moisture Content (%)
Sample 1	17.07	15.16	10.35
Sample 10	16.91	17	9.42
Sample 3	16.60	16.5	9.80

From the test result, the maximum dry density (MDD) of sample varied from 16.6 kN/m<sup>3</sup> to 17.07 kN/m<sup>3</sup> and optimum moisture content is found to be ranging from 15.16% to 17%.

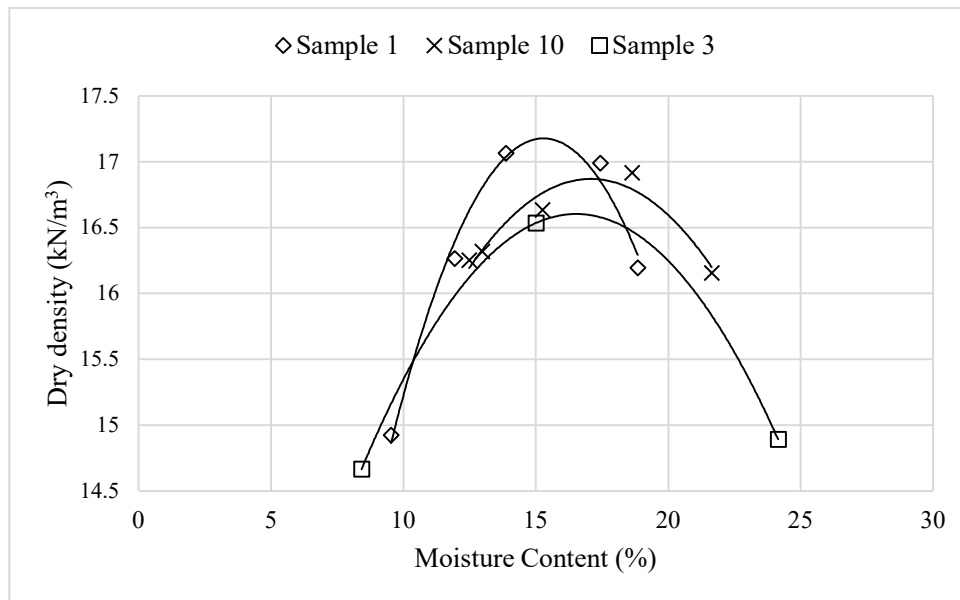


**Figure 4.2 Compaction test Result**

### 4.3.3 Permeability Test Results

Permeability test of sample 1 and sample 10 are conducted by varying void ratio of the sample in permeameter mold in lab. Field permeability test of same sample is also conducted which is discussed in the section 4.4. The permeability test results for

samples 1 and 10 are presented in Tables 4.4 and 4.5 respectively. All other samples are subjected to permeability test at a certain void ratio and their respective permeability after temperature correction are presented in Table 4.6.

**Table 4.4: Permeability Test Result of Sample No. 1**

Sample No. 1:

S.N.	Void Ratio (e)	Permeability k <sub>20</sub> (cm/s)	$\frac{e^2}{(1+e)}$	$\frac{e^3}{(1+e)}$
1	1.341	1.16E-03	0.768	1.030
2	1.146	7.83E-04	0.612	0.702
3	0.901	4.25E-04	0.427	0.385
4	0.801	3.21E-04	0.356	0.285
5	0.544	1.82E-04	0.192	0.104

**Table 4.5: Permeability Test Result of Sample No. 10**

Sample No. 10:

S.N.	Void Ratio (e)	Permeability k <sub>20</sub> (cm/s)
1	0.981	3.77E-04
2	0.840	2.75E-04
3	0.729	2.36E-04

**Table 4.6 Summary of Permeability Test of samples**

Sample No.	Initial Void Ratio	Final Void Ratio	Permeability (k) (cm/s)	k <sub>20</sub> (cm/s)	k <sub>20</sub> (@e=0.4)
Sample 2B	0.708	0.853	7.26E-04	7.82E-04	1.72E-04
Sample 2T	0.776	0.903	1.10E-03	1.18E-03	2.06E-04
Sample 3	0.708	0.829	1.53E-04	1.65E-04	3.63E-05
Sample 4	0.708	0.666	4.70E-04	5.06E-04	1.11E-04
Sample 6	0.610	0.771	2.37E-04	2.55E-04	8.29E-05
Sample 7	0.708	0.918	6.12E-04	6.59E-04	1.45E-04
Sample 8B	0.783	0.781	5.00E-04	5.39E-04	9.16E-05
Sample 8T	0.907	0.556	1.25E-04	1.35E-04	1.57E-05
Sample 9B	0.708	0.812	2.78E-04	2.99E-04	6.60E-05
Sample 9T	0.840	0.781	1.35E-04	1.45E-04	2.07E-05

Best fitted curve of permeability versus the void ratio was obtained on the logarithmic chart as shown in Figure 4.3.

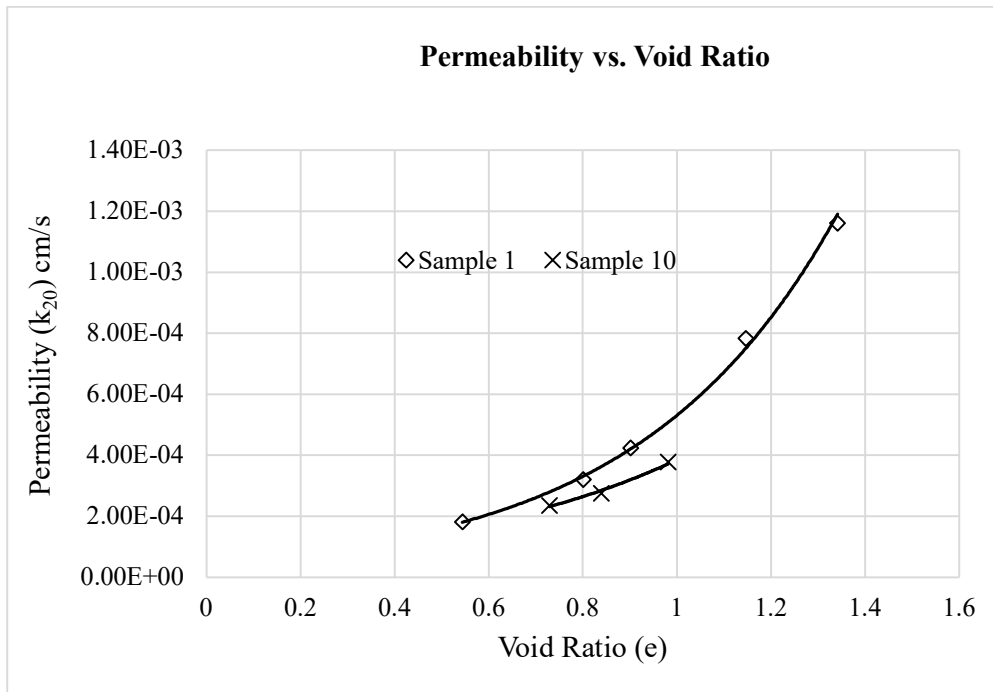


**Figure 4.3: Plot of Permeability vs. Void ratio of Samples**

For field density of 19.08 kN/m<sup>3</sup> of sample 1, the corresponding void ratio would be 0.36 using equation 3.1. From Figure 4.3 it can be extrapolated that the permeability value at field condition would be 1.17 x 10<sup>-4</sup> cm/s.

Likewise, for field density of 17.98 kN/m<sup>3</sup> of sample 10, the corresponding void ratio would be 0.4 using equation 3.1. From Figure 4.3 it can be extrapolated that the permeability value at field condition would be 1.28 x 10<sup>-4</sup> cm/s.

Furthermore, a graph is plotted between k versus  $e^3/(1+e)$  using Taylor and Kozeny-Carman equations 3.2 and 3.3 and is found to be linear as shown in Figure 4.4.

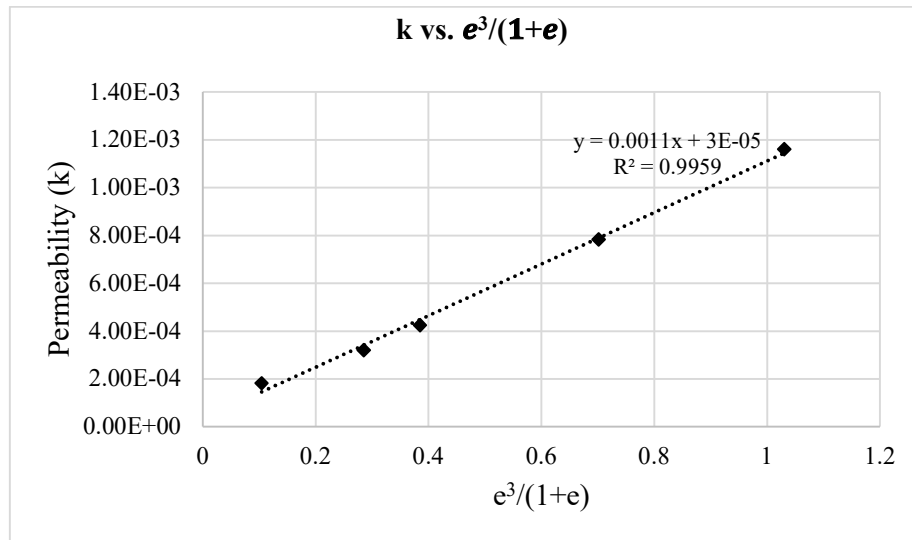


**Figure 4.4 Plot of k vs.  $e^3/(1+e)$**

A summary of test results including the percentage of gravel, sand and fines, and a ratio of permeability to the effective grain size are presented in Table 4.7. Test results for samples 1 and 10 are fitted on the Lambe and Whiteman chart (Lambe and Whitman, 1979, Pg. 286) as shown in Figure 4.5 and found that the samples are categorized as low permeable sample.

**Table 4.7: Permeability in correlation with Grain size distribution**

S.N.	Sample No.	% Gravel	% Sand	% Fines	D <sub>10</sub> (cm)	k <sub>20</sub> (cm/s)	k <sub>20</sub> /d <sub>10</sub> <sup>2</sup> (constant)
1	1	0.57	97.26	2.17	0.018	1.17E-04	0.361
2	2B	17.20	80.6	2.19	0.018	1.72E-04	0.531
3	2T	37.22	60.35	2.42	0.022	2.06E-04	0.426
4	3	2.38	95.13	2.49	0.020	3.63E-05	0.091
5	4	28.40	68.08	3.51	0.018	1.11E-04	0.344
6	6	17.42	78.08	4.49	0.015	8.29E-05	0.368
7	7	31.26	64.21	4.53	0.018	1.45E-04	0.448
8	8B	2.86	90.9	6.23	0.011	9.16E-05	0.757
9	8T	12.73	80.08	7.18	0.009	1.57E-05	0.194
10	9B	8.46	88.18	3.35	0.018	6.60E-05	0.204
11	9T	12.45	85.68	1.9	0.019	2.07E-05	0.057
12	10B	0.31	95.59	4.09	0.018	1.28E-04	0.395
13	10T	10.06	86.25	3.68	0.018	1.28E-04	0.395

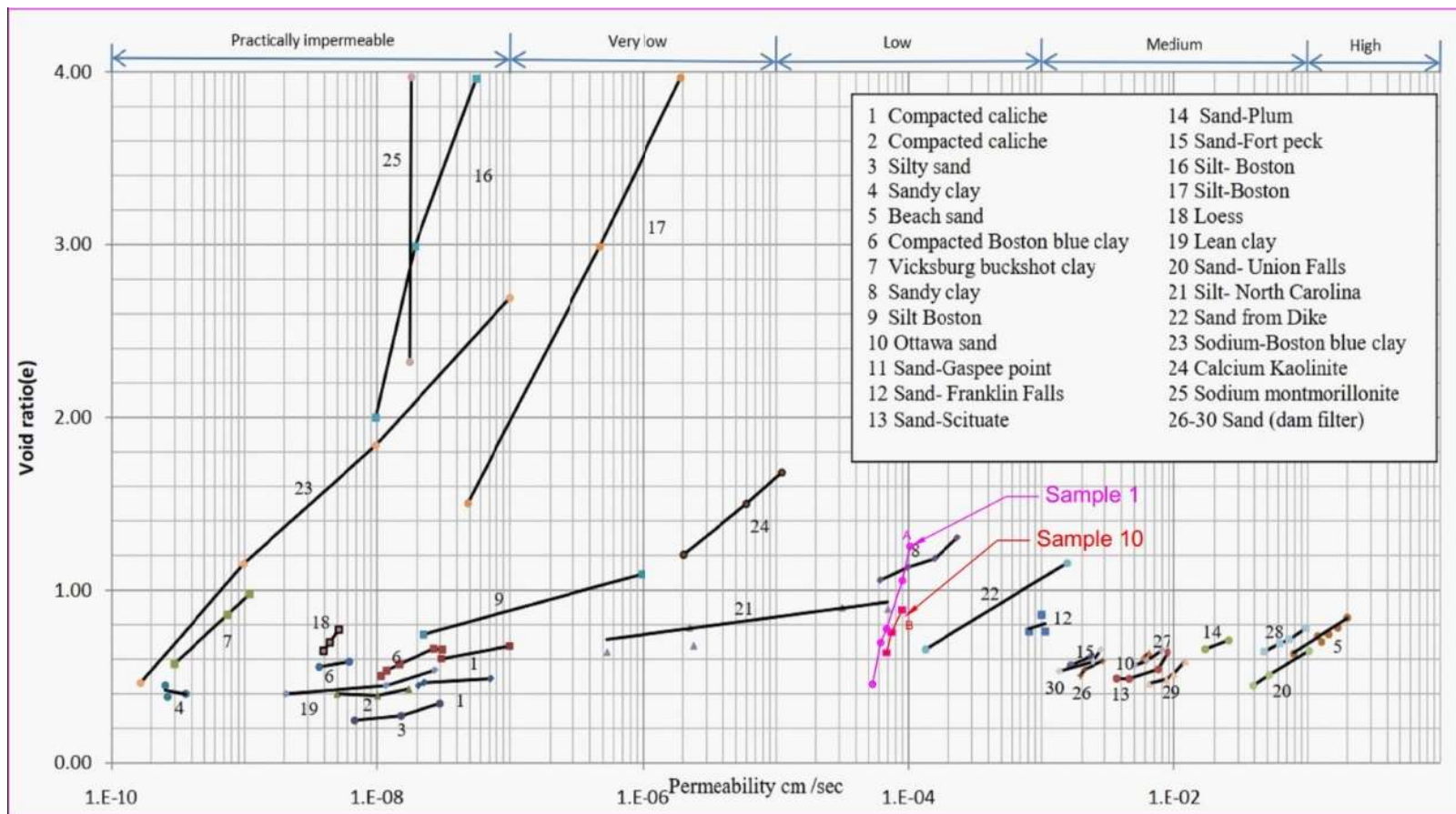


Figure 4.5 Plot of Permeability values of Sample 1 and 10 in plot digitizer of Lambe and Whitman chart

### 4.3.4 XRD

A X-Ray Diffraction test was conducted from the Nepal Academy of Science and Technology laboratory. The XRD test result is shown in Figure 4.6. The observation of the XRD test results indicates that there is the dominance of Polyolithionite and the presence of Tetramethylammonium pentaiodide, Bromotetrazole, Nordstrandite, Copper Nickel Titanium and Succinamide in the soil sample. However, the detailed assessment of the XRD is the out of scope of this research.

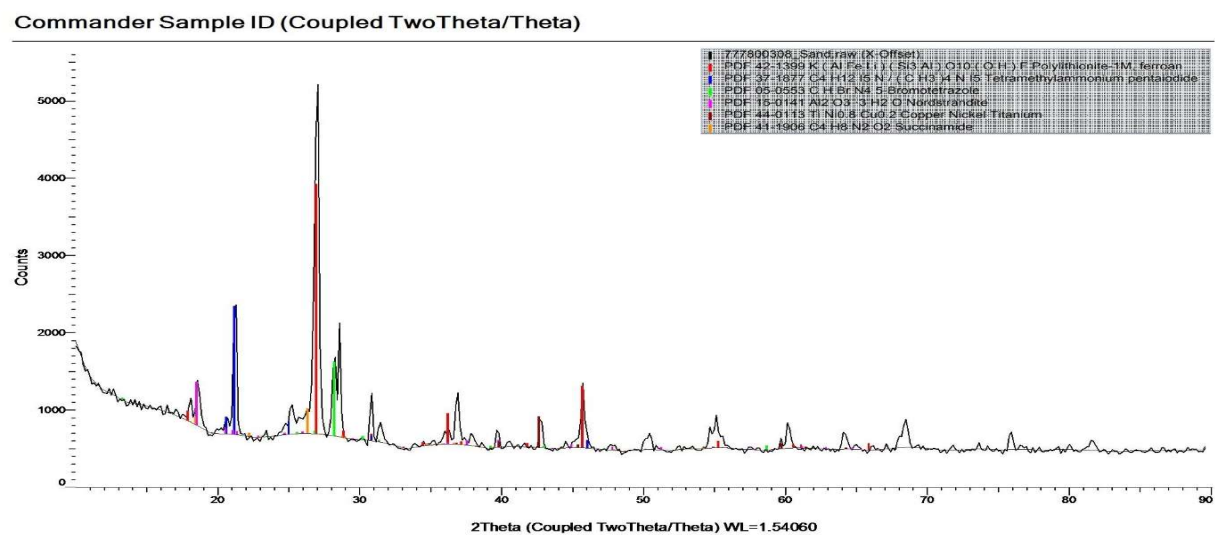


Figure 4.6: XRD test data of sample (Sample No. 10)



#### 4.4 Geotechnical Investigation

Necessary data relevant to this research was collected from the site investigation including supervision of core drilling and direct involvement on field tests. Data collected during the site investigation was used to characterize the subsurface profile of the foundation soil and results are presented in graphical form.

##### 4.4.1 Core Recovery and RQD Profile

Each core run, penetration rate, water loss, water returned as well as Rock Quality Designation (RQD) and Core Recovery Ratio of each run is recorded. A plot including the percentage of core recovery and RQD along the depth of the boreholes are presented in Figure 4.7. The central vertical line is the zero percentage and the thickness of each bar represents the value of RQD on left side of the vertical line and Core recovery ratio on the right side of the vertical line.

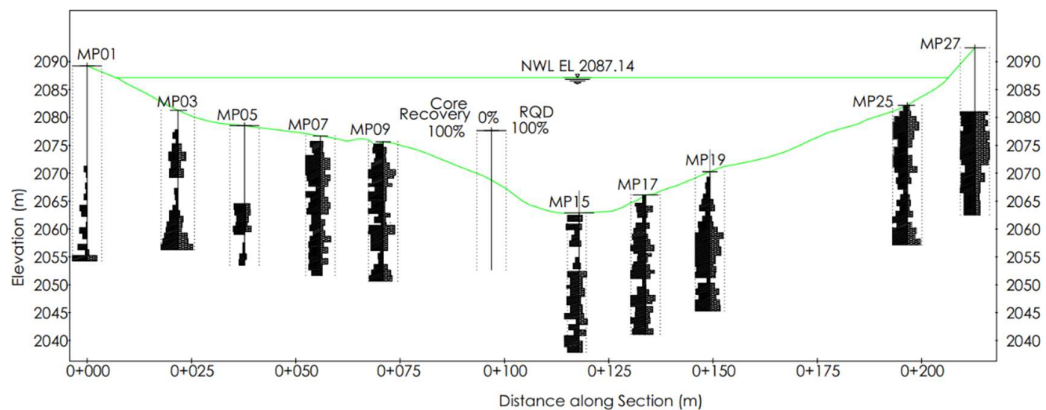


**Figure 4.7: RQD and Core Recovery obtained plot while rock coring**

##### 4.4.2 Geotechnical Model

From the site observation comprising of rock coring, drilling and field tests it is observed that the both side of embankment portions comprise colluvium soil at top and below 5m of depth highly to moderately weathered gneiss rock characterized with weak to medium strength. Around the deepest section, it comprises of relatively strong, reasonably fresh gneiss bed with some intrusions of granitic rock. A representative geotechnical model of the site is shown in Figure 4.8.



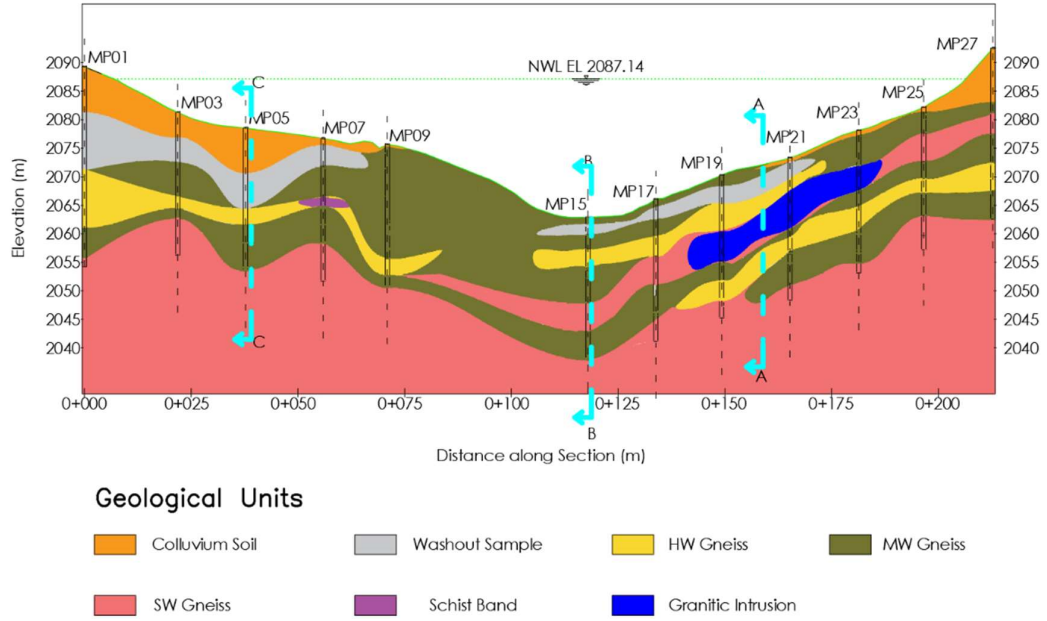


**Figure 4.8: Geotechnical Model of Dam Plinth**

#### 4.4.3 Lugeon Profile

For the hydraulic conductivity of foundation material, a comprehensive Lugeon test was performed by flowing water in varying pressure and observing its pattern. A typical test data (Borehole: MP03 and Depth 11-13m for the Lugeon test is presented in Table 4.8 and test result shown in Figure 4.9.

**Table 4.8: Typical Lugeon Test Result**

Pressure (bar)	Lugeon Value (Lu)	Flow Rate (lit./min)
1	17	8.48
2.5	12	15.11
5	8	19.44
2.5	11	14.11
1	14	7.15

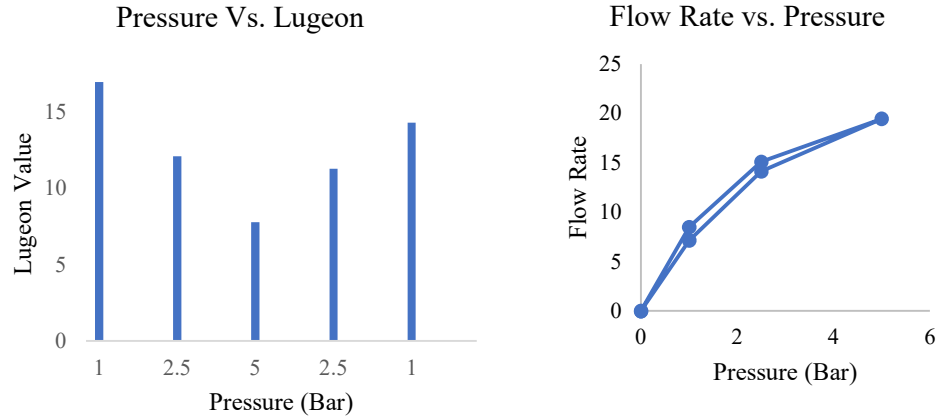


**Figure 4.9: Lugeon Pattern**

It should be noted that Figure 4.9 represents a Lugeon Pattern with values of Table 4.8, and indicates that this is a turbulent pattern (Houlsby, 1996). Thus, the corresponding Lugeon value would be the lowest at maximum pressure i.e., 8 Lugeon. A detailed calculation sheet for the Lugeon test is presented in Appendix C.

From the field tests including Lugeon and Lefranc test a representative L-Profile presenting the permeability value is presented in Figure 4.10. On the basis of Lugeon value hydraulic conductivity of the seepage model was defined and will be discussed in the Section 4.6. On the top layer (colluvium) permeability is calculated using Lefranc test and the value obtained on cm/s was converted to Lugeon value proposed by (Fell *et al.*, 2005)

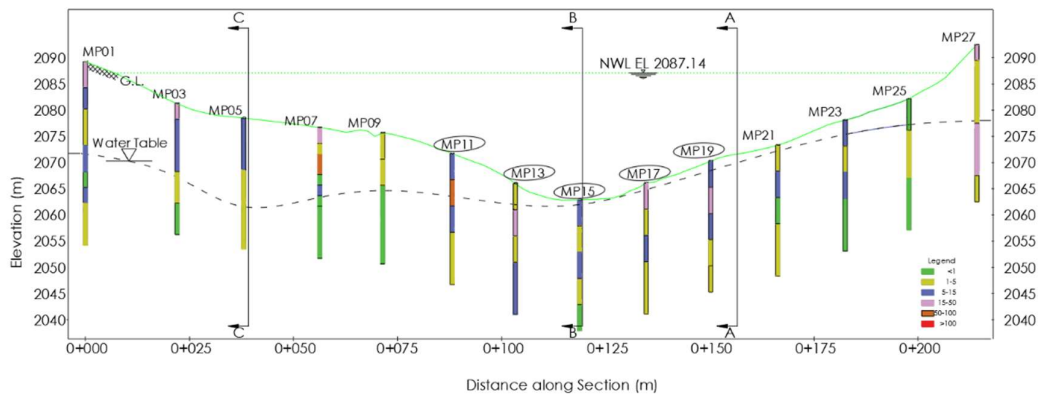


**Figure 4.10: Graphical Presentation of Lugeon Values**

In order to analyze the subsurface condition using water pressure test, Lugeon patterns were studied and the frequency of Lugeon value is also analyzed. Among 34 Water pressure tests (Lugeon Test) on rock, turbulent pattern was observed on 21 tests, Laminar flow on 4 tests, Dilatation on 8 tests and Void filling pattern on 1 test. However, washout pattern was not observed. A bar diagram showing the Lugeon value and corresponding frequency of Lugeon value are shown in Figure 11.

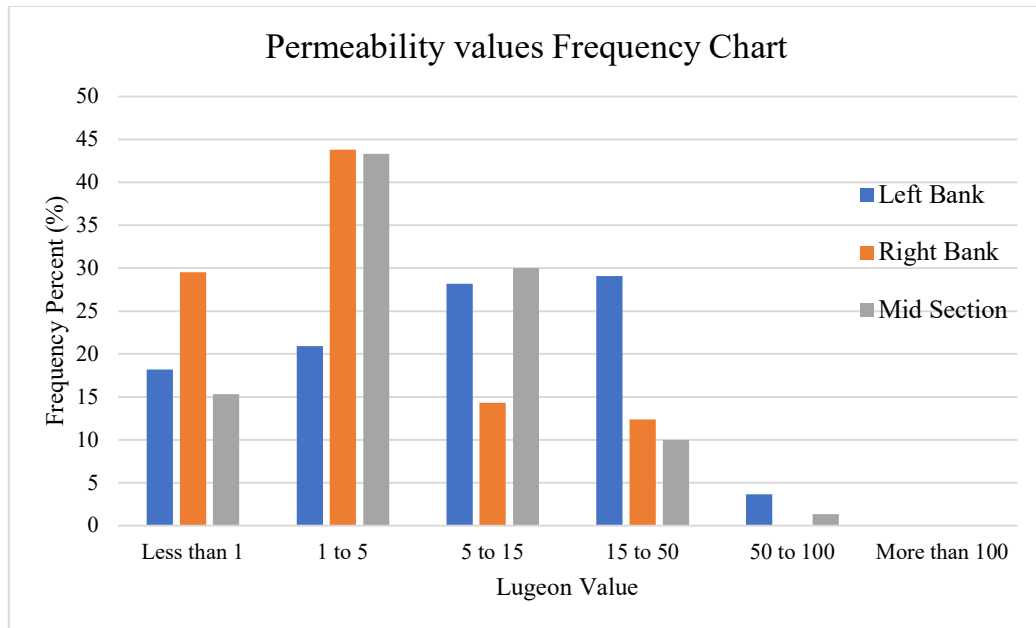


**Figure 4.11: Frequency Chart of Permeability Values in Lugeon Units**

From the test observation that more than 50% of patterns are turbulent, it can be concluded that there are mostly the rock masses exhibiting partly open to moderately wide cracks. Moreover, Lugeon profile shown in Figure 4.10 indicates the left bank is more permeable, contains more fractured rock, and exists a thick colluvium layer.

#### 4.5 Grouting

Curtain grouting was performed in 103 holes which included 26 primary holes and some secondary as well as tertiary holes. A typical test data obtained during the supervision of grouting is presented in Figure 4.12 as a result. From the observed data it can be seen that most of the points meet GIN envelope at maximum pressure as presented in Figure 4.12. Grout intake on the some of the supervised grouting holes are presented in Appendix C.

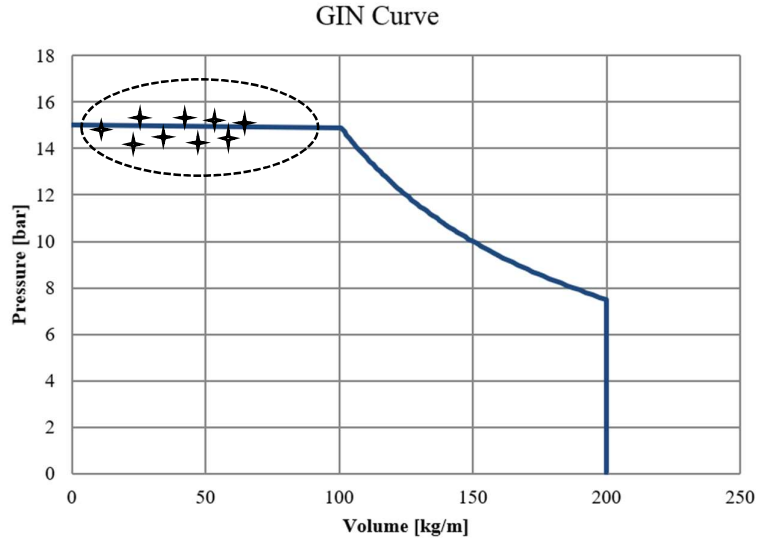


**Figure 4.12: Sample GIN curve at 15 bar pressure**

#### **4.6 Numerical Analyses**

A finite element numerical method was adopted to estimate the seepage through the dam. As the dam will be impounded up to the designed operation level, steady-state seepage analyses were conducted and results are discussed.

##### **4.6.1 General**

The dam alignment follows the natural topography of the existing valley thus the height of the water from the existing ground level to the crest is varying from the left to the right of the abutment. A total of three dam cross-sections were modeled including one cross-section representing the left abutment region, one cross-section representing the central deepest section region, and one cross-section representing the right abutment region.

Three cross-sections of the dam including A-A in the right portion, B-B in the deepest section and C-C in the left portion were chosen for the seepage models as shown in Figure 4.13.



**Figure 4.13 Dhap dam and cross-sections adopted for Seepage Model**

It can be observed in Figure 4.13 that water impoundment exists on the upstream side and three sections chosen for the seepage model at chainages of Ch 0+040, Ch 0+075 and Ch 0+145 with chainage measurement commencement from right abutment to left abutment. The three representative sections considered in the analyses are considered sufficient in this study to estimate seepage through the dam.

#### **4.6.2 GeoStudio Seep/W Software**

To estimate seepage through the dam, two-dimensional seepage analyses were carried out using the finite element program Seep/W developed by Geo-Slope International. The software calculates phreatic surfaces, pore pressures and flux (seepage per linear meter of embankment length), given user-defined geometry, hydraulic conductivity and boundary conditions. Steady-state seepage analyses were undertaken to estimate the potential development of the phreatic surface through the embankment as a result of retained water on the upstream side.

The subsurface geological profile encountered in the nearest boreholes was adopted to create the foundation of the dam in the Seep/w models. Embankment geometry was created based on the actual size of the embankment zones and concrete slab. The hydraulic conductivity values for the foundation materials obtained from the Lefranc test and the Lugeon test were employed in the seepage models. Typical values of

hydraulic conductivities were adopted in the Seep/W models for the embankment materials including concrete slab and Zones 2A to 3D.

For the analysis, a finite element square mesh of 1 m size was adopted to discretize the embankment model. Established models were run and seepage through the embankment dams was recorded at the toe in the downstream side of the dam. Total seepage through the dam is estimated by adding the product of seepage through a model and representative length of the dam for all three seepage models.

#### 4.6.3 Model Function

As discussed earlier, a total of three dam cross-sections were modeled including one cross-section representing the right abutment region (A-A), one cross-section representing the central deepest section region (B-B), and one cross-section representing the left abutment region (C-C). It should be noted that the deepest cross-section represents a critical section as this section exhibited maximum head once the water surface in the dam is in the designed operational level.

From the right abutment of the dam section first 50 m long is modeled representing section A-A, another 90 m representing section B-B and 32.2 m representing section C-C.

The hydraulic conductivity value for the embankment and foundation materials adopted in the Seep/W model are summarized in Table 4.9. The hydraulic conductivity functions produced in the Seep/W models based on the hydraulic conductivity of the materials are shown in Figure 4.14. The saturated water content values for the materials were adopted from the available database and are summarized in Table 4.9. The volumetric water content functions produced in the Seep/W models are shown in Figure 4.15.

**Table 4.9: Summary of saturated water content and hydraulic conductivity of materials**

Material	Saturated Water Content	Hydraulic Conductivity (m/s)
Zone 2A	0.38	$1 \times 10^{-5}$
Zone 2B	0.39	$1 \times 10^{-4}$
Zone 3A	0.25	$1 \times 10^{-3}$
Zone 3B	0.25	$1 \times 10^{-2}$

Material	Saturated Water Content	Hydraulic Conductivity (m/s)
Zone 3C and 3D	0.25	$1 \times 10^{-1}$
Concrete	0.5	$1 \times 10^{-12}$
Grout	-	$1 \times 10^{-12}$

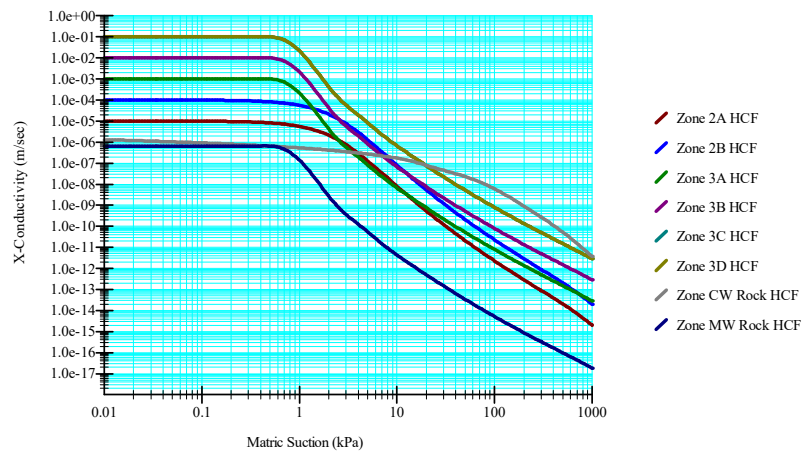


**Figure 4.14: Hydraulic Conductivity function of materials**

A hydraulic boundary condition representing the designed operational water level was applied on the upstream side of the dam. A potential seepage face boundary condition was applied at the toe region of the downstream face of the dam

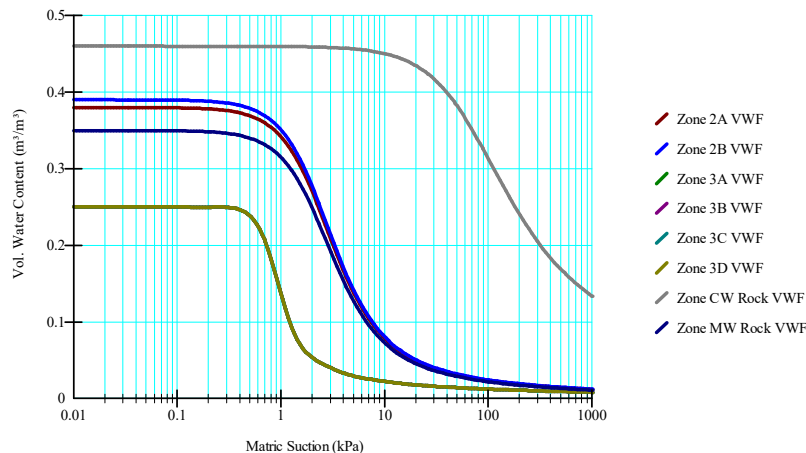


**Figure 4.15: Volumetric Water Content Function of Materials**

Based on the permeability value obtained from the Lugeon and Lefranc tests, a simplified foundation profile was established to be employed in the subsequent seepage

models. A typical foundation profile along the deepest section of the dam including permeability value and nomenclature of the materials adopted in the seepage models are summarized in Table 4.12.

**Table 4.10: Geotechnical Model Along Section B-B**

Section B-B  
Along Deepest Section (Referring Borehole MP15)

Depth (m)	Material Description	Permeability Value (m/s)	Representation on Model
0-1.3	Moderately Weathered Gneiss	1.3 x 10 <sup>-6</sup>	MW Gneiss1
1.3-3.3	Washout Sample fine sand		
3.3-5	Moderately weathered gneiss		
5-9.7	Moderately Weathered Gneiss	6.5 x 10 <sup>-7</sup>	HW Gneiss
5.4-6	Moderately weathered		
6-9.1	Highly weathered fine grained		
9.1-9.6	Moderately weathered		
9.6-14	Highly Weathered Gneiss	1.3 x 10 <sup>-6</sup>	MW Gneiss1
14-15	Slightly weathered gneiss		
15-21.2	Slightly Weathered Gneiss	6.5 x 10 <sup>-7</sup>	SW Gneiss
21.2-25	Moderately weathered Gneiss	1.3 x 10 <sup>-7</sup>	MW Gneiss2

**Table 4.11: Geotechnical Model along section A-A**

Section A-A  
Along Right Section (Referring Borehole MP19)

Depth (m)	Material Description	Permeability Value (m/s)	Representation on Model
0-0.9	Moderately Weathered Gneiss	1.95 x 10 <sup>-6</sup>	HW Gneiss
0.9-3.1	Washout Sample fine sand		
3.1-6	Moderately weathered gneiss		
6-10	Moderately Weathered Gneiss	2.6 x 10 <sup>-6</sup>	MW Gneiss1
10-15	Granitic Intrusion	1.3 x 10 <sup>-6</sup>	Granite
15-20	Moderately Weathered Gneiss	3.9 x 10 <sup>-7</sup>	MW Gneiss2
20-25	Slightly Weathered Gneiss	2.6 x 10 <sup>-7</sup>	SW Gneiss



**Table 4.12: Geotechnical Model along C-C**

Section C-C

Along Left Section (Referring Borehole MP05)

Depth (m)	Material Description	Permeability Value (m/s)	Representation on Model
0-5.2	Colluvium Soil	$1.56 \times 10^{-6}$	Colluvium2
5.2-9	Washout Fines	$1.04 \times 10^{-6}$	HW Gneiss1
9-14	Highly Weathered Gneiss	$5.2 \times 10^{-6}$	HW Gneiss2
14-25	Moderately Weathered Gneiss	$3.9 \times 10^{-7}$	MW Gneiss

#### 4.6.4 Numerical Model

Seepage models were undertaken at three locations of the dam without grouting and with grouting. It should be noted that to account for the influence of grouting in the estimated seepage, models were run by incorporating 15 m deep grouting in the upstream toe of the dam. Typical seepage model outputs including estimated seepage quantities and the observed phreatic lines for the deepest section (B-B) of the dam before grouting and after grouting are shown in Figures 16 and 17 respectively. Both models showed that the phreatic surface passed through the base of the upstream concrete slab followed by through the foundation of the dam. The phreatic surface appeared to be in shallow depth below the downstream region of the toe of the dam.

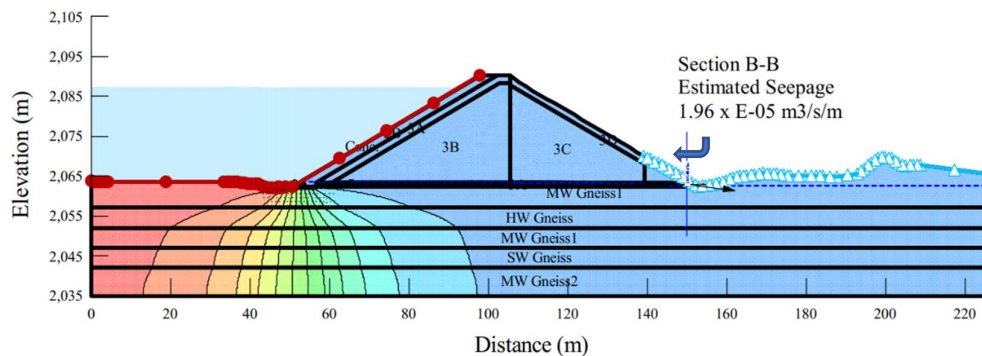


**Figure 4.16: Seepage Model of Dam along section B-B before grouting**

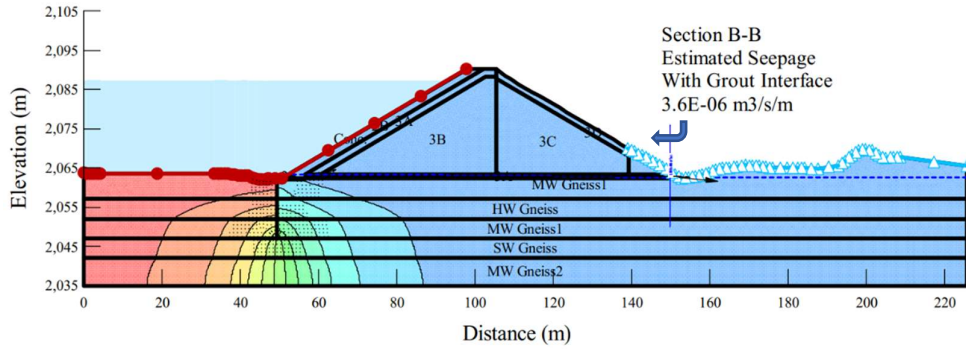


**Figure 4.17: Seepage Model of Dam along section B-B after grouting**

Similarly, seepage models along sections A-A and C-C are also prepared from respective geotechnical models as discussed in Section 4.4 and seepage model outputs are presented in Figures 4.18 to 4.21.

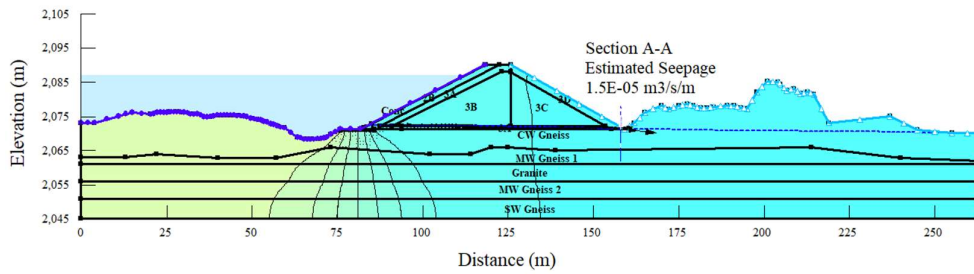


**Figure 4.18: Seepage Model of Dam along section A-A before grouting**

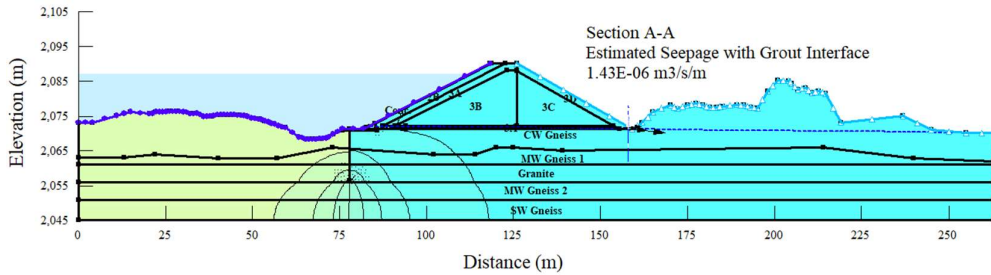


**Figure 4.19: Seepage Model of Dam along section A-A after grouting**

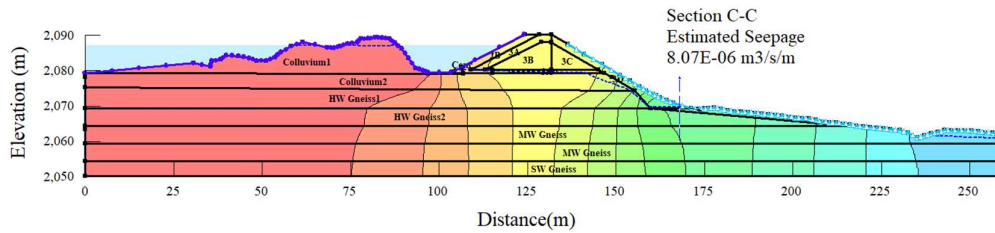


**Figure 4.20: Seepage Model of Dam along section C-C before grouting**

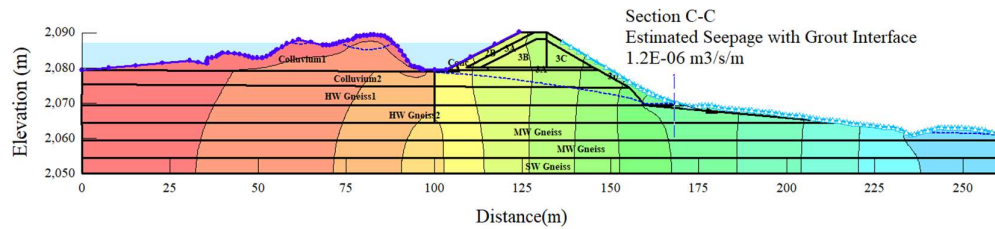


**Figure 4.21: Seepage Model of Dam along section C-C after grouting**

#### 4.7 Numerical Analyses Results

A summary of the estimated seepage or flux through the dam before grouting and after grouting is presented in Table 4.13.

**Table 4.13: Summary of Estimated Seepage on the dam**

Location	Predicted Seepage (lps)	
	Before Grouting	After Grouting
Right (Ch: 0+040) Section (A-A)	0.75	0.07
Middle (Ch: 0+075) Section (B-B)	1.76	0.32
Left (Ch: 0+145) Section (C-C)	0.25	0.04
<b>Total</b>	<b>2.77</b>	<b>0.43</b>

The seepage models from the three sections of dam indicated that the estimated seepage before grouting is 2.77 liter per second and after grouting is 0.43 liter per second. The influence of grouting in the seepage behavior of the dam is apparent indicating grouting

reduced the seepage through the foundation of the dam. It is noticed that the total water pressure head in the foundation of the dam is different with the lower water pressure head observed in the dam model with grouting. In addition, there is a slightly head loss on the downstream side of the grouting.

It can be observed from the table that seepage is reduced by approximately 6 times when the dam foundation is grouted. This indicates that there is a significant reduction in seepage following the grouting of the dam foundation and the dam after grouting is likely to exhibit insignificant amount of seepage.

#### **4.8 Sensitivity Analysis**

Hydraulic conductivity value gathered from field tests including Lugeon test and Lefranc test may contain some uncertainty and this would cause significant deviation of estimated seepage from the dam. To account for the uncertainty of the measured in-situ hydraulic conductivity, seepage analyses were conducted by varying the hydraulic conductivity of the foundation material by  $\pm 10\%$  of the measured hydraulic conductivity value during the site investigation.

A separate study undertaken by varying permeability of zoned material indicated that there is an insignificant influence in the estimated seepage quantities. The phreatic surfaces pass through the concrete face via the foundation of the dam rather than Zones 3A and 3B material. Thus sensitivity analyses undertaken by varying the hydraulic conductivity of only foundation materials are presented in this thesis.

A summary of the sensitivity analysis considering  $\pm 10\%$  of the observed hydraulic conductivity value during site investigation are presented in Table 4.14. The sensitivity analysis result for Sections A-A, B-B and C-C are shown in Figures 22, 23 and 24 respectively.

It can be observed in Table 4.14 that the seepage increase from 2.5 to 3.05 Lps once the hydraulic conductivity of the foundation materials varied by  $\pm 10\%$  of the observed value during the site investigation.

**Table 4.14: Summary of Sensitivity Analysis**

Location	Predicted Seepage (lps) after property varied to		
	110%	100%	90%
Right (Ch: 0+040) Section (A-A)	0.83	0.75	0.68
Middle (Ch: 0+075) Section (B-B)	1.94	1.76	1.59
Left (Ch: 0+145) Section (C-C)	0.28	0.25	0.23
<b>Total</b>	<b>3.05</b>	<b>2.77</b>	<b>2.5</b>

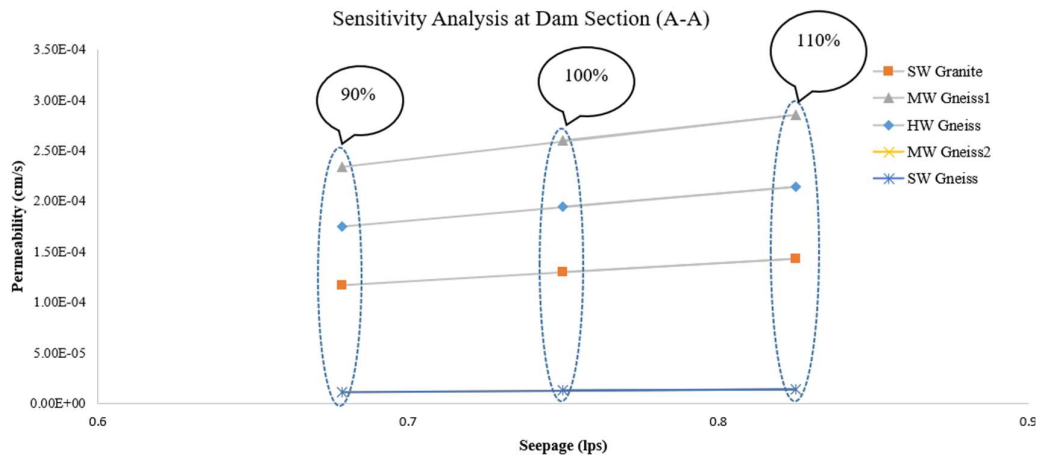


**Figure 4.22: Sensitivity Analysis at Dam Section (A-A)**

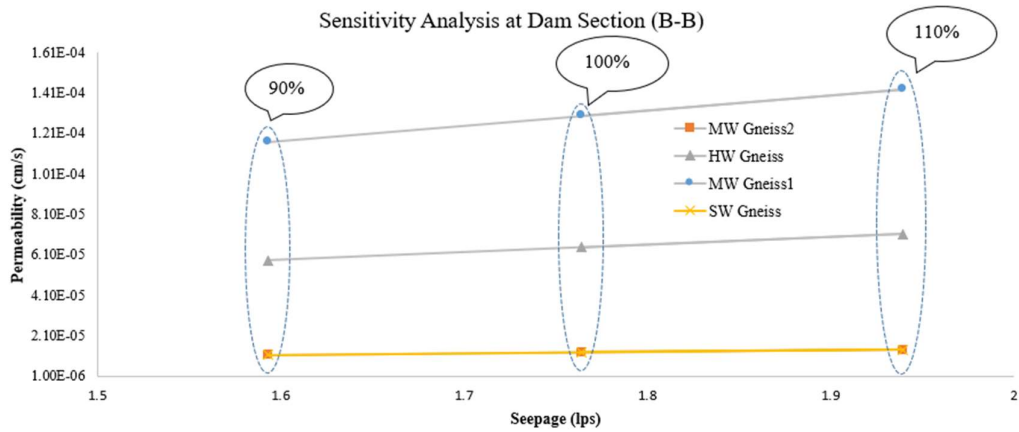


**Figure 4.23: Sensitivity Analysis at Dam Section (B-B)**

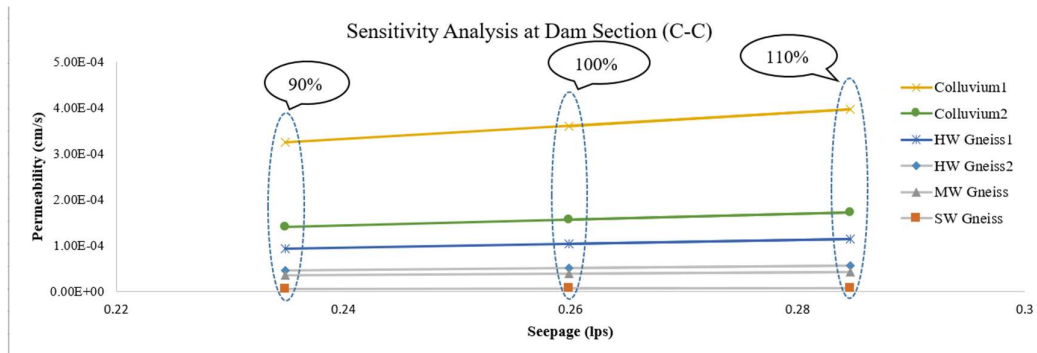


**Figure 4.24: Sensitivity Analysis at Dam Section (C-C)**

It can be observed in Figures 4.22, 4.23 and 4.24 that the estimated seepage increases with an increase in hydraulic conductivity of the foundation materials.

#### 4.9 Numerical Analyses Considering Anisotropy

In previous sections seepage models were prepared considering the same hydraulic conductivity along the horizontal direction and the vertical direction. But from the literature (eg. Shedid, 2019) it is found that hydraulic conductivity along the vertical direction ( $k_y$ ) is usually less than that along the horizontal direction ( $k_x$ ). A set of numerical models was conducted by varying the anisotropy ( $k_y/k_x$ ) of the foundation material from 0.1 to 1 and test results for models along sections A-A, B-B and C-C are shown in Figures 4.25, 4.26 and 4.27 respectively.

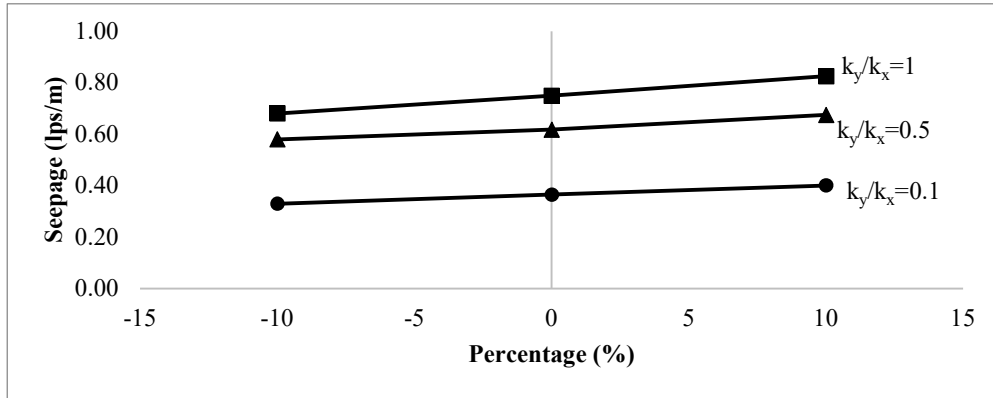


**Figure 4.25: Sensitivity Analysis by varying Anisotropy at section (A-A)**

From the analysis along section A-A, seepage quantity at 10% less permeability value with 0.1 anisotropy ratio is 0.33 lps to 0.83 lps at 10% more permeability value with 1 anisotropy ratio as presented in Table 4.15.

**Table 4.15: Estimated Seepage variation along Section A-A**

Sensitivity	Anisotropy ( $k_y/k_x$ )		
	1	0.5	0.1
-10%	0.68	0.58	0.33
0	0.75	0.62	0.37
10%	0.83	0.68	0.40

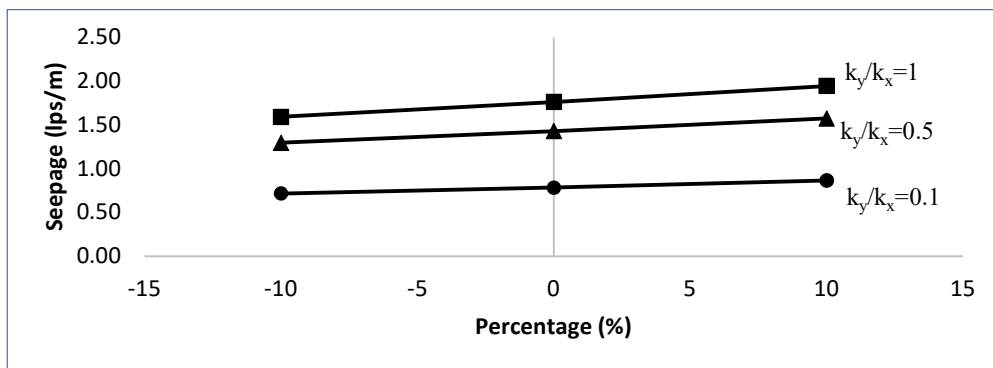


**Figure 4.26: Sensitivity Analysis by Varying Anisotropy ratio at section (B-B)**

From the analysis along section B-B, seepage quantity at 10% less permeability value with 0.1 anisotropy ratio is 0.72 lps to 1.94 lps at 10% more permeability value with 1 anisotropy ratio.

**Table 4.16: Estimated Seepage variation along Section B-B**

Section B-B			
Sensitivity	Anisotropy ( $k_y/k_x$ )		
	1	0.5	0.1
-10%	1.59	1.30	0.72
0	1.76	1.43	0.78
10%	1.94	1.58	0.87

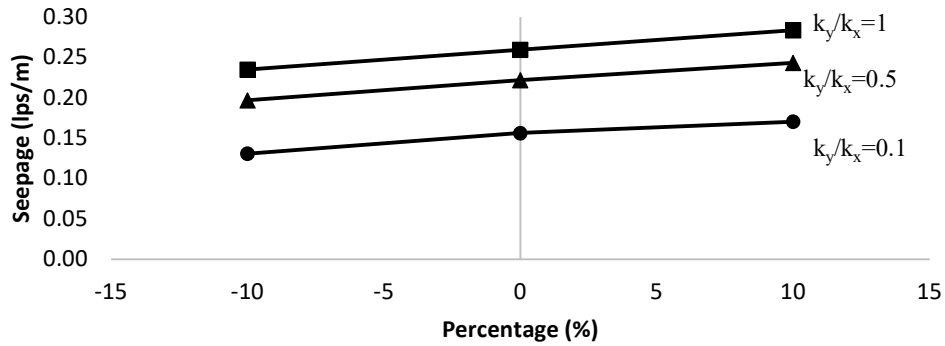


**Figure 4.27: Sensitivity Analysis by Varying Anisotropy ratio at section (C-C)**

From the analysis along section C-C, seepage quantity at 10% less permeability value with 0.1 anisotropy ratio is 0.13 lps to 0.28 lps at 10% more permeability value with 1 anisotropy ratio.

**Table 4.17: Estimated Seepage variation along Section C-C**

Section C-C			
Sensitivity	Anisotropy ( $k_y/k_x$ )		
	1	0.5	0.1
-10%	0.24	0.20	0.13
0	0.26	0.22	0.16
10%	0.28	0.24	0.17



**Table 4.18: Summary with Anisotropy**

Location	Anisotropy ranging 1 to 0.1 and Material Property Ranging -10% to +10%	
	Minimum seepage (lps)	Maximum seepage (lps)
Right (Ch: 0+040) Section (A-A)	0.33	0.83
Middle (Ch: 0+075) Section (B-B)	0.72	1.94
Left (Ch: 0+145) Section (C-C)	0.13	0.28
<b>Total</b>	<b>1.18</b>	<b>3.05</b>

The result from these analysis gives a range of 1.18 lps to 3.05 lps seepage through the foundation of dam.

**4.10 Seepage potential when water level is up to permanent outlet**

Elevation of permanent outlet is 2074.5m and so does the head boundary condition for that level is 2074.5m on numerical model. The fetch length at that level would be 91.5m. Even in dry condition the minimum water level would be up to permanent outlet point that’s why analysis here is important and two numerical models are presented below.

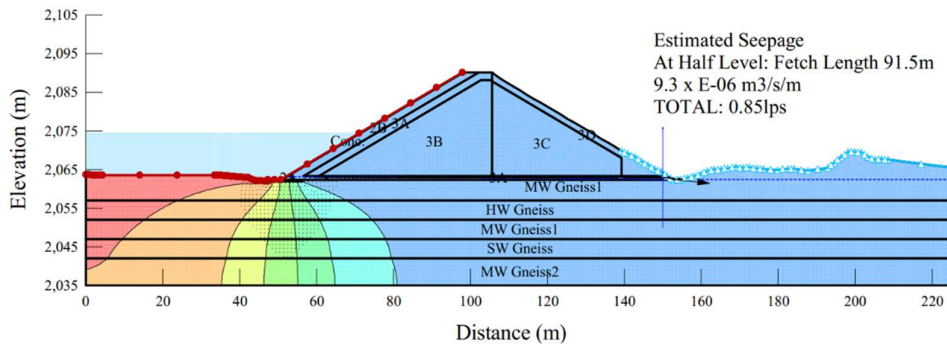


**Figure 4.28: Seepage without group on up to permanent outlet level**

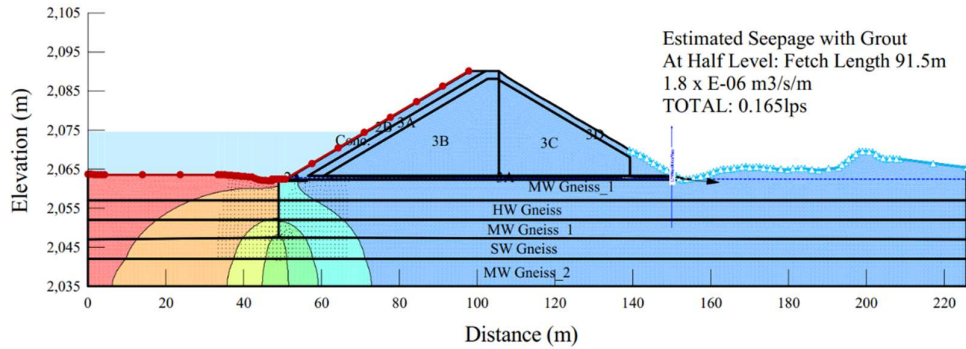


**Figure 4.29: Seepage with grout on up to permanent outlet level**

So, from the numerical model it can be concluded that when the water level would be up to the permanent outlet level estimated seepage would be 0.85lps without grout and will be reduced to 0.165lps after grout is introduced.

#### 4.11 Sensitivity analysis on grouted dam

From the earlier analysis in section 4.9 it is seen that the minimum value of seepage through the dam foundation will be on 10% less with 0.1 anisotropy ratio and maximum would be on 10% more with anisotropy ratio of 1.

Using that as a reference estimated seepage would vary from 0.362lps to 1.233lps.

**Table 4.19: Summary of estimated seepage after grout interface with sensitivity analysis**

Location	Anisotropy ranging 1 to 0.1 and Material Property Ranging -10% to +10%	
	Minimum seepage (lps)	Maximum seepage (lps)
Right (Ch: 0+040) Section (A-A)	0.104	0.440
Middle (Ch: 0+075) Section (B-B)	0.209	0.558
Left (Ch: 0+145) Section (C-C)	0.049	0.235
<b>Total</b>	<b>0.362</b>	<b>1.233</b>

Further the performance of grouted dam is observed on 10 folds and 100 folds considering the unusual behavior of top colluvium soil and results are presented. On 10 fold the seepage could be 11.5 lps and on 100 folds it could be 108lps.

#### 4.12 Discussion

To estimate the quantity of seepage necessary data was collected from laboratory testing and ongoing field investigation. Topsoil samples are brought from field and tested in laboratory for its geotechnical characterization and subsequent permeability testing which will further be used for seepage model and found that seepage quantity through the foundation of the dam would be 3.09 lps.

Field permeability tests including Lugeon and Lefranc test were conducted and found that the value obtained in laboratory and field of the same soil sample is slightly different.

Laboratory Permeability value of Sample 1 is  $1.17 \times 10^{-4}$  cm/s and field permeability value (Lefranc Test) at same point is  $2.79 \times 10^{-4}$  cm/s. Laboratory Permeability value of Sample 10 is  $1.28 \times 10^{-4}$  cm/s and field permeability value (Lefranc test) at same point is  $3.6 \times 10^{-4}$  cm/s. As permeability device is never in the same state as field and orientation of the in-situ stratum can't be duplicated and the smooth wall of permeability mold might be the reason of variance. As we are not able to calculate permeability in laboratory by compacting in field density, curve fitting may not be perfect to relate the value.

Geotechnical profile, Lugeon profile and Core Run indicated that left side of the dam is relatively weak and is more permeable. But this portion will host a lesser height of dam, correspondingly less head of water acting in this portion so there's not much problem being relatively weak zone.

The seepage model analysed by grouting of the dam foundation indicated that it will reduce the seepage quantity of the dam up to 6 times.

The sensitivity analysis conducted by varying the hydraulic conductivity value of foundation material, revealed that the seepage quantity varies from 2.5 lps to 3.04 lps.

Likewise, seepage model conducted by considering anisotropy of foundation material indicated that seepage through the foundation is likely to be in a range of 1.18 lps to 3.05 lps.

Further, the sensitivity analysis conducted on grouted dam produced a range of 0.362 lps to 1.233 lps as estimated seepage. And on 10 fold of the hydraulic conductivity value

the seepage could be 3.98 lps and on 100 folds it could be 38.65 lps through the foundation of the dam.

Also, at the water level up to permanent outlet boundary condition seepage quantity before and after grout are calculated and found to be 0.85lps and 0.165lps respectively.

## CHAPTER FIVE: CONCLUSIONS AND RECOMMENDATIONS

### 5.1 General

This research presented a study on estimating potential seepage quantity through the dam foundation with the inclusion of grouting while varying the hydraulic conductivity and anisotropy of foundation materials in Concrete face rockfill dam. For this study, Dhap dam which is at the final stage of construction is taken.

Dhap dam is a Concrete Face Rockfill Dam (CFRD), build to impound the monsoon rain and allow adequate flow in the Bagmati River during the dry seasons. The dam is 24m high and 172.7m length and expected to impound about 850,000m<sup>3</sup> water of the existing Chisapani lake. The dam characterized by diaphragm type zoned dam with concrete-faced on the upstream side and concrete is supported by a series of rockfill layers in the downstream slope of the dam is the first one built in Nepal over the Gneiss formation.

The dam here is considered as an anti-seepage dam but literature signified the importance of seepage calculation and there was a significant amount of seepage through CFRD and subsequent failures. So, to undertake a detailed seepage assessment primary data was collected from the site and both laboratory as well as field tests were conducted.

As a part of Dam construction project, there was an ongoing rock coring and drilling activities during the period of this research. So, direct supervision of the in-situ tests, rock coring and curtain grout were done, which were the primary data for seepage assessment through the dam foundation. A numerical model for the dam is prepared using Seep/W software and from the geotechnical model prepared from the field data detailed seepage assessment is carried out.

### 5.2 Conclusions

Based on laboratory test results, site-investigation test result and numerical analyses, following conclusion are drawn:

1. Shallow depth sample indicated the presence of colluvium soil varying from well graded to poorly graded sand and on which hydraulic conductivity varies from  $1.57 \times 10^{-5}$  cm/s to  $2.06 \times 10^{-4}$  cm/s obtained from Laboratory. Using this value as input parameter from the numerical analysis seepage observed on the

downstream of Dhap dam is 3.09 lps. Less value of coefficient of permeability of sand than other literatures and Free swell index of 20% of material characterized as sand is an unusual behavior and its further study is recommended.

2. The permeability value of the colluvium obtained from the laboratory tests and field permeability value (Lefranc Test) vary significantly. This may be associated with the limitations of the laboratory test equipment rather than the intrinsic characteristics of the soil.
3. From the site supervision of rock coring and drilling including the monitoring of RQD and Core recovery data it is found out that layer of colluvium soil is thicker at left abutment section. The colluvium underlain by the gneiss rock encountered was varying from highly to moderately weathered quality up to the depth of investigation. Around the deepest section good quality of gneiss rock is found which is characterized by higher value of RQD relatively strong and reasonably fresh with some intrusion of Granite was found out. The right abutment consisted of thin layer of colluvium soil underlain by slightly weathered rock.
4. Field tests viz., Lugeon Test and Lefranc Test were a part of site investigation to measure the in-site permeability of the subsurface. Lugeon tests pattern observed mostly are turbulent pattern and as per Houlsby, 1996 rock masses exhibit partly open to moderately wide cracks. The interpretation of Lugeon test data indicated that less Lugeon values are more frequent in right and deepest section and more Lugeon values are frequent in left section implying relatively permeable left abutment.
5. Grouting was introduced in dam foundation as an interface material and its effect was analyzed from the seepage modeling. It was found that with the inclusion of grouting in the Dhap dam foundation estimated seepage reduced from 2.77 lps to 0.43 lps. Thus, estimated seepage after the inclusion of grouting is approximately 6 times smaller than that estimated before the inclusion of grouting. The value obtained from numerical analysis are in the acceptable range following the literatures.

6. A sensitivity analysis conducted by varying the hydraulic conductivity of zoned material indicated there is insignificant influence in the variation of seepage through the dam. However, the seepage analyses conducted by varying the hydraulic conductivity of the foundation material by  $\pm 10\%$  revealed that seepage is likely to vary from 2.5 lps to 3.04 lps through the foundation of the dam.
7. A series of seepage analyses was conducted by varying the anisotropy ratio of the foundation materials from 0.1 to 1 to understand behavior of seepage flow in the vertical and horizontal. From the analyses of seepage model results, it is found out that seepage is likely to vary from 1.18 lps considering an anisotropy ratio of 0.1 to 3.05 lps considering an anisotropy ratio of 1 (i.e., at isotropic condition).
8. The seepage model prepared on grouted dam varying material property and anisotropy ratio gives the variance of seepage quantity from 0.362 lps to 1.233 lps. And on 10 fold of the hydraulic conductivity value the seepage could be 3.98 lps and on 100 folds it could be 38.65 lps through the foundation of the dam.
9. In half supply level (i.e., up to permanent outlet) seepage without grout is 0.85 lps and with grout is 0.165 lps.

### **5.3 Recommendations**

Based on the outcomes of this research and difficulties encountered during the site laboratory testing as well as site investigation, the following recommendations are made:

1. The permeability characteristics of the colluvium deposit of the Dhap dam need to be studied further focusing laboratory experiment. The outcome from this study will form a basis of similar dam design such as Nagmati Dam expected to be built in the downstream region of the Dhap dam.
2. The Dhap seepage dam model proposed in this study needed to be calibrated based on the actual seepage measurement after forthcoming impoundment of the dam. The calibrated seepage Dhap model can be used as supporting

document in the preliminary seepage assessment of the proposed Nagmati Dam proposed to build in the downstream region of the Dhap dam.

3. Effectiveness of consolidation grouting and curtain grouting in gneiss rock dam foundation can be further studied based on the seepage performance of dam after the impoundment.
4. Study on the Dhap dam can be further expanded including behavior of dam under the static and earthquake loadings, deformation analyses, dam break analyses and consequence category assessment, Risk assessment and mitigation strategy etc. for the successful operation of the dam.



## REFERENCES

- American Society for Testing and Material. (2007). ASTM D 698-07 Standard Test Methods for Laboratory Compaction Characteristics of Soil Using Standard Effort. *Gostroizdat*, 3, 15.
- ASTM: D 2434 – 68. (2000). Standard Test Method for Permeability of Granular Soils (Constant Head). *ASTM Book of Standards 2004*, 68(Reapproved), 1–5.
- ASTM:D4318. (2000). Liquid Limit, Plastic Limit, and Plasticity Index of Soils. *ASTM Book of Standards 2004*.
- ASTM. (n.d.). *Standard Practice for Rock Core Drilling and Sampling of Rock for Site*. 04.
- Bell, F. G. (2004). *Engineering geology and construction*. CRC Press.
- Bhattarai, S., Zhou, Y., Zhao, C., & Yadav, R. (2016). An overview on types, construction method, failure and key technical issues during construction of high dams. *Electronic Journal of Geotechnical Engineering*, 21(26), 10415–10432.
- Bowles, J. E. (1992). *Engineering Properties of Soils and Their Measurement* (4th ed.). McGraw Hill Education.
- BRBIP. (2018). *Main Dam Design Report*.
- Cambefort, H. (1987). Grouts and grouting. In *Ground Engineer's Reference Book*, 32 (pp. 1–32).
- Camilo Quinones-Rozo, C. A. J., & Andrew Yu, R. A. M. (2010). High-Pressure Concrete Plug Leakage Remediation. *Proceedings, North American Tunneling 2010*.
- Cassan, M. (1980). Les essais d'eau dans la reconnaissance des sols. *Paris, France: Eyrolles*.
- Cassan, M. (2000). Application des essais Lefranc à l'évaluation du coefficient d'anisotropie hydraulique des sols aquifères. *Revue Française de Géotechnique*, 90, 25–43.
- Cassan, M. (2005). Les essais de perméabilité sur site dans la reconnaissance des sols.

*Paris, France: Presses Des Ponts.*

- Chapuis, R. P. (2012). Predicting the saturated hydraulic conductivity of soils: A review. *Bulletin of Engineering Geology and the Environment*, 71(3), 401–434. <https://doi.org/10.1007/s10064-012-0418-7>
- Chapuis, R. P., & Sabourin, L. (1989). Effects of installation of piezometers and wells on groundwater characteristics and measurements. *Canadian Geotechnical Journal*, 26(4), 604–613.
- Chapuis, R. P., Soulie, M., & Sayegh, G. (1990). Laboratory modeling of field permeability tests in cased boreholes. *Canadian Geotechnical Journal*, 27.
- Chen, S.-K., & Zhang, X. (2016). Seepage Control in a High Concrete Face-Rock Fill Dam Based on the Node Virtual Flow Method. *The Open Construction and Building Technology Journal*, 10(1), 547–560. <https://doi.org/10.2174/1874836801610010547>
- Clements, R. P. . (1984). Post-construction deformation of rockfill dams. *Journal of Geotechnical Engineering*, 111(12), 1475. [https://doi.org/10.1061/\(ASCE\)0733-9410\(1985\)111:12\(1475\)](https://doi.org/10.1061/(ASCE)0733-9410(1985)111:12(1475))
- Cruz, P. T., Materon, B., & Freitas, M. (2010). *Concrete Face Rockfill Dams*.
- Dachler, R. (1936). Grundwasserströmung (Flow of groundwater). *Vienna, Austria: Julius Springer*.
- Dhital, M. R. (2015). *Geology of the Nepal Himalaya: regional perspective of the classic collided orogen*. Springer.
- Ewert, F. K. (2003). Discussion of Rock Type Related Criteria for Curtain Grouting. *Proceedings of the Third International Conference on Grouting in Rock and Ground Improvement*.
- Fell, R., MacGregor, P., Stapledon, D., & Bell, G. (2005). Geotechnical Engineering of Dams. In *Geotechnical Engineering of Dams*. <https://doi.org/10.1201/noe0415364409>
- Gavan, H., & Fell, R. (2003). *The deformation behaviour of embankment dams*.
- Houlsby, A. C. (1978). Routine interpretation of the lugeon water-test. *International*

- Journal of Rock Mechanics and Mining Sciences & Geomechanics Abstracts*, 15(6), 141. [https://doi.org/10.1016/0148-9062\(78\)91668-6](https://doi.org/10.1016/0148-9062(78)91668-6)
- Hvorslev, M. J. (1951). Time lag and soil permeability in ground-water observations. *Vicksburg, MS: US Army Engineering Waterways Experimental Station.*
- Icold, I. (2010). Concrete Face Rockfill Dams: Concepts for Design and Construction. *Bulletin*, 141.
- Lafhaj, Z., & Shahrour, I. (2004). Détermination de l'anisotropie de perméabilité des sols par l'essai Lefranc. *Revue Française de Géotechnique*, 109, 99–103.
- Lambe, T. W., & Whitman, R. V. (1979). *Soil Mechanics*.
- Lefranc, E. (1936). Procédé de mesure de la perméabilité des sols dans les nappes aquifères et application au calcul du débit des puits. *Le Génie Civil*, 109(15), 306-308.
- Lefranc, E. (1937). La théorie des poches absorbantes et son application à la détermination du coefficient de perméabilité en place et au calcul du débit des nappes d'eau. *Le Génie Civil*, 111(20), 409-413.
- Li, N. H. (2007). New Technology in high concrete face rock fill dam. *China Water Power Press, Beijing.*
- Lomabardi, G. (1985). The Role of Cohesion in Cement Grouting of Rock. *ICOLD-Congress, Lausanne(3)*, 235–261.
- Lugeon, M. (1933). *Barrage et Geologie.*
- Monnet, J. (2015). In situ tests in geotechnical engineering. *John Wiley and Sons.*
- Nonveiller, E. (1989). Grouting Theory in Practice. *Elsevier, Tokyo.*
- Of, M., For, T., & Limes, B. (2000). Indian Standard ) -1983 (. *Public Works*, 6932(February 1984).
- Petterson, S. A., & Molin, H. (1999). Grouting & Drilling for Grouting: Purpose, Application, Methods with Emphasis on Dam and Tunnel Projects. *Atlas Copco*, 6991 1091 01.
- Schleiss, A. J., & Pougatsch, H. (2011). Les Barrages: Du projet à la mise en service.

*Presses Polytechniques Universitaires Romandes, 17, 714.*

Şekercioğlu, E. (2007). Yapıların projelendirilmesinde mühendislik jeolojisi. *JMO Yayınları*.

Shedid, S. A. (2019). Prediction of vertical permeability and reservoir anisotropy using coring data. *Journal of Petroleum Exploration and Production Technology, 9(3)*, 2139–2143.

Shrestha, O. M. (2000). *Engineering and environmental geological map of the Kathmandu valley*. Department of mines and geology.

Taylor, D. W. (1948). Fundamentals of Soil Mechanics. *John Wile and Sons. Inc., New York, 42*.

Todd, D. K., & Mays, L. W. (2005). *Groundwater Hydrology*.

## **APPENDICES**

Appendix A: Trench Sample Collection

Appendix B: Core Logging

Appendix C: Field Tests

Appendix D: Core Log Photographs

Appendix E: Numerical Model

Appendix F: Work Schedule

## APPENDIX A: TRENCH SAMPLE COLLECTION

On 22<sup>nd</sup> March 2021, Trench/Pit sample were collected on side as described on methodology. Samples were brought to lab and subsequent tests were conducted.

**Table A1: Coordinates of Pit Location**

S.N	Easting	Northing	Elevation	Label	Sample Depths from GL	Remarks
1	347842	3076759	2100	Sample 1	0.2m and 0.8m	Field density @0.5m
2	347853	3076745	2083	Sample 2	0.1m and 0.6m	
3	347875	3076732	2081	Sample 3	0.3m	Refusal
4	347921	3076753	2062	Sample 4	0.15m	Refusal
5	347893	3076724	2058	Sample 5	0.3m	Refusal
6	347914	3076721	2060	Sample 6	0.1m and 0.6m	
7	347929	3076724	2060	Sample 7	0.4m	
8	347944	3076698	2075	Sample 8	0.1m and 0.8m	
9	347944	3076669	2090	Sample 9	0.2m and 0.9m	Field density @0.5m
10	347956	3076597	2095	Sample 10	0.2m and 0.9m	Field density @0.5m



**Figure A1: Google Images showing location of Test Pits sample**

## APPENDIX B: CORE LOGGING

From 26<sup>th</sup> April, 2021 drilling was started at the located points in the google image and from the beginning, almost all drillings were supervised on site and data were collected.



Figure B1: Google Image showing location of Boreholes

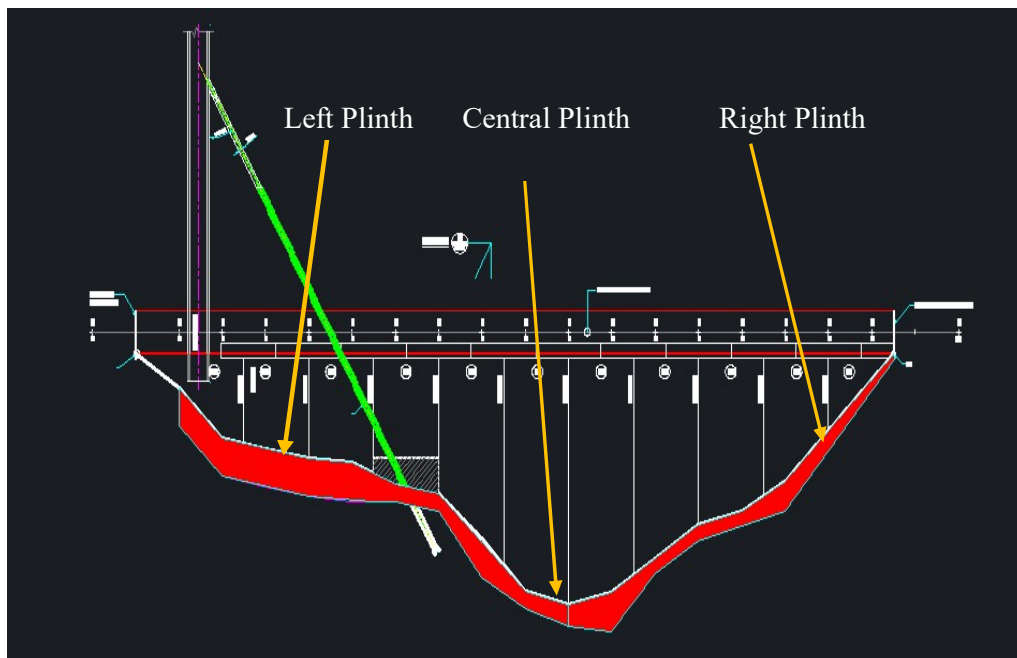


Figure B2: Red zone highlighting Plinth along which investigation is done

**Table B1: Co-ordinates of Drill Holes and some findings**

Drill Hole No.	Drill Hole Location		Elevation	Inclination	Total Depth (m)	Depth of Slightly Weathered Bed Rock(m)	No. of Packer Test	No. of LeFranc Test	Ground Water Level(m)
	Easting	Northing							
MP01	643730.326	3077117.675	2089.255	Vertical	35	34	6	6	17.5
MP03	643727.020	3077139.276	2081.272	Vertical	25	7.3	6	2	13.7
MP05	643719.367	3077153.037	2078.520	Vertical	25	16	-	-	16.8
MP07	643709.077	3077167.907	2076.687	Vertical	25	4	8		13.5
MP09	643701.030	3077180.236	2075.645	Vertical	25	4.2	4		11
MP11	643694.361	3077192.250	2071.707	Vertical			-	-	
MP13	643692.419	3077207.033	2066.000	Vertical			-	-	
MP15	643685.753	3077220.265	2062.884	Vertical	25	10.5	-	-	1
MP17	643671.616	3077226.916	2066.102	Vertical	25	9.2	-	-	1.5
MP19	643656.475	3077229.729	2070.278	Vertical	25	10.2	-	-	1.55
MP21	643641.757	3077235.717	2073.342	Vertical			-	-	
MP23	643626.190	3077239.660	2078.140	Vertical			-	-	
MP25	643611.439	3077243.137	2082.167	Vertical	25	4.8	5		5
MP27	643593.991	3077238.919	2092.086	Vertical	30	11.5	4	3	14.5



**Table B2: Core Run of Hole MP09**

Project: Dhap dam  
 Borehole: MP09  
 Inclination: Vertical  
 Water Table: 11m

Date: 26<sup>th</sup> April to 3<sup>rd</sup> May  
 Casing: 110mm for top 1m  
 Hole: 110mm, 76mm and 56mm

Run	Depth (m)		RQD %	Cr %	Penetration Rate (cm/min.)	Dia. (mm)	Core Length (m)	Remarks
	From	Top						
1	0	0.4						RCC plinth
2	0.4	1	0	65	2.9	56	0.6	
3	1	2	20	70	2.3	56	1	Mechanical breakage
4	2	3	15	50	2.9	56	1	
5	3	3.8	19	60	1.7	56	0.8	
6	3.8	5	42	80	1.4	56	1.2	
7	5	6	84	100	2.3	56	1	
8	6	6.5	72	100	1.4	56	0.5	reduced speed of rotation
9	6.5	7.5	30	74	1.4	56	1	
10	7.5	8	60	100	2.0	56	0.5	
11	8	9	20	56	2.6	56	1	
12	9	10.6	20	94	3.4	56	1.6	
13	10.6	12	10	80	4.0	56	1.4	
14	12	12.85	47	100	1.4	56	0.85	less amount of water
15	12.85	13.5	15	30	1.7	56	0.65	
16	13.5	14.5	20	60	2.3	56	1	
17	14.5	15	0	14	1.4	56	0.5	
18	15	16	78	96	2.9	56	1	
19	16	16.55	78	100	0.9	56	0.55	
20	16.55	17.5	46	94	2.3	56	0.95	
21	17.5	18.5	20	84	2.6	56	1	
22	18.5	19.5	30	83	2.9	56	1	
23	19.5	20	0	19	2.0	56	0.5	
24	20	21	0	34	1.7	40	1	BX core barrel with purpose of increasing Cr
25	21	22	0	30	2.3	40	1	
26	22	23	28	62	2.9	40	1	
27	23	24	50	80	2.6	40	1	
28	24	25	60	95	2.9	40	1	

**Table B3: Core Run of Hole MP07**

Project: Dhap dam  
 Borehole: MP07  
 Inclination: Vertical  
 Water Table: 13.5m

Date: 3<sup>rd</sup> May to 5<sup>th</sup> May  
 Casing: 110mm for top 1m  
 Hole: 110mm, 76mm and 56mm

Run	Depth (m)		RQD %	Cr %	Penetration Rate (cm/min.)	Dia. (mm)	Core Length (m)	Remarks
	From	Top						
1	0.5	1		100				Overburden
2	1	2	16	70	2.3	56	1	
3	2	3	13	55	1.9	56	1	Mechanical Breakage
4	3	3.5	22	42	2.3	56	0.45	
5	3.45	4	22	100	1.4	56	0.55	
6	4	5	64	100	1.2	56	1	
7	5	6	64	100	1.9	56	1	
8	6	7	30	100	1.2	56	1	Used less amount of water
9	7	8	65	90	1.2	56	1	
10	8	9	50	80	1.6	56	1	
11	9	10	14	30	2.1	56	1	
12	10	11	24	100	2.8	56	1	
13	11	12	25	66	3.3	56	1	
14	12	13	65	80	1.2	56	1	Return color change
15	13	14	53	92	1.4	56	1	
16	14	15	0	60	1.9	56	1	
17	15	16	28	55	1.2	56	1	
18	16	17	15	73	2.3	56	1	
19	17	18	30	50	0.7	56	1	
20	18	19	70	71	1.9	56	1	
21	19	20	20	80	2.1	56	1	
22	20	21	50	75	2.3	56	1	
23	21	22	10	80	1.6	56	1	
24	22	23	50	100	1.4	40	1	Speed Reduced
25	23	24	10	55	1.9	40	1	
26	24	25	10	60	2.3	40	1	

In similar manner core run of all holes are recorded and its RQD and Cr are presented in Figure 4.7.

Borehole log of MP15, MP19 and MP05 is presented and detailed is in geotechnical model.




















**GEOTECHNICAL LOG OF BORE HOLE**

Project: Thesis on Seepage Characteristics of Dhap Dam  
 Location: Plinth, Right Section  
 Machine: Core Drilling Rig XUL-100  
 Started: 6/10/2021  
 Completed: 6/12/2021

Coordinates (N,E) (m) 3077229.7  
 Elevation (m) 2070.28  
 Inclination w/ horizontal: 90°  
 Groundwater Table(m): 1.55m

Sheet no 1  
 643656.48

**DRILL HOLE NO. MP19**

Elevation	Drilling Depth (run wise)		Lithology		Rate of Penetration (cm/min)	Core Recovery %	Rock Quality Designation (RQD) %	Size of hole in (mm)	Water loss (full / partial / no loss)	Color of return water	Permeability		Remarks
	From	To	Description	Strata/Formation Log							Test section	Permeability value (m/s)	
2070.28	0.00	0.40	Backfilling			-	-	110	No	Brownish grey			Use of Muddy Water
2069.88	0.40	1.90	Washed out sample consisting of light grey, fine to medium grained sand with mica		2.98		-	76	No	Greyish			
2068.38	1.90	2.00	Moderately Weathered Gneiss Rock		2.70		-	76	No	Brownish grey	0 to 5	1.95E-06	Excessive use of water
2068.28	2.00	2.70	Washed out sample consisting of light grey, fine to medium grained sand with mica		2.14		-	76	No	Brownish grey			Iron Staining
2067.58	2.70	3.00	Moderately Weathered Gneiss Rock		2.40		-	76		Brownish grey			
2067.28	3.00	3.75	Washed out sample consisting of light grey fine to medium grained sand.		2.70		-	76	No	Brownish grey			Drilling is run in high speed
2066.53	3.75	4.00	Moderately to Highly Weathered Micaceous Gneiss		2.70		-	76	No	Brownish grey			
2066.28	4.00	4.50	Washed out sample consisting light grey, fine to medium grained sand.		1.58		-	76	No	Brownish grey			Weak
2065.78	4.50	5.00	Moderately to Highly Weathered Micaceous Gneiss		1.58		-	76	No	Brownish grey			
2065.28	5.00	5.50	Washed out sample consisting light grey, fine to medium grained sand.		1.30			76	No	Brownish grey			
2064.78	5.50	6.00	Moderately weathered Brownish gneiss		1.30		20	76	No	Brownish grey			
2064.28	6.00	6.30	Washed out sample consisting light grey, fine to medium grained sand.		2.14			76	No	Brownish grey			White in color
2063.98	6.30	7.00	Moderately weathered Brownish gneiss		2.23		30	76	No	Brownish grey	5 to 10	2.60E-06	
2063.28	7.00	7.70	Washed out sample consisting of light grey, fine to medium grained sand with mica		1.30		-	76	No	Brownish grey			Speed Reduced
2062.58	7.70	8.00	Highly Weathered Brownish Gneiss		1.30		-	76	No	Brownish grey			
2062.28	8.00	8.50	Washed out sample brownish fine to medium grained sand		1.86			76	No	Brownish grey			
2061.78	8.50	9.00	Moderately weathered Brownish gneiss		1.86			76	No	Brownish grey			
2061.28	9.00	9.20	Washed out sample		3.16			76	No	Brownish grey			Fresh color
2061.08	9.20	10.00	Moderately weathered Light greyish gneiss		3.16		20	76	No	Brownish grey			
2060.28	10.00	10.70	Greyish Fresh Granite		3.16	70	50	76	No	Brownish grey			Greyish

2059.58	10.70	11.00	Washed out sample		3.72	70	50	76	No	Brownish grey			
2059.28	11.00	12.00	Greysish Fresh Granite		3.72	100	95	76	No	Brownish grey			Strong
2058.28	12.00	13.00	Greysish Fresh Granite		3.72	100	60	76	No	Brownish grey	10 to 15	1.30E-06	Drilling is run in high speed
2057.28	13.00	14.00	Greysish Fresh Granite		1.30	100	75	76	No	Brownish grey			
2056.28	14.00	15.00	Greysish Fresh Granite		1.30	100	75	76	No	Brownish grey			
2055.28	15.00	16.00	Moderately Weathered Micaceous Gneiss		1.58	100	40	56	No	Brownish grey			Brownish
2054.28	16.00	17.00	Slightly to Moderately Weathered Light Greyish Micaceous Gneiss		2.14	100	20	56	No	Brownish grey			
2053.28	17.00	18.00	Slightly to Moderately Weathered Light Greyish Micaceous Gneiss		1.40	100	38	56	No	Brownish grey			
2052.28	18.00	19.00	Moderately Weathered Micaceous Gneiss		1.40	100	35	56	No	Brownish grey	15 to 20	3.90E-07	
2051.28	19.00	19.30	Moderately Weathered Micaceous Gneiss		2.70			56	No	Brownish grey			Vertical Joints
2050.98	19.30	20.00	Washout sample		0.84	30	0	56	No	Brownish grey			
2050.28	20.00	21.00	Slightly to Moderately Weathered Light Greyish Micaceous Gneiss		2.14	100	30	56/40	No	Brownish grey			Use of Muddy Water
2049.28	21.00	22.00	Moderately Weathered Gneiss Rock		2.42	90	60	56/40	No	Brownish grey			
2048.28	22.00	23.00	Slightly Weathered Micaceous Gneiss		2.70	90	40	56/40	No	Brownish grey			Excessive use of water
2047.28	23.00	24.00	Slightly Weathered Micaceous Gneiss		1.86	100	65	56/40	No	Brownish grey	20 to 25	2.60E-07	
2046.28	24.00	25.00	Slightly Weathered Micaceous Gneiss		1.58	95	67	56/40	No	Brownish grey			

Logged By: Anup Lamichhane




















**GEOTECHNICAL LOG OF BORE HOLE**

Project: Thesis on Seepage Characteristics of Dhap Dam  
 Location: Plinth, Mid Section  
 Machine: Core Drilling Rig XUL-100  
 Started: 6/1/2021  
 Completed: 6/2/2021

Coordinates (N,E) (m) 3077220.3  
 Elevation (m) 2062.88  
 Inclination w/ horizontal: 90°  
 Groundwater Table(m): 1 m

Sheet no 1  
 643685.75

**DRILL HOLE NO. MP15**

Elevation	Drilling Depth (run wise)		Lithology		Rate of Penetration (cm/min)	Core Recovery %	Rock Quality Designation (RQD) %	Size of hole in (mm)	Water loss (full / partial / no loss)	Color of return water	Permeability		Remarks
	From	To	Description	Strata/Formation Log							Test section	Permeability value (m/s)	
2062.88	0.00	0.40	Backfilling			-	-	110	No	Brownish grey			Use of Muddy Water
2061.88	0.40	1.30	Moderately Weathered Gneiss Rock		3.20	80	20	76	No	Greyish			Drilling is run in high speed
2060.88	1.30	2.00	Washed out sample consisting of light grey, fine to medium grained sand with mica		2.90	-	-	76	No	Brownish grey	0 to 5	1.30E-06	Excessive use of water
2059.88	2.00	3.00	Slightly to Moderately Weathered Gneiss Rock		2.30	90	15	76	No	Brownish grey			Iron Staining
2058.88	3.00	3.40	Moderately weathered brownish Gneiss Rock		2.90	30	-	76	No	Brownish grey			
2057.88	3.40	4.00	Washed out sample consisting of light grey fine to medium grained sand.		2.90	50	-	76	No	Brownish grey			
2056.88	4.00	4.50	Moderately to Highly Weathered Micaceous Gneiss		1.70	65	10	76	No	Brownish grey			
2055.88	4.50	5.00	Washed out sample consisting light grey, fine to medium grained sand.		1.70	-	-	76	No	Brownish grey			
2054.88	5.00	5.70	Moderately to Highly Weathered Micaceous Gneiss		1.40	-	-	76	No	Brownish grey			
2053.88	5.70	6.00	Washed out sample consisting light grey, fine to medium grained sand.		1.40	-	-	76	No	Brownish grey			
2056.88	6.00	7.00	Washed out sample consisting light grey, fine to medium grained sand.		2.30	-	-	76	No	Brownish grey			
2055.88	7.00	8.00	Washed out sample consisting of light grey, fine to medium grained sand		2.40	-	-	76	No	Brownish grey	5 to 10	6.50E-07	
2054.88	8.00	8.70	Washed out sample consisting of light grey, fine to medium grained sand with mica		1.40	25	-	76	No	Brownish grey			Speed Reduced
2054.18	8.70	9.00	Highly Weathered Brownish Gneiss		1.40		-	76	No	Brownish grey			
2053.88	9.00	9.40	Moderately weathered Brownish gneiss		2.00	40	12	76	No	Brownish grey			
2053.48	9.40	10.00	Washed out sample		2.00			76	No	Brownish grey			
2052.88	10.00	10.50	Washed out sample		3.40	80	50	76	No	Brownish grey			
2052.38	10.50	11.00	Slightly Weathered Gneiss Rock		3.40			76	No	Brownish grey			Brown color
2051.88	11.00	11.50	Moderately weathered Light greyish gneiss		3.40	60	20	76	No	Brownish grey			
2051.38	11.50	12.00	Moderately weathered Light greyish gneiss		4.00			76	No	Brownish grey			

2050.88	12.00	12.40	Moderately Weathered Micaceous Gneiss		4.00			76	No	Brownish grey			
2050.480	12.40	13.00	Wash out sample		4.00	60	20	76	No	Brownish grey	10 to 15	1.30E-06	
2049.880	13.00	14.00	Slightly Weathered Light Greyish Micaceous Gneiss		1.40	50	20	76	No	Brownish grey			
2048.880	14.00	15.00	Slightly Weathered Light Greyish Micaceous Gneiss		1.40	50	20	76	No	Brownish grey			
2047.880	15.00	15.30	Moderately Weathered Micaceous Gneiss		1.70	86	35	76	No	Brownish grey			Vertical Joints
2047.580	15.30	16.00	Washout Sample		2.30	46	8	76	No	Brownish grey			
2046.880	16.00	17.00	Slightly to Moderately Weathered Light Greyish Micaceous Gneiss		1.50	85	20	76	No	Brownish grey			
2045.880	17.00	18.00	Moderately Weathered Micaceous Gneiss		1.50	85	20	76	No	Brownish grey	15 to 20	6.50E-07	
2044.880	18.00	19.00	Moderately Weathered Micaceous Gneiss		2.90	60	30	76	No	Brownish grey			
2043.880	19.00	20.00	Slightly to Moderately Weathered Light Greyish Micaceous Gneiss		0.90	100	55	76	No	Brownish grey			
2042.880	20.00	21.00	Washed out sample consisting of light grey, fine to medium grained sand		2.30	20	0	76	No	Brownish grey			Use of Muddy Water
2041.880	21.00	22.00	Slightly Weathered Micaceous Gneiss		2.60	70	45	76	No	Brownish grey			
2040.880	22.00	23.00	Highly Weathered Gneiss Rock		2.90	35	-	76	No	Brownish grey			Excessive use of water
2039.880	23.00	24.00	Slightly Weathered Micaceous Gneiss		2.00	100	20	76	No	Brownish grey	20 to 25	1.30E-07	
2038.880	24.00	25.00	Slightly Weathered Micaceous Gneiss		1.70	80	20	76	No	Brownish grey			

Logged By: Anup Lamichhane

**GEOTECHNICAL LOG OF BORE HOLE**

Project: Thesis on Seepage Characteristics of Dhap Dam  
 Location: Plinth, Left Bank  
 Machine: Core Drilling Rig XUL-100  
 Started: 5/7/2021  
 Completed: 5/10/2021

Coordinates (N,E) (m) 3077153  
 Elevation (m) 2078.52  
 Inclination w/ horizontal: 90°  
 Groundwater Table(m): 16.8

Sheet no:1  
 643719.37

**DRILL HOLE NO. MP05**

Elevation	Drilling Depth (run wise)		Lithology Description	Strata/Formation Log	Core Recovery %	Rock Quality Designation (RQD) %	Size of hole in (mm)	Water loss (full / partial / no loss)	Color of return water	Permeability		Remarks
	From	To								Test section	Permeability value (m/s)	
2078.52	0.00	1.00	Colluvium deposit of brownish grey silt and sand (top soil)		-	-	76	No	Brownish grey			
2077.52	1.00	2.00	Colluvium deposit of brownish grey silt and sand		-	-	76	No	Brownish grey			Drilling is run on high speed
2076.52	2.00	3.00	Colluvium deposit of brownish grey silt and sand		-	-	76	No	Brownish grey			
2075.52	3.00	4.00	Washed out sample consisting of light grey, fine to medium grained sand with mica		-	-	76	No	Greyish	0 to 5	1.56E-06	
2074.52	4.00	5.00	Washout sample consisting light grey, fine to medium grained sand.		-	-	76	No	Brownish grey			
2073.52	5.00	6.00	Light grey to grey, medium to coarse grained gravelly sand.		-	-	76	No	Brownish grey			Use of muddy water
2072.52	6.00	7.00	Washed out sample consisting of light grey fine to medium grained sand.		-	-	76	No	Brownish grey			
2071.52	7.00	8.00	Washed out sample consisting light grey, fine to medium grained sand.		-	-	76	No	Brownish grey	5 to 10	1.04E-06	
2070.52	8.00	9.00	Washed out sample consisting light grey, fine to medium grained sand.		-	-	76	No	Brownish grey			
2069.52	9.00	9.90	Washed out sample consisting light grey, fine to medium grained sand.		-	-	76	No	Brownish grey			
2079.36	9.90	10.00	Boulder Rock Pieces		-	-	76	No	Brownish grey			Boulder
2068.52	10.00	11.00	Washed out sample consisting of light grey, fine to medium grained sand		-	-	76	No	Brownish grey			
2067.52	11.00	12.00	Washed out sample consisting of light grey, fine to medium grained sand with mica		-	-	76	No	Brownish grey			
2066.52	12.00	13.00	Washed out sample consisting of light grey, fine to medium grained sand with mica		-	-	76	No	Brownish grey	10 to 15	5.20E-06	
2065.52	13.00	14.00	Washed out sample consisting of light grey, fine to medium grained sand with mica		-	-	76	No	Brownish grey			
2064.52	14.00	14.27	Washed out sample consisting of light grey, fine to medium grained sand with mica	-	-	76	No	Brownish grey				
2064.25	14.27	14.61	Moderately weathered gneiss		-	-	76	No	Brownish grey			Pieces of rocks
2063.91	14.61	15.00	Slightly weathered gneiss		-	-	76	No	Brownish grey			
2063.52	15.00	15.31	Washed out sample consisting light grey, fine to medium grained sand.		-	-	76	No	Brownish grey			

2063.21	15.31	16.40	Slightly to moderately weathered gneiss		20	0	76	No	Brownish grey			
2062.12	16.40	17.12	Washed out sample consisting of light grey, fine to medium grained sand		-	-	76	No	Brownish grey			High Speed again
2061.40	17.12	17.30	Moderately weathered gneiss		-	-	76	No	Brownish grey			
2061.22	17.30	17.45	Washed out sample consisting of light grey, fine to medium grained sand		-	-	76	No	Brownish grey			
2061.07	17.45	18.00	Moderately weathered gneiss		-	-	76	No	Brownish grey			
2060.52	18.00	18.22	Washed out sample		-	-	76	No	Brownish grey			Vertical Joints
2060.30	18.22	19.00	Slightly to moderately weathered gneiss		-	-	76	No	Brownish grey			
2059.52	19.00	19.17	Washed out sample		-	-	76	No	Brownish grey	15-20	3.90E-07	
2059.35	19.17	19.50	Moderately weathered gneiss		-	-	76	No	Brownish grey			
2059.02	19.50	20.94	Washed out sample consisting of light grey, fine to medium grained sand		-	-	76	No	Brownish grey			
2057.58	20.94	21.00	Moderately weathered gneiss			-	76	No	Brownish grey			
2068.26	21.00	21.82	Washed out sample consisting of light grey, fine to medium grained sand		18	-	76	No	Brownish grey			
2067.44	21.82	22.00	Moderately weathered gneiss		-	-	76	No	Brownish grey			Iron staining
2067.26	22.00	22.83	Washed out sample consisting of light grey, fine to medium grained sand		37	-	76	No	Brownish grey			
2066.43	22.83	23.00	Moderately weathered gneiss		-	-	76	No	Brownish grey			
2066.26	23.00	23.69	Washed out sample consisting of light grey, fine to medium grained sand		33	12	76	No	Brownish grey	20-25	3.90E-07	
2065.57	23.69	24.00	Moderately weathered gneiss		33	12	76	No	Brownish grey			mostly washed
2065.26	24.00	24.55	Washed out sample consisting of light grey, fine to medium grained sand		38	-	76	No	Brownish grey			
2064.71	24.55	25.00	Moderately weathered gneiss		38	-	76	No	Brownish grey			

Logged By: Anup Lamichhane



## APPENDIX C: FIELD TESTS

**Table C1: Summary of Field Tests**

Drill Hole No.	Depth(m)	Le Franc Test Permeability(m/s)	Packer Tests	
			Lugeons	Permeability(m/s)
MP01	0 to 1	3.6E-06	-	-
MP01	3 to 4	2.1E-07	-	-
MP01	6 to 7	1.48E-07	-	-
MP01	10 to 11	4.44E-07	-	-
MP01	13.7 to 14.7	2.99E-07	-	-
MP01	17 to 18	7.19E-07	-	-
MP01	19 to 21	-	1.33	1.72E-07
MP01	22 to 24	-	0.69	9.05E-08
MP01	25 to 27	-	6.06	7.89E-07
MP01	27 to 30	-	2.21	2.87E-07
MP01	30 to 32	-	2.7	3.52E-07
MP01	32 to 35	-	1.58	2.05E-07
MP03	0.5 to 1.5	2.82E-06	-	-
MP03	3 to 4	1.24E-06	-	-
MP03	8 to 10	-	10	1.3E-06
MP03	11 to 13	-	7.78	1.01E-06
MP03	14 to 16	-	1.75	2.28E-07
MP03	17 to 19	-	2.1	2.73E-07
MP03	20 to 22	-	0.1	1.35E-08
MP03	22 to 25	-	0.5	6.8E-08
MP07	1 to 3	-	25	3.3E-06
MP07	3 to 5	-	1.87	2.43E-07
MP07	5 to 7	-	51.94	6.75E-06
MP07	7 to 9	-	54.07	7.02E-06
MP07	9 to 11	-	11.86	1.54E-06
MP07	11 to 13	-	1.77	2.31E-07
MP07	13 to 15	-	6.81	8.85E-07
MP07	15 to 20	-	0.75	9.83E-08
MP09	0 to 5	-	8	1.04E-06

Drill Hole No.	Depth(m)	Le Franc Test Permeability(m/s)	Packer Tests	
			Lugeons	Permeability(m/s)
MP09	5 to 10	-	4	5.2E-07
MP09	10 to 15	-	2	2.6E-07
MP09	20 to 25	-	0.47	6.1E-08
MP25	3 to 6	-	0.853	1.10E-07
MP25	5 to 10	-	1.18	1.53E-07
MP25	10 to 15	-	1.19	1.55E-07
MP25	15 to 20	-	0.78	1.01E-07
MP25	20 to 25	-	0.82	1.06E-07
MP27	0.5 to 1.5	2.79E-06	-	-
MP27	3 to 4	5.29E-07	-	-
MP27	6 to 7	5.18E-07	-	-
MP27	10 to 15	-	1.31	1.32E-07
MP27	15 to 20	-	10.73	1.39E-06
MP27	20 to 25	-	12	1.56E-06
MP27	25 to 30	-	2.38	3.09E-07

**Table C2: Grouting Test Results**

S.N.	Bore hole Code	Depth(m)		Duration (min.)	End Pressure(bar)	Cement (kg)	Total Cement take (kg)	Cement take per m (kg/m)	GIN
		From	To						
1	MP02	10	15	25	9	16.3	72.82	3.3	29.3
2		5	10	23	10	45.65		9.1	91.3
3		0	5	24	10	10.87		2.2	21.7
4	MP04	10	15	15	14	33.65	98.55	6.7	94.2
5		5	10	20	13	50.48		10.1	131.2
6		0	5	19	8	14.42		2.9	23.1
7	MP05	10	15	24	13	13.04	68.48	2.6	33.9
8		5	10	19	10	36.96		7.4	73.9
9		0	5	5	10	18.48		3.7	37.0
10	MP06	10	15	22	14	39.8	94.63	8.0	111.4
11		5	10	20	13	45.65		9.1	118.7

S.N.	Bore hole Code	Depth(m)		Duration (min.)	End Pressure(bar)	Cement (kg)	Total Cement take (kg)	Cement take per m (kg/m)	GIN
		From	To						
12		0	5	20	10	9.18		1.8	18.4
13		10	15	37	13	15.22		3.0	39.6
14	MP08	5	10	27	13	75	111.96	15.0	195.0
15		0	5	32	10	21.74		4.3	43.5
16		10	15	33	15	14.74		2.9	44.2
17	MP10	5	10	26	14	13.68	36.84	2.7	38.3
18		0	5	21	12	8.42		1.7	20.2
19		10	15	28	15	12.63		2.5	37.9
20	MP11	5	10	20	15	11.58	33.68	2.3	34.7
21		0	5	16	12	9.47		1.9	22.7
22		10	15	30	14	9.47		1.9	26.5
23	MP12	5	10	24	12	13.68	30.52	2.7	32.8
24		0	5	15	10	7.37		1.5	14.7
25		10	15	36	15	16.84		3.4	50.5
26	MP13	5	10	31	13	17.89	48.41	3.6	46.5
27		0	5	18	12	13.68		2.7	32.8
28		10	15	16	13	5.43		1.1	14.1
29	MP14	5	10	22	13	17.39	34.78	3.5	45.2
30		0	5	22	10	11.96		2.4	23.9
31		10	15	31	14	14.13		2.8	39.6
32	MP15	5	10	29	13	14.13	44.56	2.8	36.7
33		0	5	20	10	16.3		3.3	32.6
34		10	15	35	13	27.37		5.5	71.2
35	MP16	5	10	20	13	23.16	66.32	4.6	60.2
36		0	5	20	10	15.79		3.2	31.6
37		10	15	36	14	8.7		1.7	24.4
38	MP17	5	10	30	13	13.04	21.74	2.6	33.9
39		0	5	0	0			0.0	0.0
40		10	15	21	13	11.96		2.4	31.1
41	MP18	5	10	22	13	44.57	79.36	8.9	115.9
42		0	5	29	10	22.83		4.6	45.7

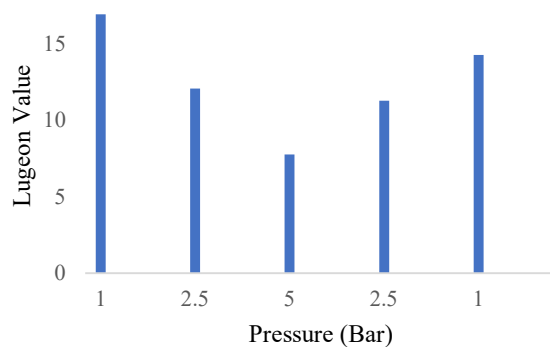
**Table C3: Sample of Comprehensive Lugeon Test Calculation**

**Packer Permeability Test (Comprehensive Lugeon Test)**

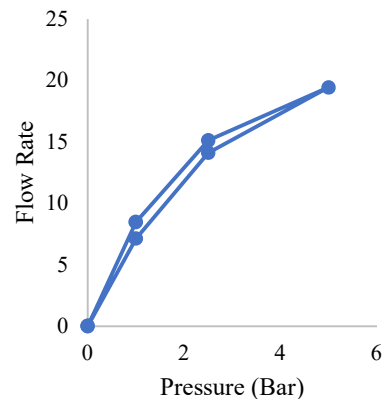
Depth: Borehole: MP03 5/30/2021  
 From: 11 m Water Table = 13.7 m 2:00 PM  
 To: 13 m  
 Length of Lugeon rod: Double Packer  
 1.35m  
 First Flow meter: 85.8 Size: 56mm (BX)

Pressure (Bar)	Time (min.)	Volume reading (lit)	Volume (litre)	Average Volume	Q (lit./min/m)	Q (lit./m in)	Pe (bar)	Lu
1	5	104.4		11.45	1.70	8.48	1	16.96
	5	116.2	11.8					
	5	127.3	11.1					
2.5	5	149.7		20.4	3.02	15.11	2.5	12.09
	5	170.8	21.1					
	5	190.5	19.7					
5	5	226.4		26.25	3.89	19.44	5	7.78
	5	252.7	26.3					
	5	278.9	26.2					
2.5	5	299.1		19.05	2.82	14.11	2.5	11.29
	5	318.3	19.2					
	5	337.2	18.9					
1	5	350.2		9.65	1.43	7.15	1	14.30
	5	359.9	9.7					
	5	369.5	9.6					

Pressure Vs. Lugeon



Flow Rate vs. Pressure



Remarks: Turbulent Flow

So, the flow is Turbulent.

And from Literature, Adopt the Lugeon at maximum pressure for turbulent flow. So, Lugeon Value = 7.78. Thus, Corresponding Permeability Value: 1.1E-06 m/s.

**Table C4: Sample of Lefranc test Calculation**

Sample Calculation of Lefranc Test

Length(L) = 100 cm  
 Diameter(d) = 76 cm  
 Radius, r = 38 cm  
 Average depth(H) = 650 cm  
 Hole No. = MP27  
 Depth = 5 to 6 m

Time(min.)	Consumed (ml or cc)
1	2900
2	2300
3	2500
4	2000
5	2170
10	9000
20	13500
30	12490

Volume Consumed= 12995 cc  
 Discharge (Q)= 21.65833333 cc/s  
 $\log(L/r)$  0.420216403  
 Permeability(k)= 5.18E-05 cm/s  
 5.18068E-07 m/s

**APPENDIX D: CORELOG PHOTOGRAPHS**



**Figure D1: MP15 (Depth 0-5m)**



**Figure D2: MP15 (Depth 5-10m)**



**Figure D3: MP15 (Depth 10-15m)**





**Figure D4: MP15 (Depth 15-20m)**



**Figure D5: MP15 (Depth 20-25m)**



**Figure D6: MP19 (Depth 0-5m)**



**Figure D4: MP19 (Depth 5-10m)**



**Figure D5: MP19 (Depth 10-15m)**



**Figure D6: MP19 (Depth 15-20m)**





**Figure D4: MP19 (Depth 20-25m)**



**Figure D5: MP05 (Depth 0-5m)**



**Figure D6: MP05 (Depth 5-10m)**



**Figure D4: MP05(Depth 10-15m)**



**Figure D5: MP05 (Depth 15-20m)**



**Figure D6: MP05 (Depth 20-25m)**

## APPENDIX E: NUMERICAL MODEL

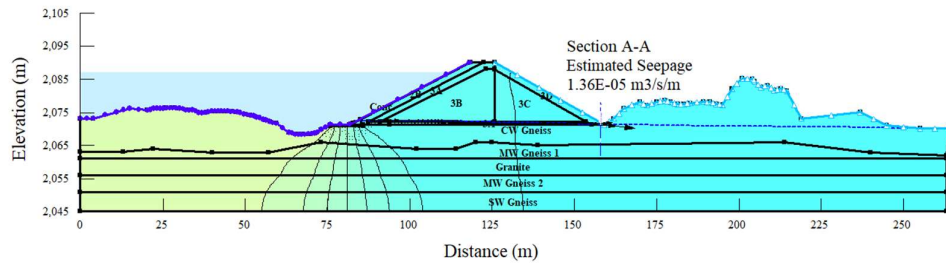


Figure E1: Right\_90\_1

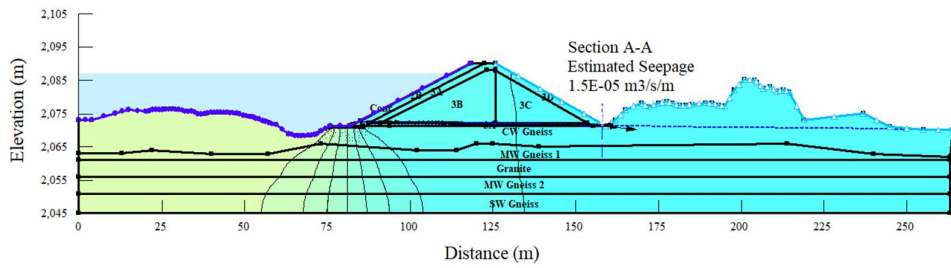


Figure E2: Right\_100\_1

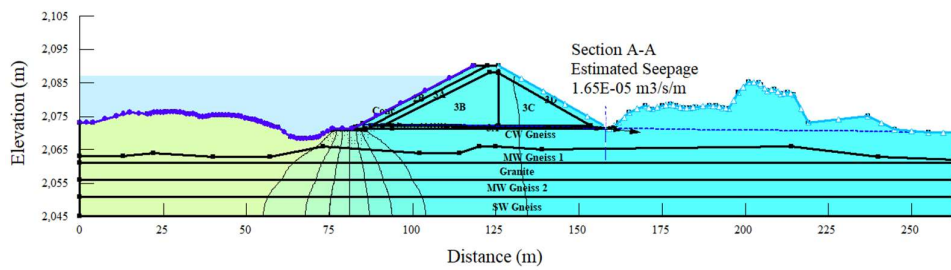
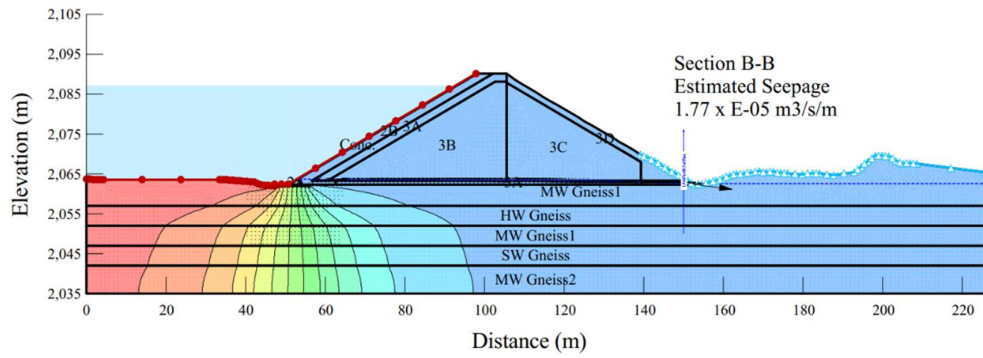
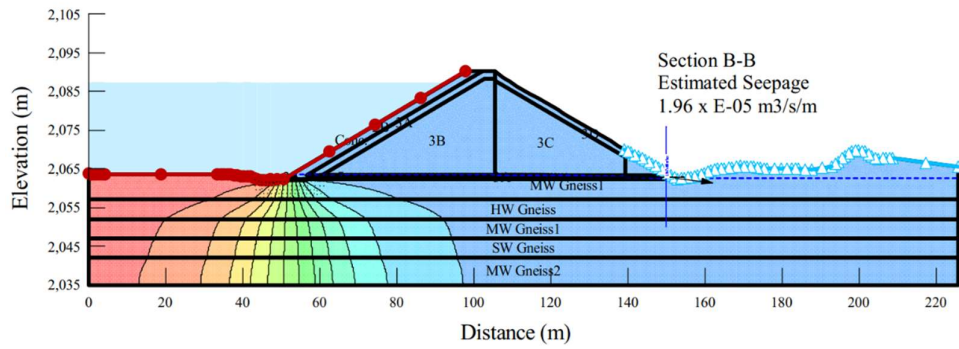


Figure E3: Right\_110\_1





**Figure E4: Deep\_90\_1**



**Figure E5: Deep\_100\_1**

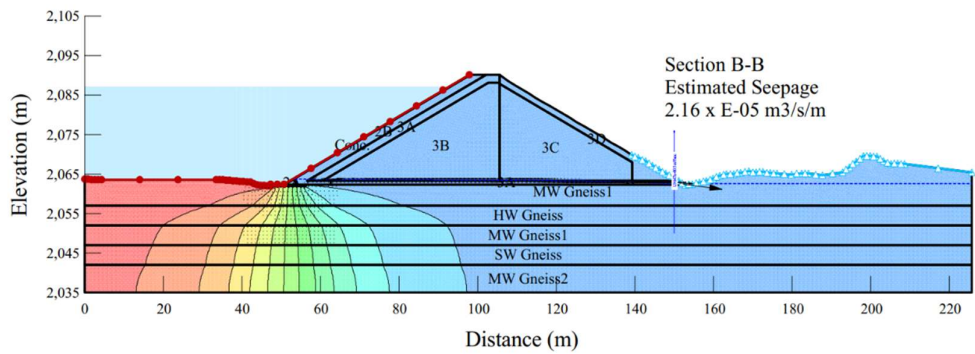


**Figure E6: Deep\_110\_1**

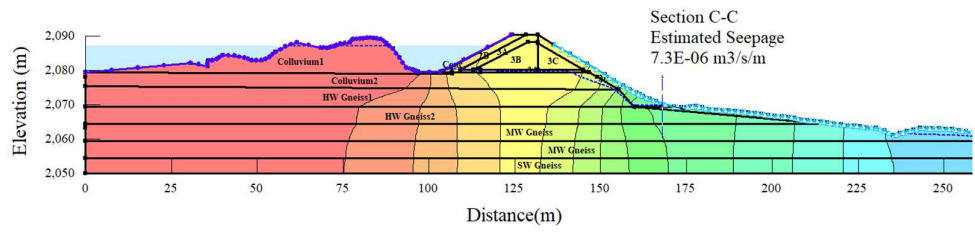


Figure E7: Left\_90\_1

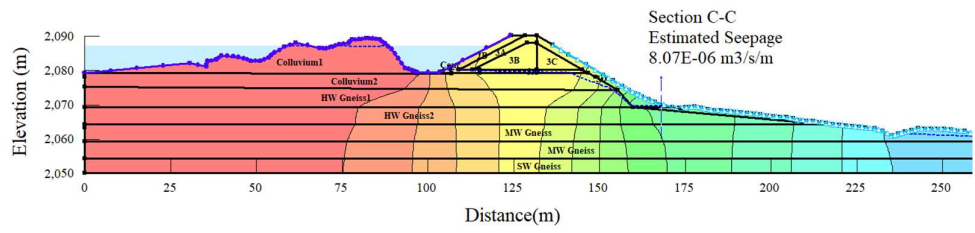


Figure E8: Left\_100\_1

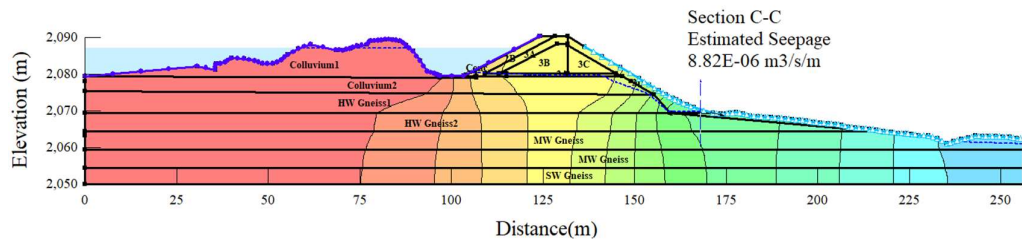


Figure E9: Left\_110\_1

## APPENDIX F: WORK SCHEDULE

Date		Tasks	Status	Remarks
From	To			
7-Jan-2021		Preliminary Title Defense	Completed	Starting of Thesis Work
21-Jan	23-Jan	Observation of Previous Core Samples and Site Visit	Completed	Inception work
23-Jan	11-Feb	Study of Available reports from BRBIP	Completed	Literature Reviews and more
25-Feb	3-Mar	Topic Defense and Report Submission	Completed	Finalized the topic
12-Mar		Proposal and Presentation to BRBIP	Completed	Permission to work from Government
22-Mar	25-Mar	Trench Sample Collection	Completed	Site works
27-Mar	26-Apr	Laboratory tests of all samples and their analysis, Geotechnical Characterization	Completed	Lab Works
29-Apr	18-Jun	Field Program, Drilling of all 13 holes, Field Tests and Grouting works	Completed	Field Stay
18-Jun	23-Jul	Numerical Modeling of single section and Report Preparation	Completed	Software works
26-Jul		Mid-Term Thesis Submission	Completed	Upto completed
7-Jan	31-Aug	Literature Review works	Continuous	Throughout thesis
7-Jan	31-Aug	Weekly Meeting with Supervisor	Continuous	Throughout thesis
26-Jul	6-Aug	Preparation for Presentation and Further Interpretation	Completed	
6-Aug		Mid-term thesis defense	Completed	

Date		Tasks	Status	Remarks
From	To			
6-Aug	22-Aug	Complete Numerical Analysis, Preparation of Borehole Log profiles, Sensitivity Analyses, Incorporate comments (if any)	Completed	Software and formatting works
15-Aug		Paper Submission	Completed	IOEGC Paper
15-Aug	1-Sep.	Final formatting, Approval from Supervisor, and Thesis Submission	Completed	
September, 2021		Final Thesis Defense	Completed	Accepted
September, 2021		Final Thesis Submission	Completed	

## LAB AND SITE PHOTOGRAPHS



**Figure 1: Field Density Test**



**Figure 2: Sample Collection**



**Figure 3: Sample Transport to Lab**



**Figure 4: Sieve Analysis in Lab**



**Figure 5: Standard Proctor test**



**Figure 6: Constant head test setup**



**Figure 7: Sample Preservation in Lab**



**Figure 8: Free Swell Test**





**Figure 9: Grouting seen while drilling**



**Figure 10: Lugeon Test**



**Figure 11: Labeling Core Box**



**Figure 12: Digital Flow Meter**



**Figure 13: Lefranc Test**

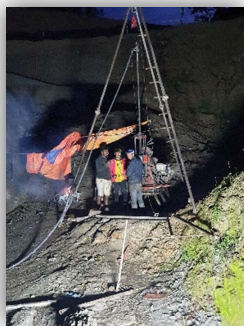


**Figure 14: Drilling works at night**



**Figure 15: Flow cone test on grouting**